TECHNISCHE UNIVERSITÄT MÜNCHEN

Fakultät für Medizin

Lehrstuhl für Diabetesforschung / Beta-Zell-Biologie

The Role of Oct4 in murine endoderm development

Stefan Hasenöder

Vollständiger Abdruck der von der Fakultät für Medizin der Technischen Universität München zur Erlangung des akademischen Grades eines

Doktors der Naturwissenschaften

genehmigten Dissertation.

Vorsitzender: Univ.-Prof. Dr. Michael John Atkinson

Prüfer der Dissertation:

1. Univ.-Prof. Dr. Heiko Lickert
2. Univ.-Prof. Angelika Schnieke, Ph.D.

Die Dissertation wurde am 28.05.2015 bei der Technischen Universität München eingereicht und durch die Fakultät für Medizin am 18.11.2015 angenommen.

Content

List of figures

List of tables

1 Summary

Oct4 is the key transcription factor for pluripotency and incorporated into a network together with Nanog and Sox2. Recent studies have shown that Oct4 function reaches beyond the maintenance of pluripotency and plays a role during early embryonic development (Deveale et al. 2013; Morrison & Brickman 2006; Reim et al. 2004). We therefore wanted to investigate the function of Oct4 in mesendoderm and endoderm formation during early mouse embryonic development. Since the full knock-out of Oct4 is lethal before implantation (Nichols et al. 1998), we conditionally deleted Oct4 in Foxa2+ mesendodermal and endodermal progenitors during gastrulation.

Oct4 CKO embryos displayed malformation of the hindgut endoderm as well as rare defects in neural development. Furthermore, the establishment of left-right (LR) asymmetry was perturbed in Oct4 CKO embryos. The likely cause was the malformation and morphological defects at the node, including aberrant ciliation, which can impair nodal flow and therefore LR asymmetry formation. These patterning defects are further supported by mRNA profiling on embryonic tissue, which showed misregulation of genes important for posterior development, patterning and LR asymmetry formation. This also includes several important signaling pathways such as Tgf-β and Wnt.

To further investigate the consequences of Oct4 deletion on endoderm formation, we generated Oct4 CKO embryonic stem cells (ESC). *In vitro* differentiation towards endoderm using an EpiSC differentiation assay exhibited a cell fate switch from definitive endoderm to axial mesoderm. Moreover, activation of Wnt/β-catenin and Nodal/Tgf-β signaling pathways was drastically reduced.

In concordance with the hindgut defect *in vivo*, Oct4 CKO ES cells failed to form Cdx2+ hindgut endoderm *in vitro*. mRNA transcriptome analysis in Oct4 mutant ES cells revealed misregulation of genes involved in germ layer formation as well as Wnt and Tgf-β signaling. Additionally, chromatin IP (ChIP) analysis showed that regulatory regions of several misregulated genes were bound by Oct4 in pluripotent and endodermal wild type cells.

Upon Oct4 deletion the active enhancer mark H3K27ac was reduced in these regions which indicates a role of Oct4 in epigenetic gene activation.

Conclusively, Oct4 is required for posterior endoderm development, mesendoderm lineage decisions and proper node formation. Oct4 mediates this function by activation of Wnt/β-catenin and Tgf-β signaling pathways.

2 Zusammenfassung

Oct4, zusammen mit Nanog und Sox2, spielt eine wesentliche Rolle bei der Erhaltung des pluripotenten Charakters von Stammzellen. Desweitern wurde gezeigt, dass Oct4 über die Pluripotenz hinaus auch in der frühen embryonalen Entwicklung eine wichtige Rolle spielt. Aus diesem Grund interessieren wir uns für die Funktion von Oct4 bei der Bildung des Mesentoderms und Entoderms während der Mausentwicklung. Da der vollständige Knock-out von Oct4 noch vor der Einnistung letal ist, entwickelten wir ein System zur konditionellen Inaktivierung von Oct4 (CKO) in Foxa2 exprimierenden Zellen und deren Tochterzellen.

Unsere Analysen zeigen, dass die Bildung des posterioren Entoderms in Oct4 CKO Embryonen stark beeinträchtigt ist. Des Weiteren ist die Ausbildung der Links-rechts Achse gestört, was zu Heterotaxie und Links-Isomerismus der Lunge führt Dies wird durch Fehler der Primitivknoten- und Zilienbildung verursacht. Die Untersuchung der mRNA Expression in mutanten Embryonen zeigte zudem, eine Fehlregulierung von Genen, welche für die Musterbildung, posteriore Entwicklung, und RL Achsenbildung wichtig sind. Darüber hinaus sind Signalwege die entscheidende Rolle während der embryonalen Entwicklung spielen betroffen, wie zum Beispiel Tgf-β/Nodal und Wnt/beta-catenin.

Um die Funktion von Oct4 in der Entodermentwicklung genauer zu untersuchen, generierten wir konditionelle embryonale Stammzellen (ES) und differenzierten diese zu Entodermzellen. Die fehlerhafte Bildung dieser Zellen zeigte, dass Oct4 wichtig für die Entwicklung von definitivem Endoderm und im Besonderen posteriorem Endoderm ist. Die konditionelle Inaktivierung von Oct4 führt außerdem zu einer deutlichen Aktivitätsverringerung der Tgf-β und Wnt Signalwege, welche für diese Prozesse wichtig sind. Die Bindung von Oct4 an regulatorische Elemente deregulierten Gene deutet zudem auf einen direkten Mechanismus hin. Zudem zeigten die Oct4 regulierten Gene in den Mutanten eine Reduzierung der Histonmodifikation H3K27ac, welche aktive Enhancer charakterisiert.

Zusammenfassend ergibt sich, dass Oct4 während der frühen Entoderm Bildung eine wichtige Rolle in der Aktivierung der Wnt und Tgf-β Signalwege spielt, und somit eine

entscheidende Funktion für die Differenzierung des Entoderms, korrekte Bildung des Primitivknotens und der Rechts-links Achse spielt.

3 Introduction

3.1 Early embryonic development

Life starts with the fusion of a sperm with an oocyte followed by massive expansion of the cell population. An organism develops from a single cell via morula and blastocyst stage. At the morula stage 2 distinct cell lineages segregate, the Oct4 expressing inner cell mass (ICM) and the surrounding Cdx2 expressing trophoblast (Niwa et al. 2005a). The transcription factors (TFs) Oct4, Nanog and Sox2 form the core pluripotency network which is important for proper formation of the ICM (Avilion et al. 2003; Chambers et al. 2003; Nichols et al. 1998; Mitsui et al. 2003). The two TFs Oct4 and Cdx2 play an important role in this lineage segregation by reciprocal repression (Niwa et al. 2005a). In the trophoblast Cdx2 is required to restrict Oct4 and Nodal expression to the ICM (Ralston & Rossant 2008). The trophoblast gives rise to trophectoderm which later forms structures like the ectoplacental cone and extra embryonic ectoderm whereas the ICM gives rise to the embryo proper. At embryonic day (E) 4.5 the primitive endoderm (PrE) segregates from the ICM on the luminal side of the ICM (Figure 1A). The cells which become PrE upregulate the TFs Sox17 and Gata6 in a mosaic pattern and sort out in a precise spatio-temporal manner (Morris et al. 2010; Chazaud et al. 2006). This process is dependent on Grb2 MAP kinase and Fgf signaling pathways (Chazaud et al. 2006; Goldin & Papaioannou 2003; Morris et al. 2010). Cells of the PrE form the extra-embryonic parietal endoderm and the visceral endoderm (VE). The epithelial layer of VE surrounds the epiblast and plays an important role for embryonic patterning by secreting signaling molecules to the underlying epiblast (Perea-Gomez et al. 2001; Yamamoto et al. 2004a; Arnold & Robertson 2009).

3.2 Patterning of the embryo

Formation of the proximal - distal axis

From the blastocyst stage the embryo develops further into the egg cylinder where the first axis, namely the proximal-distal (P-D) axis, is established (Figure 1). In the egg cylinder the proximal extraembryonic ectoderm (ExE) is located juxtaposed to the distal epiblast. At E5.5,

bone morphogenic protein (BMP) signaling in the ExE induces Wnt3, which activates Nodal expression in the adjacent epiblast. Nodal expression in the epiblast activates Dickkopf homologue 1 (*Dkk1*), left-right determination factor 1 (*Lefty1*), *Hex* and *Cerberus* like protein 1 (*Cer1*) expression in the distal visceral endoderm (DVE). These factors antagonize Wnt/β-catenin and Tgf-β/Nodal signaling from the ExE and thereby form a proximal-distal signaling gradient with the highest concentrations at the proximal side of the embryo (Arnold & Robertson 2009; Perea-Gomez et al. 2002; Perea-Gomez et al. 2001) (Figure 1B).

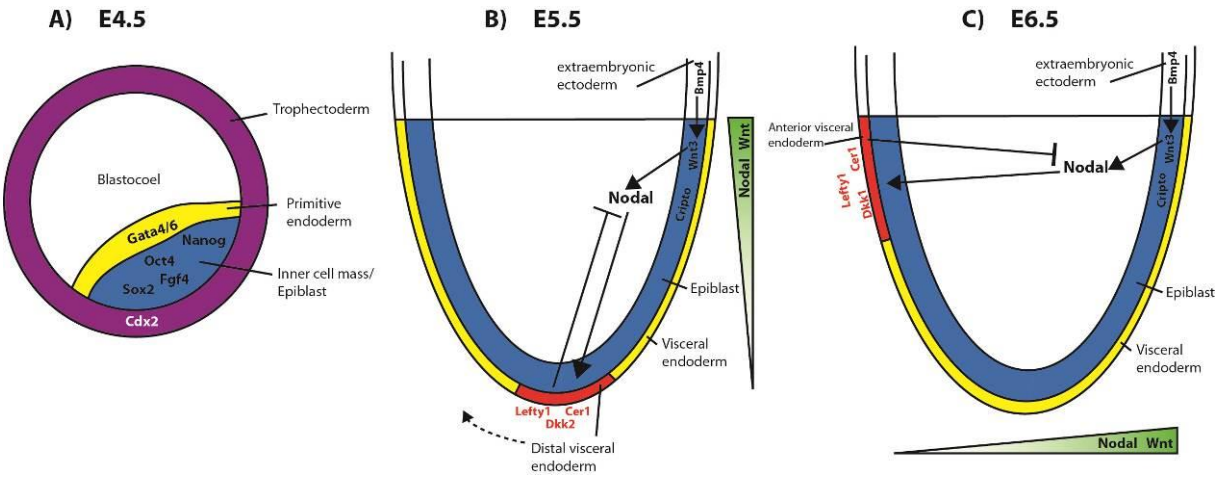

Figure 1: Early embryonic development
(A) The embryo at E4.5 consist of Trophectoderm (violet, Cdx2+), Primitive endoderm (yellow, Gata4/6+) and the inner cell mass (blue, Oct4+, Sox2+, Nanog+, Fgf4+). (B) At E5.5 distal visceral endoderm (DVE) cells are specified. (C) Visceral endoderm (VE) cell on the anterior side form the anterior visceral endoderm (AVE) and secret antagonists of Tgf-β/Nodal and Wnt/β-cat (depicted in red) to establish signaling gradients with the highest concentration on the posterior side of the embryo.
The PrE and VE are shown in yellow, TE in violet, ICM and Epiblast in blue and DVE and AVE in red.

Formation of the anterior-posterior (AP) axis

Specification of the AP axis results from the movement of the DVE to one side of the embryos which defines the anterior side. It was suggested that this movement results from active migration of the DVE cells (Srinivas et al. 2004) or from proliferating cells in a region with high nodal activity (Yamamoto et al. 2004a; Ding et al. 1998), which displaces the DVE. These anterior most cells are called anterior visceral endoderm (AVE). It has been shown that Nodal and Eomes play important roles in the formation of the AVE (Brennan et al.

2001a). AVE cells express characteristic markers like the Wnt antagonist *Dkk1* (Mukhopadhyay et al. 2001; Glinka et al. 1998), *hHex* (JP et al. 2000), *Otx2* (Ang & Rossant 1994a; Simeone et al. 1992; Simeone et al. 1993), *Hesx1* (Thomas & Beddington 1996; Hermesz et al. 1996) and *Lim1* (Barnes et al. 1994; Shawlot & Behringer 1995). The AVE produces Wnt and Tgf-β signaling antagonists like *Dkk1*, *Cer1* and *Lefty1* on the anterior side (Fig 1C). This generates an AP gradient of Wnt and Tgf-β signaling with their highest concentration on the posterior side of the embryo (Figure 1C). Blocked signaling on the anterior side allows cell to acquire a neuroectodermal fate whereas high Wnt and Nodal signaling activity on the posterior triggers the formation of the primitive streak (PS) and formation of mesoderm and endoderm (see Gastrulation and formation of endoderm)(Conlon et al. 1994).

Establishment of the left-right (LR) asymmetry

After the PD and the AP axis are determined the embryo establishes the left-right (LR) axis. Even though our body has a superficial bilateralism, the internal organs of vertebrates show a LR asymmetry as seen in the asymmetric looping of the heart and intestine as well as lung and the liver. A central structure in this process is the embryonic node, which possesses motile cilia in the so called pit cells (Nonaka et al. 1998). For the correct positioning of the cilia the planar cell polarity (PCP) pathway plays an important role (Hashimoto et al. 2010; Song et al. 2010). The clock-wise rotation of these cilia generates a leftward nodal flow on the surface of the ventral node which transports Nodal and particles containing Shh as well as retinoic acid (RA) to the left side of the embryo (Hirokawa et al. 2006; Tanaka et al. 2005; Brennan et al. 2002a) (Figure 2A). Non-motile cilia in the perinodal crown cells around the node sense the leftward flow though chemosensory and mechanosensory mechanisms to trigger left side specific signaling cascades (Hirokawa et al. 2006; Tabin & Vogan 2003). Nodal flow also increases higher levels of the Nodal antagonist Cerl2 on the right side of the node via Ca^{2+} signaling to restrict Nodal signaling to the left (Yoshiba et al. 2012; Yoshiba & Hamada 2014). The asymmetric distribution of Nodal is the key factor for breaking the symmetry of the embryo (Collignon et al. 1996; Brennan et al. 2001b; Brennan et al. 2002a). In the left lateral plate mesoderm (LPM) Nodal triggers the expression of its antagonist

Lefty2 (Yoshioka et al. 1998; Meno et al. 1999; Meno et al. 2001). Nodal antagonist Lefty1 forms a barrier in the midline and restricts Nodal expression to the left side (Meno et al. 1998). In the left LPM Nodal signaling induces the expression of Pitx2 via the co-activator Cited2, which is important for asymmetric morphogenesis of visceral organs (Campione et al. 1999; Lin et al. 1999; Yoshioka et al. 1998; Weninger et al. 2005; S. D. Bamforth et al. 2004) (Figure 2B).

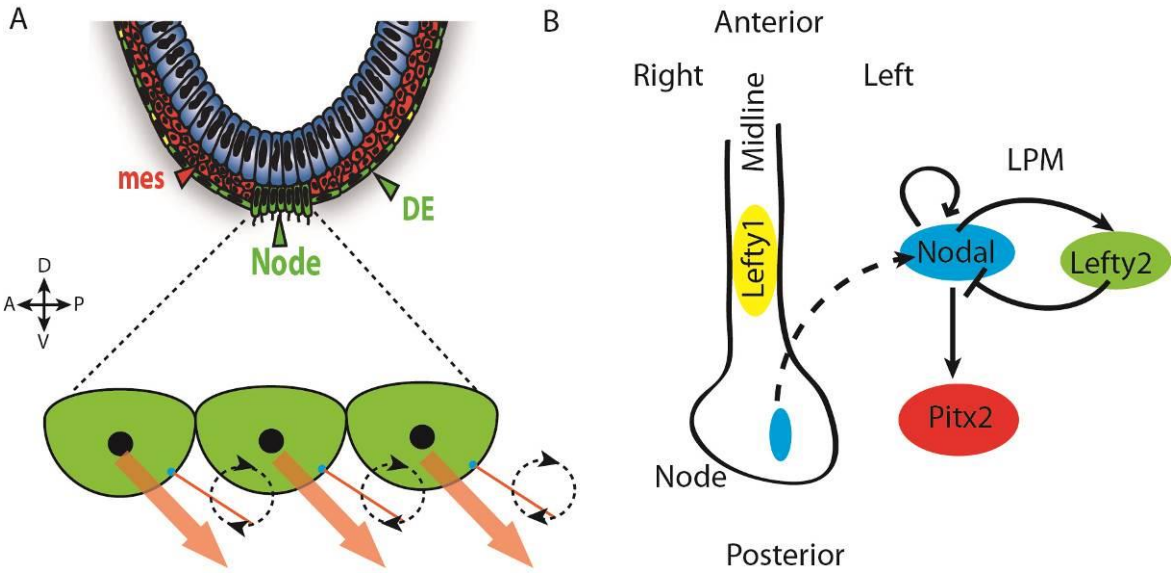

Figure 2: Establishment of the LR asymmetry
(A) Enlarged view of node pit cells. Cilia on the posterior side of the cells (red lines) rotate clock-wise to generate a leftward nodal flow. (B) Nodal signals in the left lateral plate mesoderm (LPM) induce expression of Lefty2 and Pitx2. Lefty1 is expressed in the midline (adapted from Shiratori et al. 2006).

3.3 Gastrulation and formation of endoderm

The formation of the three germ layers, ectoderm, mesoderm and endoderm starts at E6.5 and becomes visible by formation of the primitive streak (PS) (Figure 3B). Before the PS is morphologically visible, precursors of endoderm and mesoderm are already specified in the posterior epiblast (Burtscher & Lickert 2009) (Figure 3A). Expression of the forkhead transcription factor (TF) Foxa2 (Hnf3β) marks endoderm progenitors (and also the VE) whereas expression of the T-box TF Brachyury (T) marks the posterior mesodermal population. Cells which are co-expressing T and Foxa2 give rise to the axial mesoderm (node

and notochord) (Burtscher & Lickert 2009). Initiation of endoderm formation is triggered by Tgf-β/Nodal signaling whereas Wnt/β-catenin signaling is important to develop endoderm from bipotential progenitors instead of pre-cardiac mesoderm (Lickert et al. 2002).

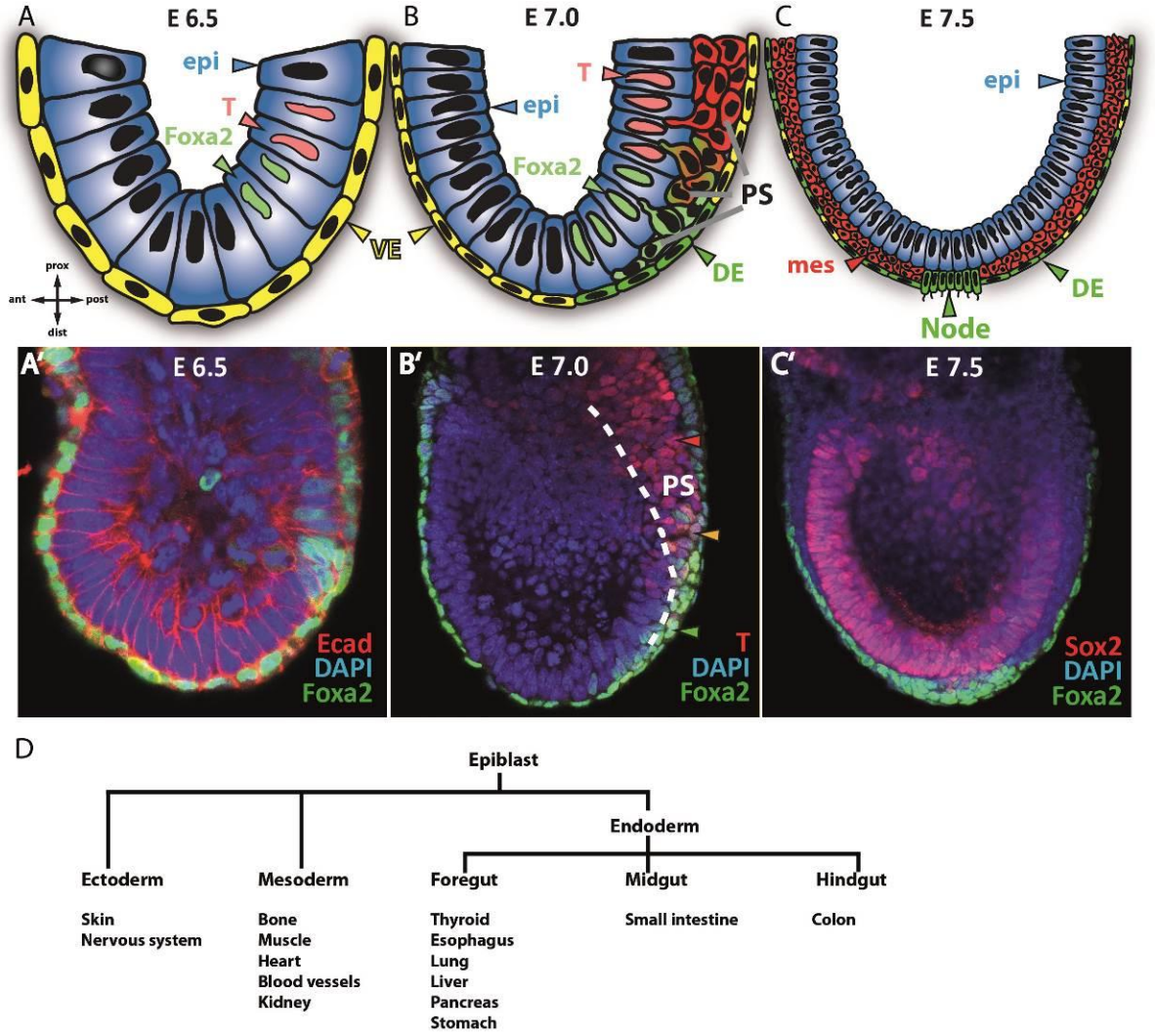

Figure 3: Formation of the three germ layers

(A) Cells in the epiblast (Epi) express Foxa2 (Foxa2+) and T (T+) before the primitive streak (PS) is formed. (B and C) During gastrulation T+ cells undergo epithelial-mesenchymal transition and intercalate between Epi and visceral endoderm (VE) to form the mesoderm (Mes). Foxa2+ cells leave the Epiblast and intercalate into the VE, forming the definitive endoderm (DE). These cell populations form the PS. (A'-C') Immuno staining of embryos at the indicated stages with mesendodermal (Foxa2, T) and anterior Epi (Sox2) markers. (D) Organs and tissues generated from the respective germ layers. Modified from Biospektrum 5/2011.

Endoderm progenitor cells from the anterior PS expressing Foxa2 lose their epithelial morphology and apical-basal polarity and leave the epiblast. At this step the cells start expressing the Sry-box TF Sox17 (Burtscher et al. 2012), intercalate into the VE layer and disperse these cells. The remaining VE cells mix with endodermal cells and are mainly incorporated into the hindgut (Kwon et al. 2008).

At E7.5 the three germ layers endoderm, mesoderm and ectoderm are specified (Figure 3C). The endodermal gut tube is formed at E8.5 after the gastrulation is completed. The endoderm at this stage is already patterned along the anterior and posterior axis, marked by expression of *Hhex, Sox2, Foxa2 or Cdx1, Cdx2, Cdx4* respectively (Zorn & Wells 2009).

In this context it has been demonstrated that growth factors like Fgf4 and Fgf8 pattern the endoderm in a concentration dependent manner (Boulet & Capecchi 2012; Wells & Melton 2000; Gregorieff et al. 2004). Also signals from the canonical Wnt pathway are involved in posterior development (Leyns et al. 1997; Lickert et al. 2000; Pilon et al. 2006). As development progresses the foregut will give rise to thyroid, esophagus, trachea, lung, liver, biliary tree, stomach and pancreas; whereas the midgut forms the small intestine and the hindgut forms the colon (Zorn & Wells 2009)(Figure 3D).

3.4 **Mouse embryonic stem cells**

To study aspects of embryonic development *in vitro,* a culture system was established more than three decades ago that allows culture of embryonic cells in a pluripotent state outside the embryo. These so called pluripotent embryonic stem cells (ESC) were first derived and cultured from mouse ICM in 1981 (Evans JM; Kaufman MH 1981) and later also from human blastocysts (Thomson et al. 1998). For maintenance of the pluripotent state in mouse ESCs signaling of the leukemia inhibitory factor (LIF), Wnt and Tgf-β/Bmp4 pathways are required (ten Berge et al. 2011; Williams et al. 1988; Qi et al. 2004), which are produced from embryonic fibroblast feeder cells or contained in fetal bovine serum which is added to the culture medium.

ES cells bare a great potential because of their pluripotent state. They can self-renew, be expanded for extensive periods in an undifferentiated state and have the ability to differentiate into all cell types and tissues of the body (Keller 2005). In 1984 mouse ESCs were genetically modified and opened the possibility to generate genetic mouse models (Soriano et al. 1986; Bradley et al. 1984). Because they can be differentiated into all cell lineages *in vitro* ESCs also have a great potential for cell replacement therapy in human diseases in the future.

3.5 **Naïve ESCs**

ESCs can also be cultured in a so called naïve or ground state by inhibition of differentiation inducing factors like Fgf4 and mitogen-activated protein (MAP) kinase signaling and activation of the Wnt signaling pathway for exended self-renewal. By using two chemical inhibitors for Fgf receptor kinase MEK and Gsk3β (2i conditions) ESCs become independent from extrinsic stimuli and differentiation-inducing signaling is blocked (Ying et al. 2008a; Wray et al. 2011; Nichols & Smith 2009). In this ground state ES cells resemble cells of the ICM before implantation of the embryo, express naive markers like Rex1 and Fgf4 and have two active X-Chromosomes in female cells (Nichols & Smith 2009).

3.6 **Primed/Epi Stem Cell**

After implantation of the blastocyst into the uterus the epiblast develops into a cup shaped structure and one of the X Chromosomes in female embryos undergoes random inactivation (Heard 2004). These epiblast stem cells (EpiSC) can be isolated and cultured *in vitro* using culture conditions containing basic fibroblast growth factor (bFgf) and ActivinA (Brons et al. 2007; Tesar et al. 2007). These cells still express the core pluripotency factors Oct4, Sox and Nanog, possess one inactive X chromosome in female cells and can be propagated and differentiated *in vitro*. EpiSCs cannot contribute to blastocyst chimeras but can be reverted back into a naïve state by induced expression of the TF Klf4 under 2i conditions (Guo et al. 2009). ESCs can also be differentiated into EpiSCs *in vitro* by culturing them in serum free medium with the addition of Activin and bFgf (Guo et al. 2009). Mouse EpiSCs are closer

related to human ESCs than mouse ESCs and also require bFgf and Activin signaling for their propagation and show a similar flattened morphology (Brons et al. 2007; Tesar et al. 2007). Differentiation of ESCs to DE vie EpiSCs closer resembles the processes in embryos where the ICM first forms the epiblast before differentiating into the endoderm layer.

3.7 **In vitro differentiation of ES cells into endoderm**

For extended analysis pluripotent ESCs can be differentiated *in vitro* into cells of all germlayers (Keller 1995). To differentiate ESCs into endoderm *in vitro* Wnt and Activin A (a Tgfβ/Nodal pathway agonist) are used to activate the respective pathways and trigger the expression of Foxa2 and T (Gadue et al. 2005; Gadue et al. 2006a). During differentiation ESCs down-regulate Oct4 and other factors of the pluripotency network and up-regulate Foxa2 and T in mesendoderm cells which then differentiate further into $Foxa2^{+}$,$Sox17^{+}$ definitive endoderm cells (Kanai-Azuma et al. 2002; Hudson et al. 1997; D'Amour et al. 2005). By addition of high levels of Wnt3a and Fgf4 endodermal cells can also be further differentiated into posterior hindgut or intestinal cells (Sherwood et al. 2011; Jason R. Spence et al. 2010a; Wells & Melton 2000).

3.8 **Wnt/β-catenin signaling pathway**

A major signaling pathway during embryonic development is the canonical Wnt/β-catenin pathway. Secreted Wnt protein is palmitoylated by the membrane bound O-acyltransferase porcupine (Porc) to generate the active protein (Kadowaki et al. 1996). Wnt then binds to frizzled receptors, which are seven-transmembrane proteins and cooperate with the single transmembrane molecules LRP-5 and -6 which function as co-receptors (Pinson et al. 2000)

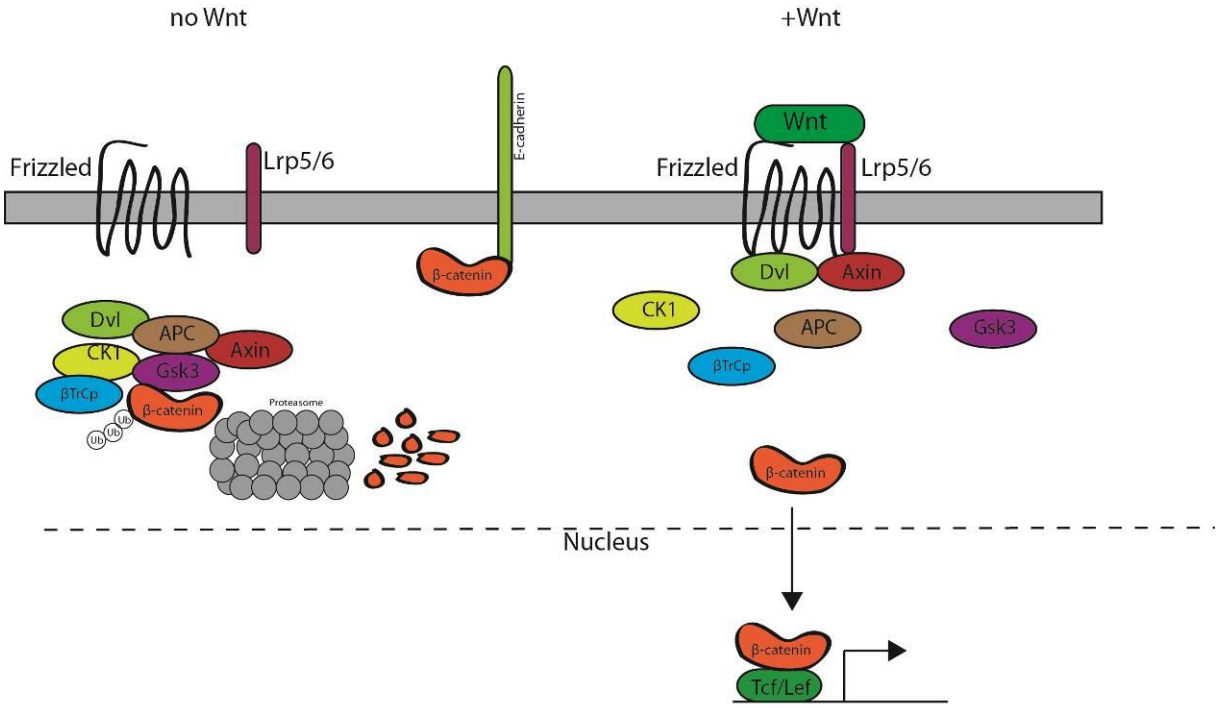

Figure 4: Wnt/β-catenin signaling pathway
Without the Wnt ligand β-catenin is marked by the destruction complex for proteasomal degradation. Upon binding of Wnt to the Frizzled receptor the destruction complex is destabilized and β-catenin can translocate to the nucleus, interact with Tcf/Lef and activate transcription of target genes. B-catenin is also found at adherens junctions bound to E-cadherin.

(Figure 4). When Wnt is bound to the receptor, Dishevelled blocks the degradation of β-catenin. The stabilized β-catenin accumulates and translocates to the nucleus where it activates its target genes together with T-cell-factor (Tcf) and Lymphoid enhancer factor (Lef) (Schneider et al. 1996). In the absence of Wnt signaling β-catenin is phosphorylated by CK1 and GSK3α/β in a complex with Axin and APC proteins, ubiquitinylated and targeted for destruction by the proteasome (Clevers 2006; Reya & Clevers 2005).

The Wnt pathway can be regulated by secreted inhibitors on several levels. Cerberus (Cer) and secreted Frizzled like proteins (sFRPs) can directly bind to Wnt to inhibit receptor binding while Dickkopf (Dkk) proteins bind the co-receptor LRP5/6 to inhibit pathway activation (Glinka et al. 1998; Rattner et al. 1997; Bafico et al. 2001; Piccolo et al. 1999). The canonical Wnt pathway plays important roles in early embryonic development and mesendoderm differentiation in the mouse (Arnold et al. 2000; Dunty et al. 2008; Lickert et al. 2000, Yamaguchi et al. 1999). The signaling ligand Wnt3a has been shown to be required

for formation of the primary axis in the mouse and formation of the PS by directing movement of the VE (Liu et al. 1999; Kimura-Yoshida et al. 2005). It has been shown that conditional deletion of β-catenin changes cell fate from endoderm to pre-cardiac mesoderm and results in formation of multiple hearts (Lickert et al. 2002).

3.9 **Tgf-β/Nodal signaling**

The Tgf-β signaling pathway is involved in various aspects of embryonic development and plays an important role in the maintenance of pluripotency and differentiation of ESCs (Gadue et al. 2006a; K. Zhang et al. 2010; Qi et al. 2004). The ligands of this pathway are members of the Tgf-β superfamily and bind to type I and type II receptors.

One major component in this signaling pathway is bone morphogenetic protein 4 (Bmp4). Upon binding, the receptors phosphorylate the downstream effectors Smad 1/5/8 which then bind to Smad4 and activate target genes. Activated type IA receptor can also inactivate p38 and Erk MAP kinases to support self-renewal of ESCs (Qi et al. 2004). BMP signaling can be antagonized by Noggin and Chordin, which play important roles in patterning the embryo (Yoshiki Sasai et al. 1994).

Likewise ligands like Nodal or Activin bind to type I (Alk4) and type II (ActRIIA and ActRIIB) receptors and the EGF-CFC co-receptor (Cripto, Cryptic) (Figure 5). Receptor activation leads to phosphorylation of Smad 2/3. These associate with Smad4 and together with the TFs FoxH1 or Mixer activate downstream target genes like Foxa2, Lefty2 and Pitx2 (Norris et al. 2002). In this pathway the EGF-CFC co-receptors Cripto and Cryptic are involved through their interaction with Alk4 (Shen 2007). Extracellular inhibitors Lefty 1 and Lefty 2 block the formation of receptor complexes through their interaction with EGF-CFC proteins to modulate signaling activity (Cheng et al. 2004; Chen & Shen 2004). Also members of the Cerberus protein family can block nodal signaling by their direct interaction with the nodal ligands (Piccolo et al. 1999).

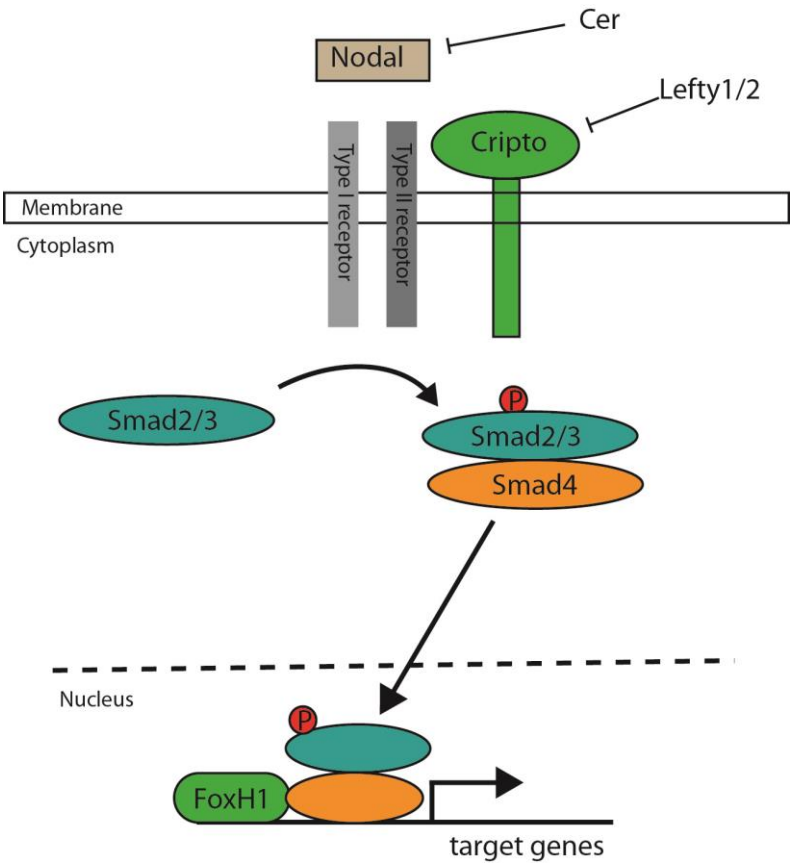

Figure 5: Tgf-β nodal signaling pathway
Nodal binds to type I and II receptors which leads to phosphorylation of smad2/3 proteins. Activated smad2/3 associate with smad4, translocates to the nucleus and activates targets genes. Cerberus and Lefty are soluble antagonists which can interact with Nodal; Lefty can also interact with the co-receptors to inhibit their function.

3.10 The pluripotency TF Oct4

Structure and expression of Oct4

The TF Oct4 (Oct3, Pou5f1) belongs to class V octamer-binding POU TFs. The Oct4 protein consist of an N-terminal POU specific domain and a C-terminal POU homeodomain. These two domains can bind DNA through their helix-turn-helix structure and are connected by a variable linker.

Oct4 is expressed in the oocyte, the ICM, the epiblast, PS, mesoderm and notochord during embryonic development. When the epiblast differentiates into the three germ layers Oct4 expression is down regulated and from the 8-somite stage restricted to primordial germ cells (PGC) (Rosner et al. 1990; Schöler et al. 1990; Downs 2008; Palmieri et al. 1994). The distal regulatory element of the Oct4 promoter drives expression in the pre-implantation embryo whereas the proximal element directs the epiblast specific expression (Downs 2008; Yeom et al. 1996). Interestingly the expression of Oct4 protein diminishes in an anterior to posterior

manner and the Oct4 gene becomes silenced through Dnmt3a/b and G9a mediated epigenetic mechanisms (Feldman et al. 2006; Athanasiadou et al. 2010).

Function in pluripotency

Knock-out of Oct4 in mice results in loss of pluripotency of ICM cells and their differentiation into the trophoblast lineage (Nichols et al. 1998). No ES cells can be generated from an Oct4 deficient embryo and development arrests at E3.5. Oct4 is a major component of the core pluripotency network acting together with Nanog and Sox2 and through auto-regulatory loops maintains their expression. (Zhang et al. 2007; Ambrosetti et al. 1997). These TFs maintain ESCs in a pluripotent state by activating other important pluripotency associated genes while repressing lineage specific TFs (Chambers & Tomlinson 2009; Young 2011; Silva & Smith 2008; Chambers 2004). These three factors also bind and repress genes encoding cell lineage specific regulators and thereby preventing ESCs from the exit of pluripotency (Loh et al. 2006; Marson et al. 2008a). Oct4, Sox2 and Nanog co-occupy many of their targets together with Smad1 and Stat3 which links the core pluripotency network to BMP and LIF signaling (Chen et al. 2008). Oct4also possesses a repressive function through its interaction with the NuRD complex, the SWI/SNF complex, histone deacetylases (HDACs) and other chromatin modifying complexes, which link the pluripotency network to epigenetic mechanisms for silencing developmental genes (Wang et al. 2006; Ding et al. 2012; Liang et al. 2008; Pardo et al. 2010; van den Berg et al. 2010). Most of these complexes are transcriptional repressors suggesting that Oct4 is mostly involved in repression of lineage specific genes to maintain ESCs in an undifferentiated state.

During the early events of embryonic development and lineage segregation Oct4 regulates the separation of TE and ICM through negative regulation of Cdx2 (Niwa et al. 2005a). It has been demonstrated that Oct4 recruits the histone H3K9 methyltransferase ESET (Setdb1) to repress TE specific genes, like Cdx2 in the ICM (Yuan et al. 2009a). Also in the next lineage decision where primitive endoderm (PE) cells segregate from the ICM it was shown that Oct4 and Sox2 important by directly activating Fgf4 (Yuan et al. 1995).

Oct4 does not act in a simple on/off fashion but carries out its function in a dose dependent manner. A decrease of Oct4 levels in ESCs results in loss of pluripotency and differentiation towards TE Upon increase of Oct4 levels the cells differentiate into a mesoderm and PrE-like state (Niwa et al. 2000). On the other hand it was recently shown that reduced levels of Oct4 result in a stabilized pluripotent state and sustained levels do not interfere with early development (Karwacki-Neisius et al. 2013). Later in development Oct4 is dispensable for renewal of somatic stem cells but it is still required for survival of germ cells (Kehler et al. 2004; Lengner et al. 2007).

Oct4 and differentiation

Despite its function in the maintenance of pluripotency it has been demonstrated in various species *in vivo* and in ESCs *in vitro* that Oct4 also plays a role during early differentiation into endoderm and lineage commitment (Burgess et al. 2002; Zeineddine et al. 2006; Deveale et al. 2013; Lunde et al. 2004; Radzisheuskaya et al. 2013; Reim et al. 2004; Thomson et al. 2011; Morrison & Brickman 2006). During the early phases of differentiation of ESCs from naive to primed pluripotency Oct4 activates Otx2 and together activate enhancers of epiblast genes (Yang et al. 2014; Buecker et al. 2014).

It was reported that Oct4 binds to the Meis1 promoter during neural differentiation, Mesp1 during embryoid body (EB) differentiation and to the *Brachyury* promoter during mesendodermal differentiation to activate lineage specific programs (Yamada et al. 2013; Li et al. 2013a; Thomson et al. 2011). This also supports the concept that Oct4 regulates developmental genes during differentiation.

A major advance in stem cell technology was the reprogramming of somatic cells into a stem cell like state, so called induced pluripotent stem cells (iPSC), by the four Yamanaka TFs Oct4, Sox2, Klf4 and c-Myc (Masui et al. 2007; Okita et al. 2007). Here it has been shown that Oct4 can only be replaced by the orphan nuclear receptor Nr5a2 which points out the major role Oct4 plays in pluripotency (Heng et al. 2010).

Oct4 function was also linked to Wnt and other signaling pathways in ESCs. Oct4 represses Wnt/β-catenin signaling during self-renewal and is bound in a complex with E-Cadherin associated with cell membranes (Faunes et al. 2013; Davidson et al. 2012). It has also been

demonstrated that Oct4 interacts with nuclear β-catenin, which results in its degradation (Abu-Remaileh et al. 2010). Through interactions with other proteins Oct4 is involved in the regulation of Tgf-β, Notch and Wnt signaling pathways (van den Berg et al. 2010).

Taken together, these data indicate that Oct4 is involved in modulating Wnt and Tgf-β signaling and can regulate some early steps during development and cell differentiation. Nevertheless it is still unknown in what process of endodermal development Oct4 function is required.

3.11 **The endoderm TF Foxa2**

The forkhead transcription factor Foxa2 (Hepatocyte nuclear factor 3β/Hnf3β) belongs to the family of TFs which contain a forkhead domain as DNA binding motif (Weigel & Jäckle 1990; Lai et al. 1990; Ang et al. 1993; Sasaki & Hogan 1993).

In the embryo Foxa2 is expressed in VE, DE and also in organizer tissues like the node and its derivatives. It is also expressed in the floor plate of the neural tube. Later in development Foxa2 is still expressed in epithelia of endodermal organs like pancreas, lung, liver, intestine and others. Foxa2 is essential for formation of foregut endoderm, the node and notochord and complete knock-out results in embryonic lethality at E8.5 (Ang & Rossant 1994a; Weinstein et al. 1994). Its expression in the AVE is also important for AP axis generation by activating Wnt antagonists Dkk1 and Cerl (Kimura-Yoshida et al. 2007). Surprisingly it is not required for mid and hindgut endoderm formation. This can be explained by other Fox TFs that might compensate for the loss (McKnight et al. 2010). Before the start of gastrulation Foxa2 is already expressed in epiblast cells which are primed to become endoderm in the anterior region of the PS (Burtscher & Lickert 2009; Ang et al. 1993). Loss of Foxa2 results in endodermal cells unable to intercalate into the outside epithelium and fail to establish proper cellular junctions (Burtscher & Lickert 2009).

Additionally, Foxa2 was also shown to be involved in floorplate development and patterning of the neural tube (Sasaki & Hogan 1994; Filosa et al. 1997). In later embryonic development

it plays a role in lung, liver and pancreas maturation and function (Chung et al. 2013; Lee et al. 2005; Wolfrum et al. 2004; Wan et al. 2004; Gao et al. 2008; Lee et al. 2002).

Foxa2 acts as a pioneer factor in development by opening up compacted chromatin in conjunction with chromatin remodeling complexes and thereby making it accessible for other TFs (Cirillo et al. 2002; Li et al. 2012; McPherson et al. 1993). This function could explain the fact that Foxa2 plays an important role in various different tissues during and after gastrulation.

3.12 **The endoderm TF Sox17**

Sox17 belongs to the family of Sry-related HMG box genes which consists of 20 members and was originally identified in mouse testis (Kanai et al. 1996; Francois et al. 2010). It has been shown to play an important role in development and formation and differentiation of gut endoderm (Kanai-Azuma et al. 2002), cardiac mesoderm (Liu et al. 2007; Sakamoto et al. 2007) and for lineage segregation in the ventral foregut (Jason R Spence et al. 2010). Sox17 has also been implicated in LR-asymmetry determination (Aamar & Dawid 2010) and in differentiation of respiratory cells (Park et al. 2006).

Sox17 is expressed in definitive endoderm but also in VE (Kanai-Azuma et al. 2002; Burtscher et al. 2012) and it has been shown to be regulated by Wnt/β-cat signaling in the specification of embryonic organizer tissues and endoderm (Engert et al. 2013b; Sinner et al. 2004).

3.13 **Epigenetic gene regulation**

All cells in an organism, except germ cells and immune cells, have the same DNA content which means that in the progression from pluripotent to lineage restricted somatic cells genes which are not needed have to be inactivated. On the other hand genes or groups of genes which are necessary for lineage specification and development have to be activated in a precise spatio-temporal manner. These processes are regulated by signaling pathways and TF networks as described before. Another level of regulation comes from epigenetic mechanisms, like histone modifications and DNA methylation. Epigenetic regulators can

reorganize the chromatin structure to allow or prevent binding of TFs to DNA and activate target genes or permanently repress genes (Smith & Meissner 2013; Chen & Dent 2013; Atkinson & Armstrong 2008).

DNA methylation

A major mechanism for gene silencing is methylation of cytosine at the 5' position (5mC) at CpG dinucleotides which can be found throughout the genome. Unmethylated CpG domains are enriched in 5' regions of genes, promoters and CpG islands. Promoters of imprinted genes or genes located on the inactive X-chromosome are also often methylated. On the other hand it was demonstrated that active genes show methylation within gene bodies (Suzuki & Bird 2008). De novo methylation is carried out by the DNA methyltransferases Dnmt3a and b whereas Dnmt1 is mostly responsible for maintenance of methylation marks in proliferating cells (Goll & Bestor 2002). Dnmt3L has no catalytic activity but is required for de novo methylation through cooperation with the Dnmt3 methyl transferases (Hata et al. 2002). During differentiation methylation marks on CpGs are dynamic and undergo extensive changes. It was also shown that DNA methylation patterns during differentiation of ESCs are well correlated with histone methylation patterns (Meissner et al. 2008).

DNA hydroxymethylation

DNA hydroxymethylation at cytosine 5 (5hmC) is generated from 5mC by TET family enzymes and is mostly associated with euchromatin. This mark is linked to increasing transcription levels and plays a role in activating several pluripotency related genes (Ficz et al. 2011; Ito, D/'Alessio, et al. 2010). In ESCs 5hmC is mostly found at transcriptional start sites (TSS) and within gene bodies (Ficz et al. 2011). Aberrant 5hmC plays a role in several forms of leukemia and in some has prognostic value (Cimmino et al. 2011).

Histone modifications

Modifications of core histone tails like methylation, phosphorylation, acetylation and ubiquitination regulate the activity of genes and also the structure of the genome. Histone modifications together with DNA methylation can grossly speaking divide the genome into silent heterochromatin and active euchromatin. Silent heterochromatin is in general characterized by low levels of acetylation and high levels of methylated histone H3 lysine 9

(H3K9) and H3K27. These sites can then recruit specific binding proteins which can further modify chromatin. Euchromatin on the other hand has high levels of acetylation and trimethylated H3K4 and H3K36 (Kouzarides 2007).

Pluripotent ESCs are characterized by elevated global transcription and their genome undergoes large scale epigenetic silencing upon differentiation (Efroni et al. 2008). This in part results from so called bivalent domains which are characterized by histones with the active H3K3me3 and the inactive H3K27me3 mark at the same time (Bernstein et al. 2006). These domains are found at subsets of developmental genes and keep them in a silent but poised state from which they can be activated during differentiation.

In promoters acetylated lysine 27 at histone H3 (H3K27ac) plays a special role. This mark can distinguish active from inactive or poised enhancers, which contain H3K4me1 alone (Creyghton et al. 2010a). In combination with the TFs Oct4 and Otx2 the pattern of this active enhancer mark is reorganized in the transition from naïve to primed pluripotency and plays an important role for the activation of epiblast genes like Fgf5 (Buecker et al. 2014). Also H3K56ac has been shown to play a role in pluripotency in ESCs. This chromatin mark interacts with the core pluripotency TF Oct4 and is important for the maintenance of pluripotency (Tan et al. 2013). These recent publications indicate that Oct4 is involved in epigenetic regulation of several target genes; still it is unclear if this function extends to early events of germ layer formation.

3.14 **Aims of the study**

Pluripotent cells are characterized by their ability to self-renew and differentiate into all cell types of the body. During embryogenesis, epiblast cells exit their pluripotent state in order to differentiate into more specialized cell types, which become more and more restricted in their differentiation potential. Oct4 is a major transcription factor required for maintenance of the pluripotent state (Nichols et al. 1998). However, recent reports in frog and fish demonstrated that Oct4 is also required during lineage differentiation and endoderm formation (Thomson et al. 2011; Reim et al. 2004; Morrison & Brickman 2006; Deveale et al.

2013; Zeineddine et al. 2006). This suggests that Oct4 does not only maintain pluripotency but is also involved in endoderm formation during development.

In mouse, complete knock-out of Oct4 is embryonic lethal before implantation whereas deletion of Oct4 in somatic stem cells does not have any visible effects (Nichols et al. 1998; Lengner et al. 2007). To unravel potential roles of Oct 4 in endoderm formation in the mouse we conditionally deleted Oct4 in Foxa2 lineage cells. The conditional knock-out (CKO) allows us to specifically study the function of Oct4 in Foxa2 expressing endoderm and axial mesoderm progenitors and their progeny, namely definitive endoderm, node and notochord. Using the R26R lineage reporter allele we can follow the fate of the Oct4 depleted cells and visualize resulting defects during embryonic development. Furthermore, we use a fluorescent live reporter of Foxa2 expression to isolate differentiated Oct4 CKO ES cells in. This purified cell population allows us to specifically analyze changes in signaling pathways and gene expression upon Oct4 deletion

4 Results

4.1 Conditional knock out of Oct4 in in Foxa2 expressing mesendoderm and endoderm

Oct4 is a major transcription factor, working in a network together with Sox2 and Nanog to maintain mouse embryonic stem cells (mESC) in a pluripotent state (Lengner et al. 2008; Loh et al. 2006). Since Oct4 has been shown to play a role in endoderm formation of Xenopus and Zebrafish (Morrison & Brickman 2006; Reim et al. 2004) we hypothesized that Oct4 has an evolutionary conserved function also in mouse endoderm formation. To specifically address Oct4 function in endoderm we conditionally deleted the Oct4 gene in Foxa2 expressing mesendoderm progenitors and their respective lineage. The Foxa2 lineage comprises the definitive endoderm, gut tube, axial mesoderm, node, notochord, floorplate of the neural tube and the epithelium of all endodermal organs (Horn et al. 2012). We used the Foxa2^{2AiCre} mouse line where a codon-improved Cre recombinase (iCre) is fused to the coding region of Foxa2 via T2A (Horn et al. 2012). The T2A sequence leads to ribosomal skipping which results in the production of two proteins at equimolar amounts (Figure 6A). Additionally, we made use of a conditional mouse model in which the essential promoter and the 1st exon of Oct4 are flanked by 2 loxP sites (Oct4 ^{flox}) (Figure 6B) (Kehler et al. 2004). To generate Oct4 conditional knock out (CKO) and control embryos, a male mouse homozygous for Foxa2 ^{2AiCre} and with one Oct4^{flox} allele recombined in all cells by a ubiquitous R26 Cre (Oct4 flox deleted; Oct4^{FD}) was mated with a Oct4$^{flox/flox}$ homozygous female. For live or lineage analysis female mice also had either two Foxa2-Venus fusion (FVF) (Burtscher et al. 2013) or Rosa26 lac-Z reporter (R26R; (Soriano 1999)) alleles respectively (Figure 6C). In the R26R allele a LacZ lineage reporter is integrated into the Rosa 26 locus to ensure uniform and ubiquitous expression upon Cre mediated recombination. By Foxa2^{2AiCre} mediated recombination all descendants of Foxa2 expressing cells can be visualized by X-Gal staining.

Matings resulted either Foxa2$^{2AiCre/+}$; Oct4$^{FD/flox}$ (Oct4 CKO) or Foxa2$^{2AiCre/+}$; Oct4$^{wt/flox}$ (control) embryos at an expected mendelian ratio of 1:1 (Figure 6C). Embryos were identified by genomic PCR genotyping for the Oct4 flox allele (see material and methods) (Figure 6D).

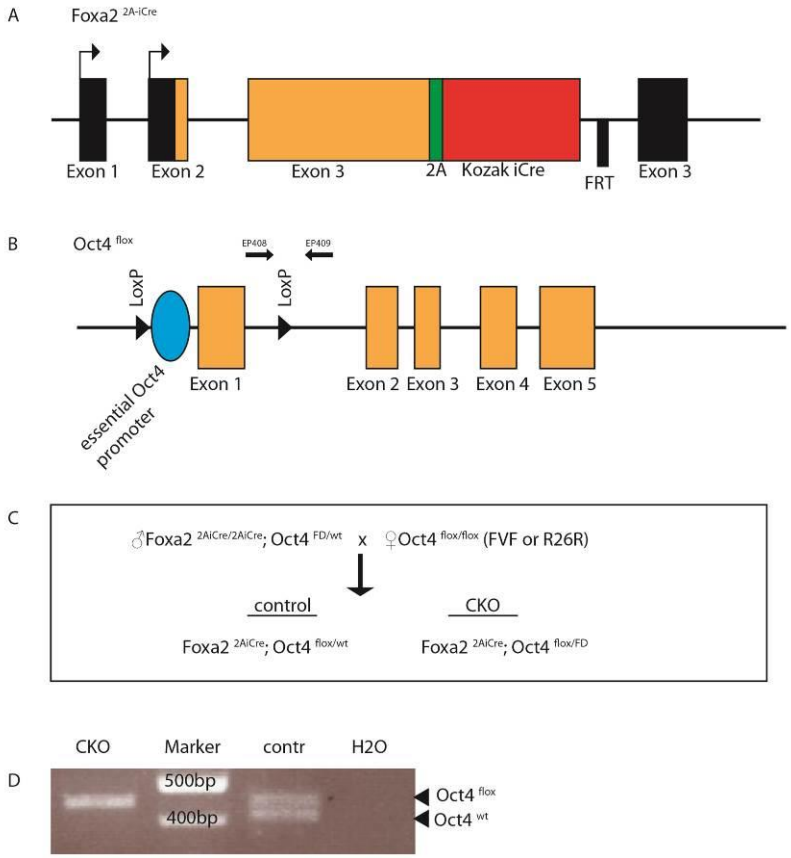

Figure 6: Generation and genotyping of Oct4 CKO embryos
(A) Schematic illustration of the Foxa2 ^{2AiCre} allele, Foxa2 exons are depicted as black boxes and the ORF as orange boxes. The T2A sequence and the iCre recombinase are inserted after exon 3 (for details see (Horn et al. 2012). (B) Schematic illustration of the Oct4 ^{flox} allele, the 200bp Oct4 essential promoter (blue oval) and the first exon are flanked by LoxP sites and can be excised upon Cre recombination (for details see (Kehler et al. 2004)). (C) Mouse mating scheme to generate Oct4 CKO and control embryos. Males are homozygous for Foxa2 2AiCre and have an Oct4 $^{FD/wt}$ (FD=flox deleted) allele. Females are homozygous for Oct4 ^{flox} and have either a homozygous Foxa2 Venus fusion (FVF) or Rosa 26 reporter (R26R) allele. By mating these mice Oct4 control (Foxa2 ^{2AiCre};Oct4 $^{flox/wt}$) and CKO (Foxa2 ^{2AiCre};Oct4 $^{flox/FD}$) mice are generated. (D) Genotyping of embryos with primers EP408 and 409 (see (B)). Control embryos generate a 415bp wt and a 449bp Oct4 ^{flox} band whereas CKO embryos generate a 449bp Oct4 ^{flox} band.

Oct4 is known to be expressed in the inner cell mass (ICM) of the blastocyst and also later in the epiblast, which gives rise to the embryo proper. Foxa2 expression can be detected in pre-streak embryos in the posterior epiblast at low levels and is further expressed in the PS, node and notochord and the DE (Burtscher & Lickert 2009). In these cells Foxa2 and Oct4 are co-expressed and Oct4 is deleted in CKO embryos. Oct4 expression can be detected in few cells in the DE at comparable levels to the epiblast after gastrulation at E7.5 (Figure 7A – D'

white arrow heads). In CKO embryos deletion of Oct4 protein was observed in Foxa2 expressing cells in the posterior epiblast before these cells ingress into the PS (Figure 7E-G'). Compared to the control, reduction in Oct4 levels is shifted earlier in CKO embryos through Cre mediated recombination. The absence of Oct4 protein in Foxa2 expressing epiblast cells also shows that the Oct4 protein is absent within a few hours after genomic recombination Cells which turn on Foxa2 in

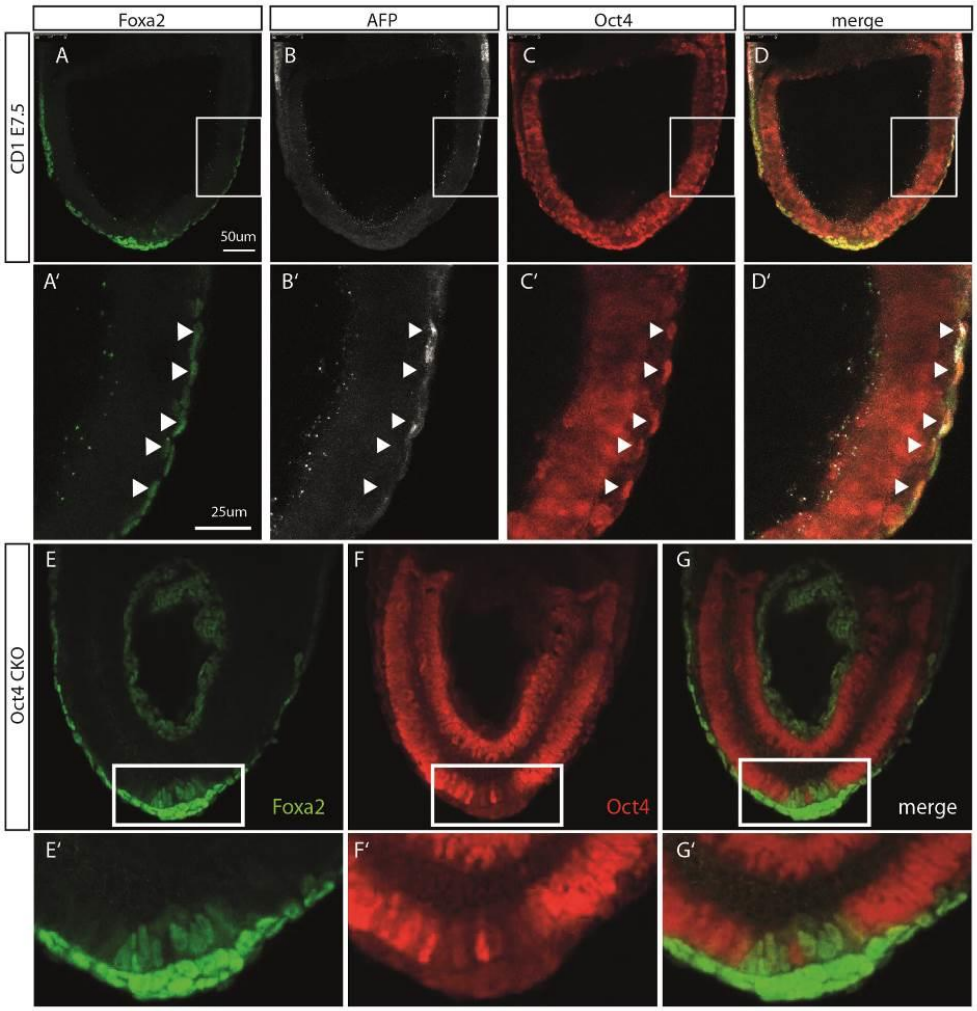

Figure 7: Localization of Oct4 in DE and deletion of Oct4 in CKO embryos
(A-D') Localization of Oct4 in DE in E7.5 wt CD1 embryos by immuno fluorescent staining. E7.5 Embryos were stained with antibodies against Foxa2 (green), Oct4 (red) and AFP (white). Oct4 protein is localized in the epiblast and in several cells in the DE layer overlapping with Foxa2 staining; white box in A – D is shown enlarged in A'-D', arrowhead shows Foxa2 – Oct4 double positive cell. (B) Antibody staining of Oct4 CKO embryos against GFP (FVF) and Oct4 shows specific deletion of the Oct4 protein in Foxa2 expressing epiblast cells (enlarged in E' - G'). Scale bars are 50µm for images in A - D and 25µm for enlarged images in A' - D'.

the epiblast lose their epithelial morphology and intercalate into the primitive streak within 2-3 hours and form the definitive endoderm (Burtscher et al. 2013). These results demonstrate that Oct4 protein is depleted in Foxa2 positive cells in the epiblast and all daughter cells.

4.2 CKO embryos die embryonically or shortly after birth

All Oct4 KO embryos die at E3.5 (Nichols et al. 1998). To analyze effects of Oct4 conditional deletion on lethality mendelian ratios of recovered embryos and pups between E7.5 and after birth (postanatal day,3 P3) were calculated.

The expected proportion of Oct4 CKO embryos using the mating strategy indicated above is 50% (Figure 6C). This ratio can be observed until E12.5, whereas from E13.5 the ratio is decreasing and after postanatal day 3 (P>3) no mutant animals were recovered (Figure 8). Oct4 CKO mice were often born dead or died neonatally within the first three days. Between E7.5 and E12.5 resorbed embryos were recovered which could not be genotyped.

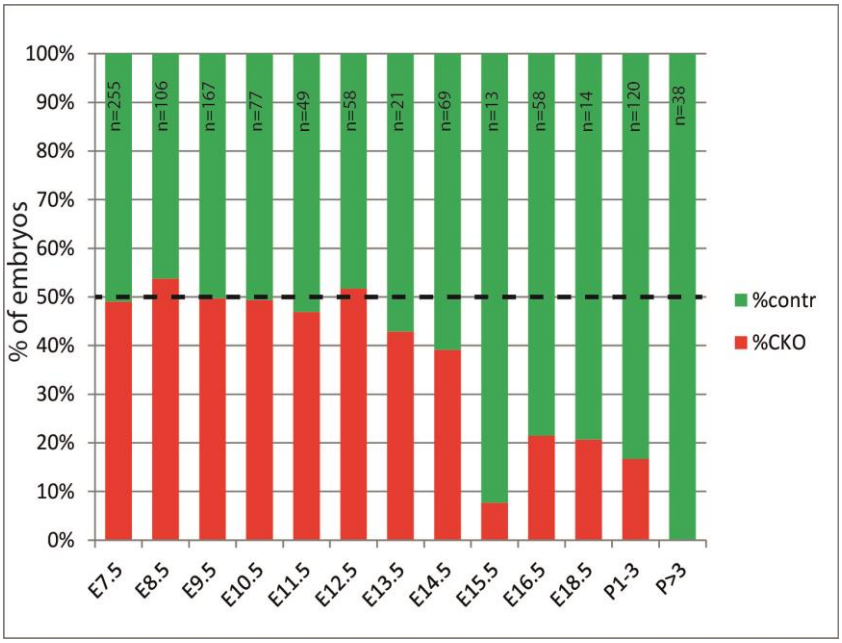

Figure 8: Mendelian ratios
Plugs were dissected at the indicated embryonic stages E7.5-E18.5 or 1- >3 days after birth (P1-3, P>3) and genotyped as shown in Fig 1D. Percentages of CKO (red) and control (green) embryos and total number of analyzed embryos (n) are shown. Dashed black line shows expected percentage of control and Oct4 CKO embryos of 50%.

4.3 Oct4 mutant embryos have an exencephalus phenotype

The notochord and the floor plate of the neural tube are derived from the Foxa2 cell lineage where Oct4 is depleted in mutant embryos (Figure 10A). It has been described that Oct4 is required for hindbrain patterning in Xenopus embryos, but the mechanism remains largely unclear (Morrison & Brickman 2006). To identify effects of Oct4 deletion on neural development we monitored developmental abnormalities during embryonic development.

Between embryonic day E11.5 and E14.5 some exencephali were observed in Oct4 CKO embryos (9/197 embryos) whereas control embryos did not exhibit open brain phenotypes (0/173) (Figure 9: Open brain phenotype). The exposure of the brain in an open brain phenotype can result in a birth trauma but is rarely the cause of prenatal lethality in Oct4 CKO embryos.

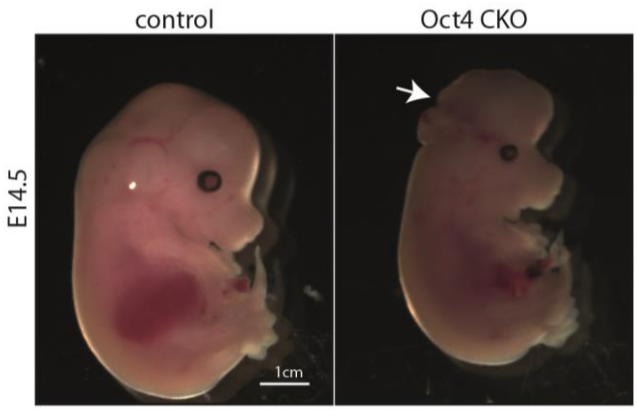

Figure 9: Open brain phenotype
Image of E14.5 littermates of Oct4 control and CKO embryos. Arrow in right image shows open brain. Scale bar 1cm

To test if the open brain phenotype could be caused by patterning defects of the neural tube we analyzed expression of DV patterning markers Foxa2, Nkx2.2 and Olig2 in the neural tube at E10.5. These markers are expressed in specific DV domains in the neural tube at this stage (Figure 10B). Immuno-staining of cryo-sections of Oct4 CKO and control embryos at the same position of the AP axis did not reveal any obvious differences in the expression patterns of these markers (n=4 each). In mutant and control groups Foxa2 was expressed in the floor plate of the neural tube and Nkx2.2 and Olig2 are expressed in their respective domains (Figure 10C, D).

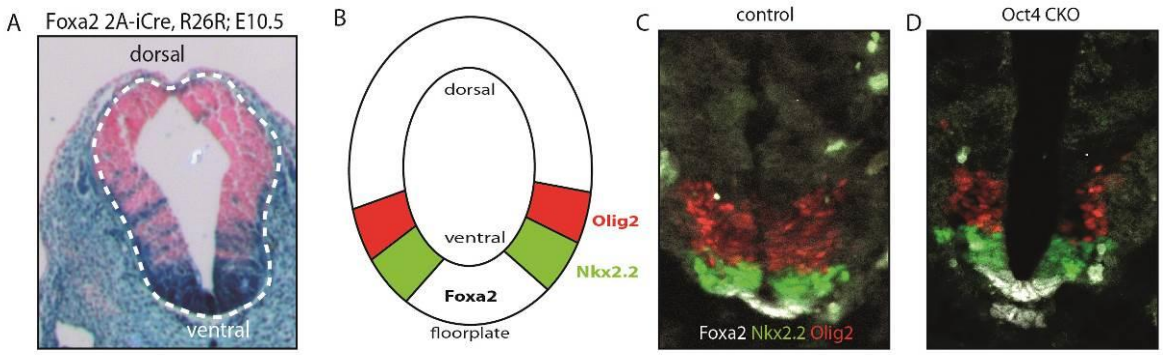

Figure 10: neural tube patterning at E10.5
(A) shows lineage tracing of Foxa2 expressing cells by crossing Foxa2 2AiCre with R26R mice. Embryos were dissected at E10.5 and stained with X-gal. Image shows cross-section through the neural tube. (B) Schematic view of the Foxa2, Olig2 and Nkx2.2 expression domains in the neural tube. Staining of E10.5 control (C) and Oct4 CKO (D) with Foxa2 (white), Nkx2.2 (green) and Olig2 (red) are shown

These results show that the open brain phenotype observed in Oct4 CKO embryos is not caused by patterning defect of the neural tube at E10.5. However, it is possible that Oct4 depletion affects cilia formation in the floorplate of the neural tube which can cause neural tube defects (Katsanis 2006)(see also 4.10).

4.4 Oct4 CKO cells can contribute to endodermal organs

Foxa2 is continuously expressed in cells from the early DE to fully developed endoderm derived organs such as lung, liver, pancreas etc. Cells of the Foxa2 lineage form the epithelial lining of all endodermal organs. Foxa2 and Oct4 are co-expressed in the epiblast where Oct4 gets deleted in CKO embryos. We thus asked whether Oct4 function during gastrulation is required for the formation of Foxa2 lineage cells in endodermal organs.

Since live pups are relatively rare and die shortly after birth, embryos were isolated at E18.5 when organs are fully formed and used for further analysis. Gross morphological analysis showed that all organs are formed in Oct4 mutant embryos at E18.5. To analyze the contribution of the Oct4 deleted Foxa2 lineage cells to organs we used the R26R allele for lineage tracing by staining with X-gal. Oct4 CKO cells contributed to endodermal tissues like pancreas and the intestinal epithelium (Figure 11 B-E). Foxa2 lineage cells also contributed

to mesodermal tissues like the atria of the heart (Figure 11A, A'). In heart an increase of Foxa2+ lineage cells was observed in Oct4 CKO compared to control embryos but could not be further quantified. Unexpectedly we did not find Foxa2 lineage cells covering the epithelial lining of the stomach. However X-gal staining was observed in small regions of the stomach. This might result from incomplete penetrance of the staining solution into the stomach.

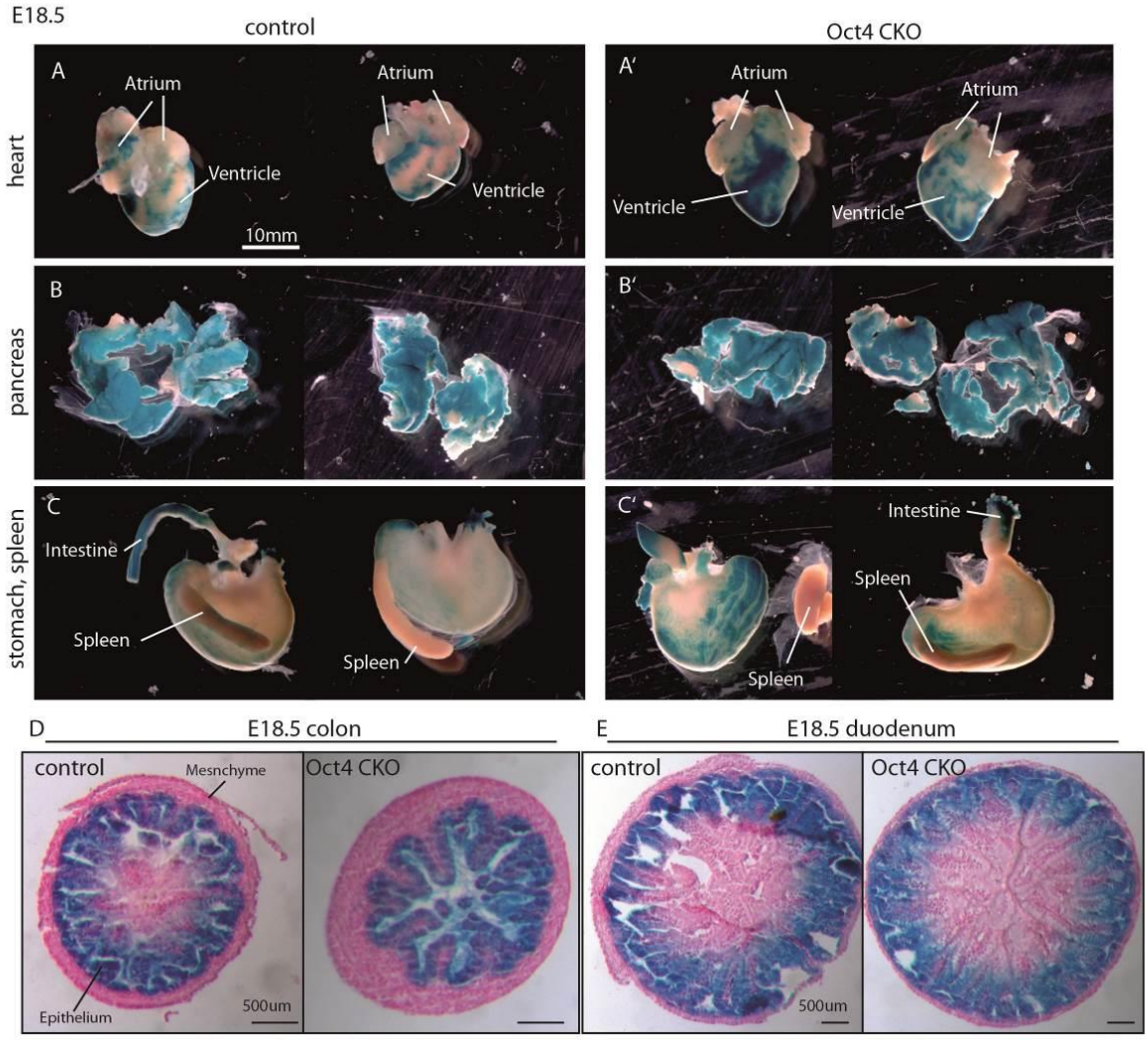

Figure 11: Contribution of CKO cells to organs
Control and Oct4 CKO E18.5 embryos were dissected and organs stained with X-gal to show the Foxa2 lineage. (A, A') shows hearts, (B, B') shows pancreas and (C, C') shows stomach and spleen. Sections of E18.5 colon (D) and duodenum (E) stained with X-gal for R26R and NFR as counterstaining. Scale bar for A-C' 10mm, for D and E 500µm.

Our results show that Oct4 CKO embryos form all internal organs and Oct4 depleted cells can contribute to endoderm derived organs and to the Foxa2 lineage in the heart and stomach.

4.5 **Oct4 is required for Foxa2 lineage contribution to somites**

Wnt3a/β-catenin signaling is essential for the specification of paraxial mesoderm fates during gastrulation and the recruitment of mesendoderm progenitors to the paraxial mesoderm (Galceran et al. 1999; Yamaguchi et al. 1999). Somites are derived from paraxial mesoderm and further differentiate into axial skeleton, the muscle of the trunk and the dermis of the body wall (Tam 1981). Oct4 has been shown to be involved in the regulation of Wnt/β-catenin signaling (Abu-Remaileh et al. 2010; Marikawa et al. 2011; Li et al. 2013a; Faunes et al. 2013) and Wnt3a levels are reduced in Oct4 CKO embryos (table 1). We thus asked whether conditional deletion of Oct4 has an effect on formation of somites.

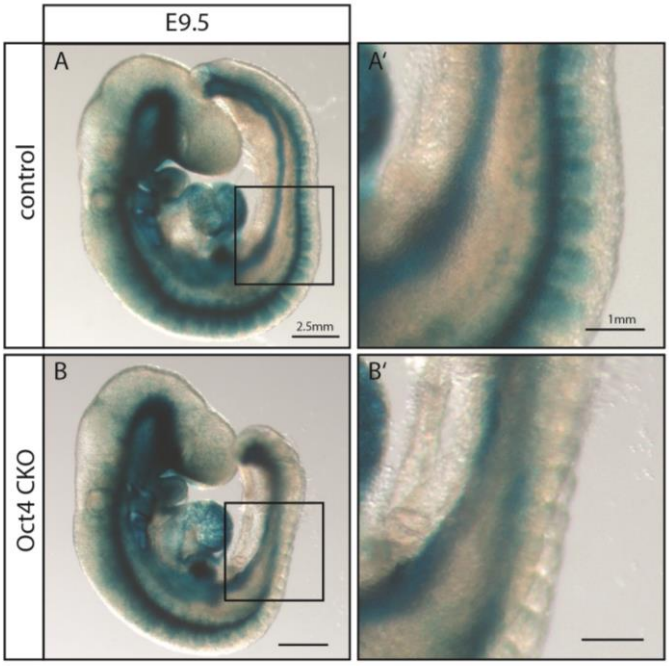

Figure 12: Contribution of Foxa2 lineage cells to somites
E9.5 control (A,A') and Oct4 CKO (B,B') embryos harboring a R26R allele were dissected and stained with X-gal to show the Foxa2 lineage. Scale bars are 2,5mm in A and B and 1mm in A' and B'.

To analyze the contribution of Oct4 depleted cells to somites Oct4 control and CKO embryos were dissected at E9.5 and stained with X-gal, which labels Foxa2 lineage cells in blue to visualize contribution of Oct4 depleted cells to somites.

At E9.5 Oct4 CKO and control embryos formed all anatomical structures including somites (Figure 12A-B'). However Oct4 CKO embryos showed a complete absence of Foxa2+ lineage cells in somites of the posterior part of the embryo (43/45 embryos) compared to control embryos (Figure 12 A – B'). Somites in the anterior part of the mutant embryos did not display this defect.

These results demonstrate that Oct4 depleted Foxa2 expressing cells fail to contribute to posterior somites, which develop from paraxial mesoderm.

4.6 **Oct4 mutant embryos lack hindgut endoderm**

It has been shown that Oct4 expression is down regulated in all germ layers from anterior to posterior during embryonic development and that deletion of Oct4 can cause posterior truncations in Xenopus (Morrison & Brickman 2006, Yeom et al. 1996).

Gross morphology shows that Oct4 CKO embryos have kinked tails at E9.5 (15/45 embryos)(Figure13A). This phenotype is known as curly tail has so far been associated with neural tube defects (van Straaten & Copp 2001). However, since defects in one germ layer can affect other germ layers, we morphologically analyzed the structure of hindgut endoderm in mutant embryos at E9.5. In Oct4 CKO embryos we observed an absence of the hindgut pocket and endoderm, while in control littermates it was correctly formed at E8.5 (

Figure 13B, white arrow head). For closer analysis we used the R26R lineage reporter to specifically stain Foxa2 lineage cells. At E9.5, control embryos clearly show β-gal staining in the Foxa2 lineage notochord and floor plate (

Figure 13C, grey arrow head) as well as in the hindgut endoderm (Figure 13C, grey arrow head and white dashed line), while in Oct4 CKO embryos no β-gal staining was observed in the hindgut. In paraffin sections of the embryo the hindgut endoderm is clearly visible in control but completely absent in Oct4 CKO embryos (Figure 13, C' – D''). The remaining blue staining in the posterior results from the floor plate of the neural tube and the notochord, which appear normally formed (Figure 13D, grey arrow head). The foregut endoderm is correctly formed in control and Oct4 CKO embryos.

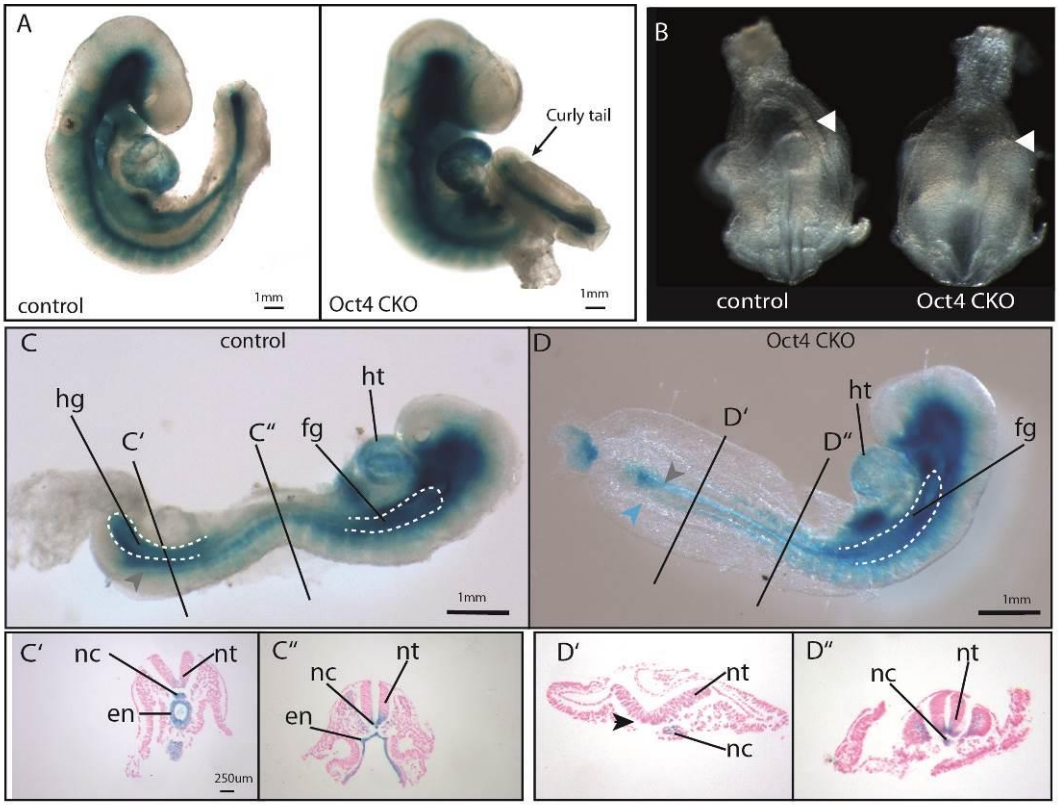

Figure 13: Oct4 CKO embryos lack hindgut endoderm
(A) Oct4 CKO embryos at E9.5 show a curly tail phenotype. (B) At E8.5 a lack of hindgut endoderm is visible, white arrow head shows position of posterior endoderm. (C and D) At E9.5 Foxa2 lineage staining by R26R shows absence of β-gal staining in the hindgut endoderm in Oct4 CKO embryos (D, blue arrow head) whereas the notochord and floor plate are not affected (grey arrow head). (C'-D'') show cross sections through the embryos in C and D as indicated. Sections were counterstained with nuclear fast red (NFR). Scale bars are 1mm in A, C, D and 250µm in C' - D''. Paraffin sections are cut at 8µm thickness. nc – notochord, nt – neural tube, en – endodermal gut tube, ht – heart, fg – foregut, hg - hindgut

These results indicate that Oct4 is required in the Foxa2 lineage for proper formation of the posterior endoderm and morphogenesis of the hindgut.

4.7 **Oct4 CKO cells can contribute to the intestinal crypt stem cell compartment**

Oct4 CKO embryos show an absence of hindgut endoderm but it could be possible that embryos which only show mild defects and form a colon have defects in formation of intestinal stem cells. Iit has been shown by others that Oct4 is not required for self-renewal of somatic stem cells (Lengner et al. 2007). In this study however Oct4 was deleted in somatic stem cells after birth. We therefore asked if deletion of the pluripotency factor Oct4 in Foxa2 expressing endodermal cells at the progenitor stage has an effect on formation and maintenance of the intestinal stem cell niche.

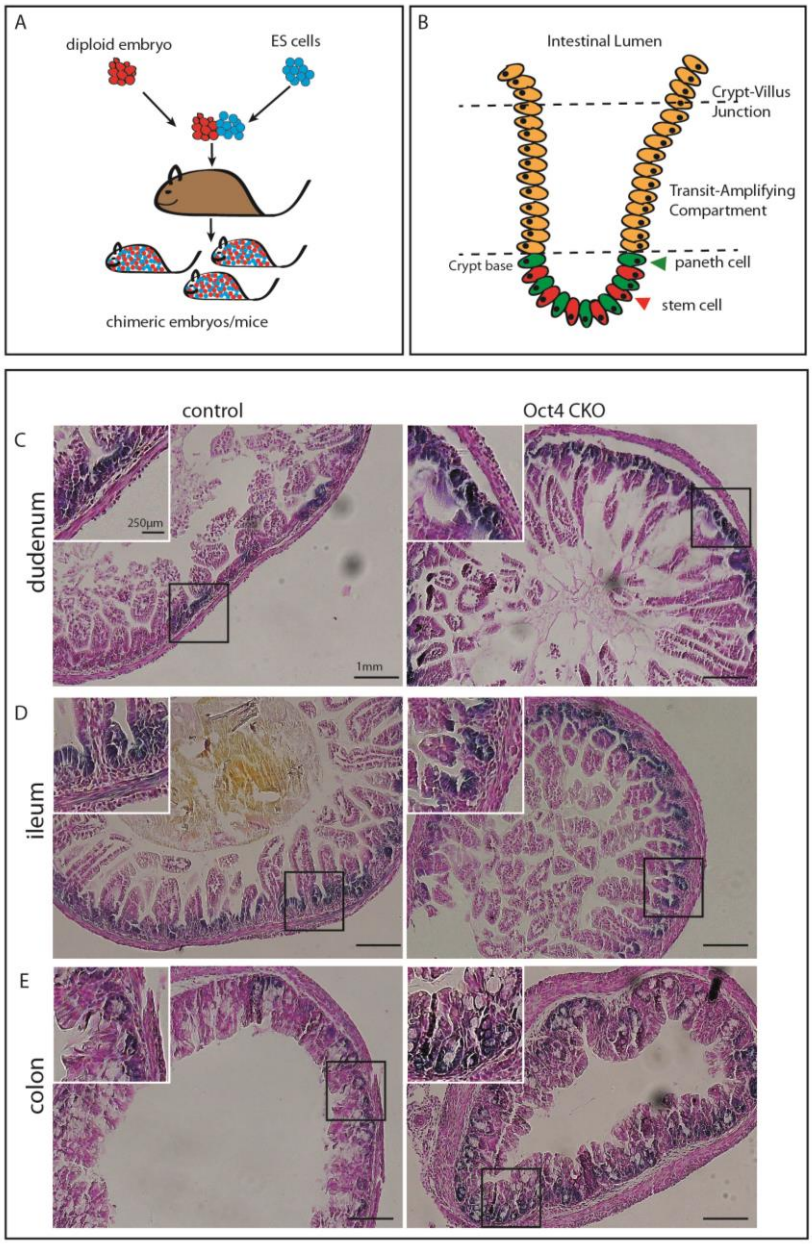

Figure 14: Diploid aggregation of CKO ES cells
(A) Scheme of diploid aggregation for generation of chimeras. Diploid embryo cells and ES are fused ant transplanted into a pseudo pregnant mouse, chimeric embryos or mice can be used for analysis. (B) Scheme of an intestinal crypt (adapted from Baker et al. 2008). In the crypt base supporting paneth cells (green) and intestinal stem cells are residing. Sections of P6 duodenum (C), ileum (D) and colon (E) from control and Oct4 CKO ES cells. ES cells contain a R26R allele and are stained by X-gal, counterstaining with nuclear fast red (NFR). Scale bars are 1mm, in insets 250µm.

The intestine is divided into villi and crypts. The crypt compartment is composed of adult stem cells which self-renew and give rise to all cells of the intestinal epithelium and paneth cells which have a supportive function (Clevers 2013; Barker et al. 2008)(Figure 14B).

To overcome lethality of Oct4 mutants we made use of the diploid aggregation system where E2.5 wild type morula are aggregated with ESCs and transferred into pseudo pregnant female mice (Figure 14A) (Bradley et al. 1984). Control and CKO ESCs have a R26R allele to follow the fate of these cells by X-gal staining. This system allows us to generate chimeric mice from Oct4 CKO and control ESCs and identify tissues derived from ESCs. Intestines of mice were dissected, stained with X-gal and paraffin sections were used for analysis. In the duodenum, ileum and jejunum in chimeric animals at postnatal day six (P6) blue staining was observed in the crypt compartment of duodenum, ileum and jejunum (Figure 14C - E). This result shows Oct4 CKO cells can still contribute to the intestinal stem cell compartment.

4.8 **Oct4 CKO embryos do not show obvious defects in early endoderm formation**

Since we observed effects in endodermal hindgut formation at E9.5 we wondered whether defects in endoderm formation during gastrulation cause this phenotype. Alternatively, it is possible that reduced proliferation or increased apoptosis in the endoderm results in a reduction of tissue and embryo growth and size. To distinguish between these possibilities, we first dissected Oct4 CKO and control embryos after germ layer formation is completed and analyzed endodermal marker expression by immunofluorescence staining at E7.5. Foxa2, Sox17 and the cell-cell adhesion molecule N-Cadherin (N-Cad, Cdh2) were used as markers of definitive endoderm. Both, Foxa2 and Sox17 did not reveal any visible differences in control and Oct4 CKO embryos (Figure 15A - B'). Also the epithelial marker N-Cad is expressed in the endoderm layer in control and Oct4 CKO embryos.

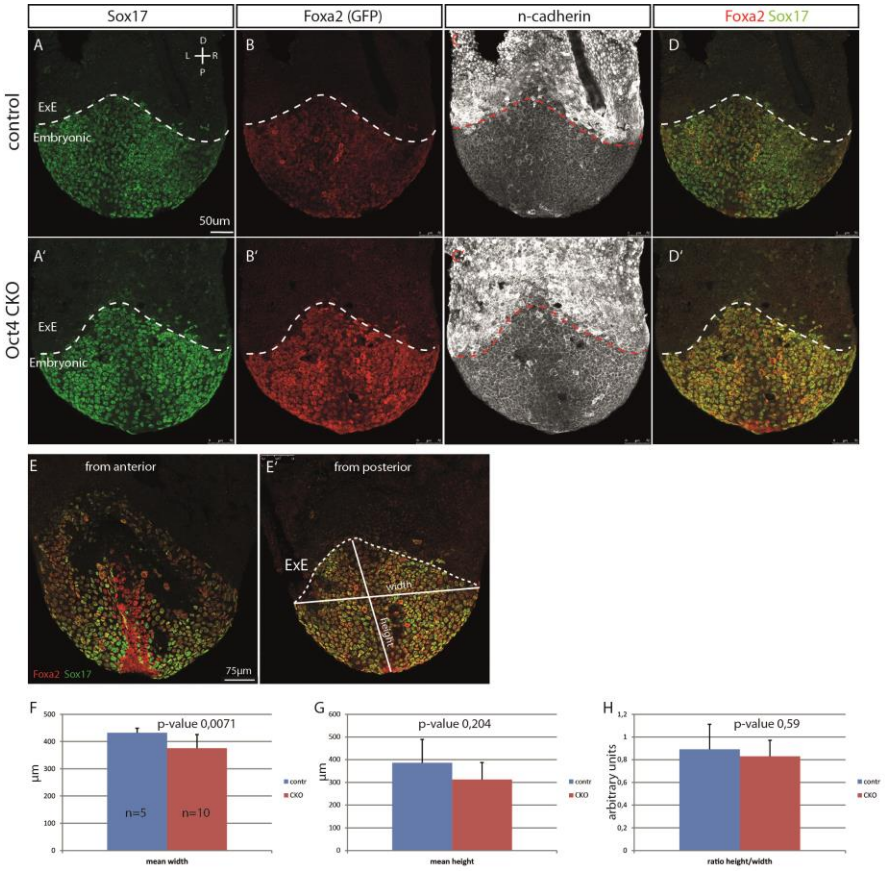

Figure 15: Analysis of early endoderm formation
Immunostaining of control (A-D) and Oct4 CKO (A'-D') embryos against Sox17 (green), Foxa2 (red) and N-cadherin (white), posterior view (dashed line shows border of embryonic and extra embryonic (ExE) part). Control embryo shown from anterior and posterior (E, E' respectively), in (E') border of extra embryonic and embryonic part is indicated by dashed line, width and height measured are indicated by solid lines. (F-H) shows measurements of width, height and ratio of width to height as indicated in (E') for control (blue) and Oct4 CKO (red) embryos. Mean values and standard deviations are shown. ExE – extra embryonic endoderm, D – distal, P – proximal, L – left, R - right. Scale bars are 50µm for A – D' and 75µm for E and E'.

To determine size differences the height of the posterior definitive endoderm, marked by Foxa2 and Sox17, from the distal tip to the most proximal extent of the embryonic endoderm and the width of the embryo were measured (Figure 15E'). Oct4 CKO embryos showed a slight reduction in height and width compared to the control but the ratio of height to width of the endoderm was not significantly changed (Figure 15F - H).

These results show that Oct4 mutant embryos had no obvious defect early endoderm formation and express the definitive endoderm markers Foxa2 and Sox17.

4.9 Conditional deletion of Oct4 causes a defect in left-right asymmetry specification

Foxa2 is expressed in axial mesoderm tissues like node, notochord and prechordal plate. These structures are important for establishment of the LR and DV axis (Ang & Rossant

1994b). Therefore we asked whether Oct4 deletion in these tissues has an effect on establishment of the LR axis.

Global establishment of LR asymmetry becomes morphologically first visible by the rightward looping of the heart tube (Irfan S Kathiriya & Srivastava 2000). At E9.5, all control embryos show rightward heart looping (n=22) (Figure 16A-B'), whereas in 32% of the Oct4 CKO embryos (n=25) the heart is looped to the left (Figure 16C-D').

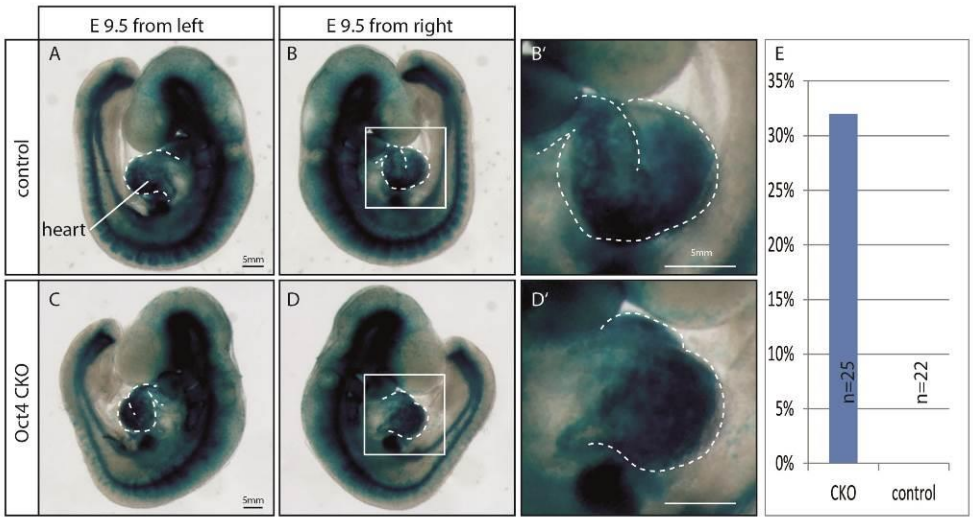

Figure 16: Heart looping defects in CKO embryos
Control and Oct4 CKO embryos were dissected at E9.5 and stained with X-gal. Control ((A,B) and Oct4 CKO (C,D) are shown from the left and right side and a vien on the heart from the right side is shown enlarged (B',D'). (E) 32% of the CKO embryos (n=25) and 0% of the control embryos (n=22) show heart looping to the left.

This phenotype can also be found in the *situs inversus* phenotype and is generally caused by improper establishment of the LR asymmetry of the embryo.

It has been shown that defects in LR asymmetry also effect formation of the lung (Meno et al. 2001). In the mouse the lung consists of four lobes on the right side (right cranial, caudal, accessory and middle lobe) and one lobe on the left side (Figure 17B).

All control embryos display normal lung morphology between E11.5 and P1 (n=47) (Figure 17A - F), whereas 82,7% (n=29) of Oct4 CKO embryos have pulmonary left isomerism (Figure 17A' – F'). This phenotype is characterized by absence of the right middle and accessory lobes, and the right caudal and cranial lobes are fused.

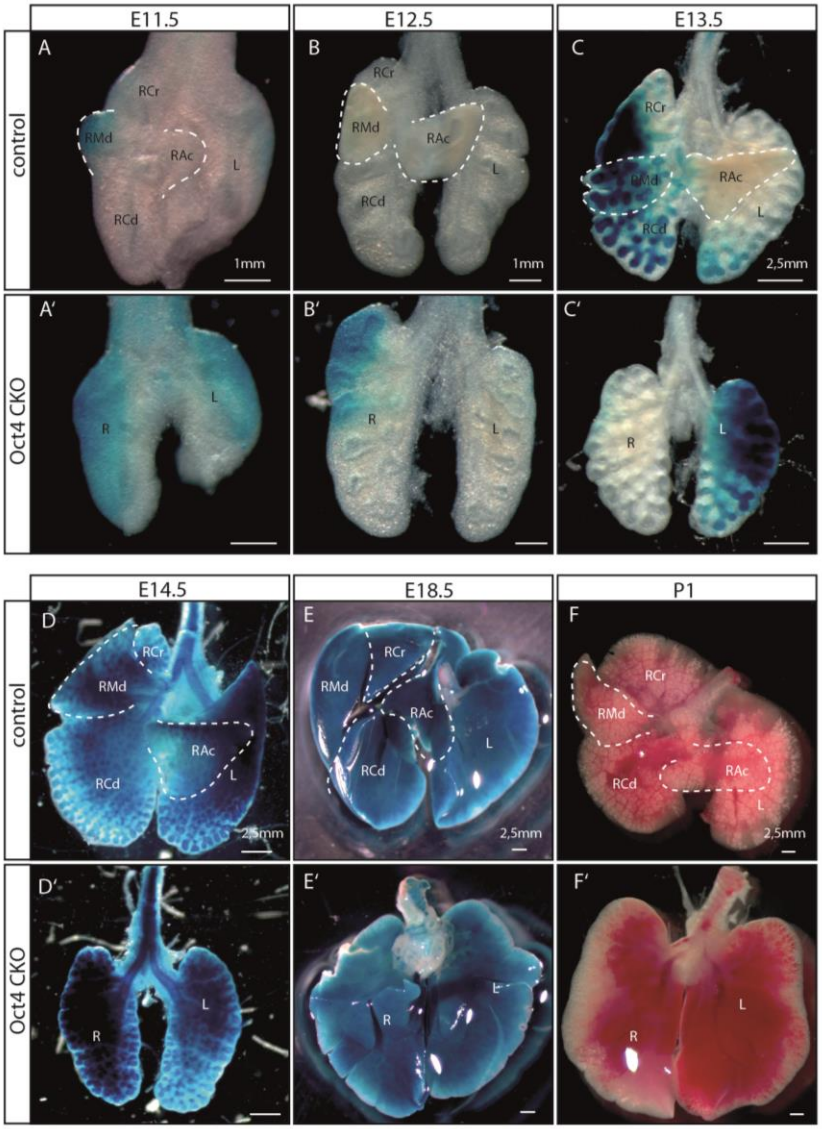

Figure 17: Oct4 CKO embryos show pulmonary left isomerism
Lungs of control (A-F) and Oct4 CKO (A'-F') were dissected from E11.5 to P1 and stained with X-gal (except for P1). White dashed lines in (A and B) show right middle and accessory lobes. For (B): L – left lobe, RCr – right cranial lobe, RMd – right middle lobe, RCd – right caudal lobe. Scale bars are 1mm (A-B'), 2,5mm (C-F')

To analyze this phenotype in more detail control and Oct4 CKO lungs were stained for Gata4, E-Cadherin (E-Cad) and Phospho Histone H3 (PH3) at E12.5. Gata4 was shown to be necessary for pulmonary lobar development and patterning (Ackerman et al. 2007), E-cad stains the epithelial lining of the ducts in the lung and PH3 marks cells in mitosis. In control lungs all lobes are developed and Gata4 is expressed in some cells of the mesenchyme. E-Cad shows normal expression in the epithelium of the developing duct system. The proliferation marker PH3 shows that a large proportion of the cells are in mitosis (Figure 18D, D'). In Oct4 CKO embryos only 2 lobes are present (Figure 18A'-E'). The ductal epithelium is formed which can be seen by E-Cad staining (Figure 18C'). The proportion of proliferating cells, marked by PH3, is comparable between CKO and control lungs (Figure

18D, D'). Interestingly expression of the transcription factor Gata4 is more abundant in CKO lungs than in the control (Figure 18 B, B'). The interaction of Gata4 with Fog2 (Zfpm2) is required for normal lung development (Ackerman et al. 2007). Since Fog2 expression is reduced in Oct4 CKO embryos (data not shown) the upregulation of Gata4 could be a compensatory mechanism.

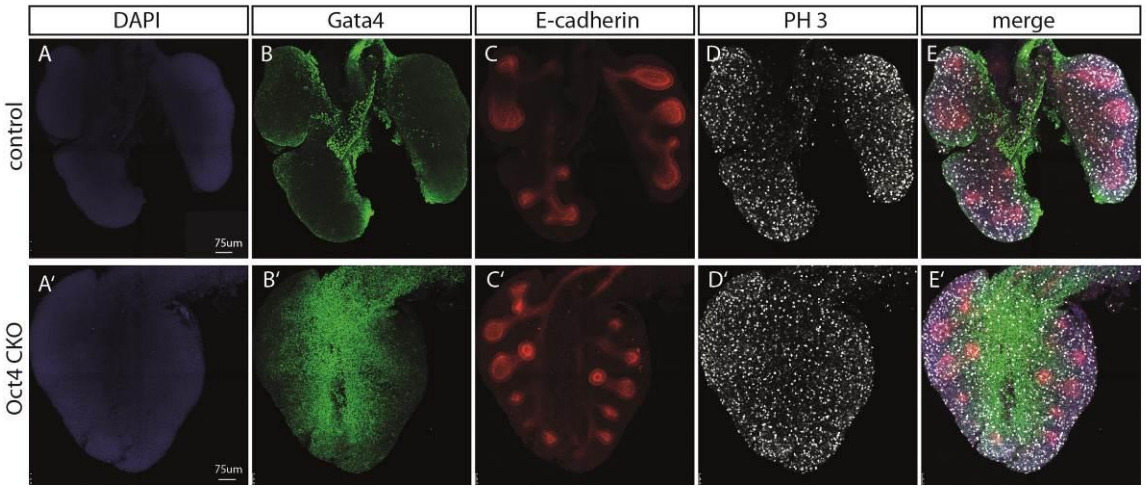

Figure 18: Analysis of pulmonary left isomerism by IF staining
Control and Oct4 CKO lungs were immuno stained at E12.5 for Gata4 (B, B', green), E-cadherin (C, C', red) and phospho histone H3 (PH3, D, D', white). DAPI was used as counter stain (A,A'). CKO lungs show more cells expressing Gata4 (B,B') and a comparable level of proliferating cells marked by PH3 (D,D'). Scale bar is 75µm in all images. Figures show z-projection of confocal images.

Taken together the heart looping and pulmonary left isomerism phenotype clearly show that Oct4 function in Foxa2+ lineage cells is required for proper establishment of the LR asymmetry during embryonic development.

4.10 **Oct CKO embryos show defects in node and cilia morphology**

The LR axis is established by asymmetric distribution of signaling molecules in the node through nodal flow, which is generated by motile cilia (Nonaka et al. 1998). Since we observe LR defects in Oct4 mutants and Oct4 is deleted in the Foxa2 lineage in the node we asked whether Oct4 is involved in correct formation of the node cells and/or the node cilia.

For this we performed immunostaining on embryos at the head fold stage (HF, E7.75) and used Chordin as a node specific marker (Y Sasai et al. 1994). In control embryos Chordin is expressed in the node region with no obvious differences in the Oct4 CKO embryos (Figure 19A - E', white arrow heads indicating the node). This shows that the node cells are formed in mutant embryos.

We then examined node morphology in more detail by staining embryos with Foxa2 and T as markers for axial mesoderm including the node and acetylated tubulin (acet-tub) for node cilia. At the late HF stage the node is positioned at the distal tip of the embryo. Co-staining of Foxa2 and T can be observed in the node of control and Oct4 mutant embryos confirming that the node is formed. In control embryos the node shows a clear separation between pit and crown cells (Figure 19G-J). In Oct4 mutant embryos however the borders of the node are not clearly defined and pit and crown cells are not properly separated (Figure 19G' - J'). At E8.0, the node is positioned more on the posterior side of the embryo. The node of control embryos shows a clearly defined structure with expression of Foxa2 and T in all cells (Figure 19L-O). On the other hand, the node in Oct4 CKO embryos lacks defined borders and several cells within the node do not express Foxa2 and T (Figure 19K' and N', white arrow heads). In the node of control embryos cilia are uniformly positioned on the posterior side of the node cells (Figure 19M). However, node cilia in Oct4 mutant embryos are mostly absent or randomly oriented (Figure 19 M').

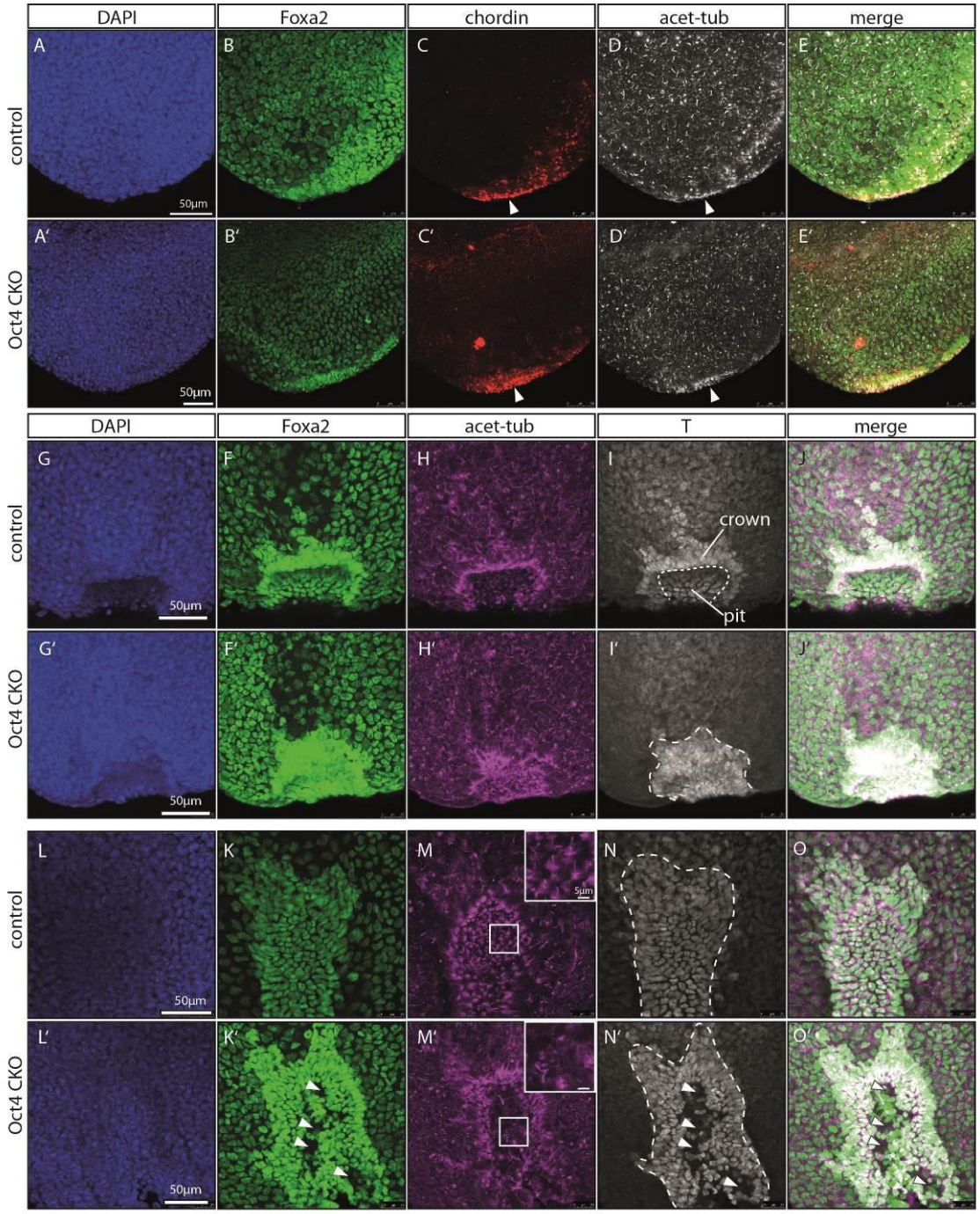

Figure 19: Disruption of node architecture in Oct4 CKO embryos

Immuno staining of E7.5 and E8.0 control and Oct4 embryos. (A-E) shows a E7.5 control embryo stained for DAPI (blue), Foxa2 (green), chordin (red) and acetylated tubulin (white). (E) shows merge of Foxa2, chordin and Acetylated tubulin. (A'-E') shows an Oct4 CKO embryo with the same staining as the control. White arrow heads in D and D' show the position of the node. (G-J') shows the node of E8.0 embryos at the most distal position at the late headfold stage stained for DAPI (blue), Foxa2 (green), acetylated tubulin (violet) and T/Brachury(white). (F-J) shows control embryo, (G'-J') Oct4 CKO embryo. Immuno staining of the node of control (L-O) and Oct4 CKO (L'-O') embryos on the posterior side of the embryos shows improper formation of node cells and cilia (Staining as in F-J'; white arrow head in K' and N' show cells without Foxa2 and T staining)).

Scale bars are 50µm, 5µm in insets in M and M'. White dotted line shows border of nodal pit and crown cells (I) and outline of the node structure (I', N, N')

These results indicate that Oct4 is required in Foxa2 expressing mesendodermal cells for proper specification and organization of node cells and for correct formation and orientation of motile cilia. Malformation of the node structure and absence of nodal cilia offers an explanation for the LR asymmetry defects observed in Oct4 mutant embryos.

4.11 mRNA profiling of E7.5 Oct4 CKO embryos shows misregulation of important endoderm and signaling genes

To analyze the effect of Oct4 deletion in the mesendoderm on a molecular level we compared mRNA expression profiles of control and CKO embryos using Affymetrix GeneChip® analysis at E7.5 (in collaboration with M. Irmler, IDG). When gastrulation is completed no obvious morphological phenotype was detected in the Oct4 CKO embryos. To decipher early effects of Oct4 deletion we dissected 6 Oct4 CKO (ko_1,3,12,13,14,15) and 4 control (ctrl_2,5,10,11) embryos at stages between neural plate (NP) and late bud (LB) stage during gastrulation. mRNA was extracted from the embryonic part for microarray analysis and extra embryonic tissue was used for genotyping. Cluster analysis of the data with Hclust software showed that control and Oct4 CKO embryos are clustered in independent groups with exception of ko12 and ko13, which cluster more to the controls (Figure 20). This could be caused by slight time differences in Cre mediated Oct4 deletion.

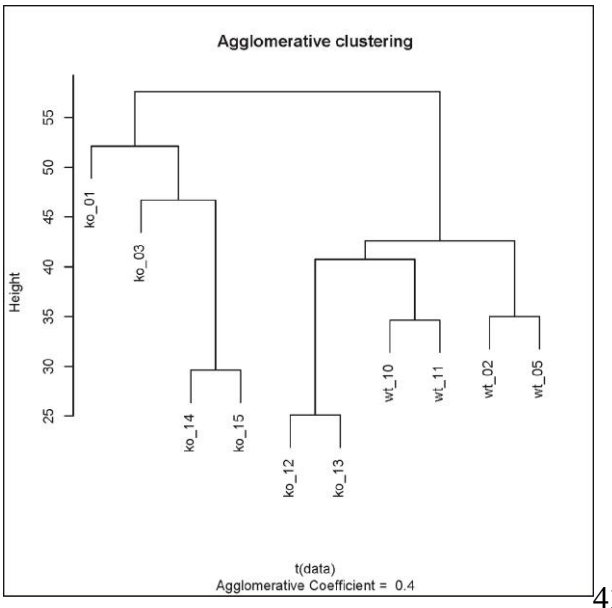

Figure 20: Cluster analysis mRNA expression profiling
Agglomerative clustering of mRNA expression arrays from E7.5 Oct4 CKO (ko_01,03,14,05,12,13) and control embryos (wt_10,11,02,05) is shown

Comparison of mRNA expression between Oct4 CKO and control embryos exhibited differential expression of 600 probesets with a false discovery rate (FDR) <5%. Of these, 151 are up- and 449 downregulated (Figure 21A). With a FDR <10% we find 1938 probesets misregulated. On the GeneChip array several genes are detected by more than one probeset. Our further analysis we restricted to genes with a FDR<10% and a fold change (FC) of >1.5x (CKO vs. control) to focus on significant changes. From these 522 genes 133 were up regulated and 389 genes down regulated in Oct4 CKO embryos. Gene ontology (GO) analysis of misregulated genes revealed an enrichment of primitive streak, endoderm, mesoderm, germ layers and somites within genes upregulated in CKO embryos (Figure 21B).

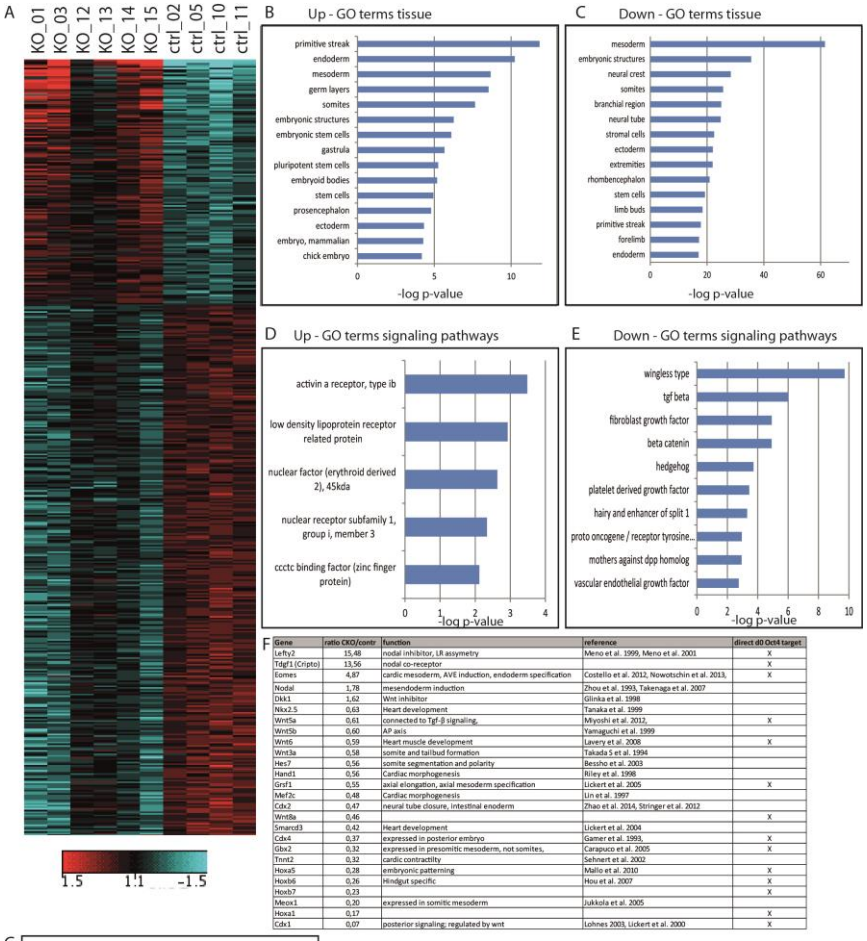

Gene	ratio CKO/contr	function	reference	direct d0 Oct4 target
Lefty2	15,48	nodal inhibitor, LR assymetry	Meno et al. 1999, Meno et al. 2001	X
Tdgf1 (Cripto)	13,56	nodal co-receptor		X
Eomes	4,87	cardic mesoderm, AVE induction, endoderm specification	Costello et al. 2012, Nowotschin et al. 2013,	X
Nodal	1,78	mesendoderm induction	Zhou et al. 1993, Takenaga et al. 2007	
Dkk1	1,62	Wnt inhibitor	Glinka et al. 1998	
Nkx2.5	0,63	Heart development	Tanaka et al. 1999	
Wnt5a	0,61	connected to Tgf-β signaling,	Miyoshi et al. 2012,	X
Wnt5b	0,60	AP axis	Yamaguchi et al. 1999	
Wnt6	0,59	Heart muscle development	Lavery et al. 2008	X
Wnt3a	0,58	somite and tailbud formation	Takada S et al. 1994	
Hes7	0,56	somite segmentation and polarity	Bessho et al. 2003	
Hand1	0,56	Cardiac morphogenesis	Riley et al. 1998	
Grsf1	0,55	axial elongation, axial mesoderm specification	Lickert et al. 2005	X
Mef2c	0,48	Cardiac morphogenesis	Lin et al. 1997	
Cdx2	0,47	neural tube closure, intestinal enoderm	Zhao et al. 2014, Stringer et al. 2012	
Wnt8a	0,46			X
Smarcd3	0,42	Heart development	Lickert et al. 2004	
Cdx4	0,37	expressed in posterior embryo	Gamer et al. 1993,	X
Gbx2	0,32	expressed in presomitic mesoderm, not somites,	Carapuco et al. 2005	X
Tnni2	0,32	cardic contractility	Sehnert et al. 2002	
Hoxa5	0,28	embryonic patterning	Mallo et al. 2010	X
Hoxb6	0,26	Hindgut specific	Hou et al. 2007	X
Hoxb7	0,23			X
Meox1	0,20	expressed in somitic mesoderm	Jukkola et al. 2005	
Hoxa1	0,17			X
Cdx1	0,07	posterior signaling; regulated by wnt	Lohnes 2003, Lickert et al. 2000	X

Figure 21: Microarray analysis of Oct4 CKO E7.5 embryos

(A) Heatmap of 6 Oct4 CKO and 4 control embryos. GO term analysis of the top upregulated genes for tissues (B) and signaling pathways (D) and of the top down regulated genes for tissues (C) and signaling pathways (E). (F) List of top up/ down regulated genes with important function for embryonic development of which several have been described as bound by Oct4. (G) Dotblot of the top up/ down regulated genes. Red dots indicate Oct4 bound genes.

In down regulated genes we find enrichment for mesoderm, embryonic structures, neural crest and somites (Figure 21C). This shows that misregulated genes in Oct4 CKO embryos are associated with gastrulation and neurulation. GO term analysis identified signaling pathways like Wnt, Tgf-β, Fgf and hedgehog signaling within down regulated genes (Figure 21E). All of these pathways play important roles during embryonic development and patterning. In the set of upregulated genes the most prominent pathway is ActivinA receptor which, as part of the Tgf-β/Nodal pathway is important for endoderm formation (Figure 21D).

CKO/contr	cdx1	hoxb1	aldh1a2	dkk1	cdx2	fzd10	wnt8a	grsf1	cdx4	Oct4
array	0,07	0,38	0,12	1,62	0,47	0,63	0,46	0,55	0,37	not significant
qPCR	0,23	0,48	0,48	2,17	0,51	0,28	0,83	0,93	0,79	0,5

Figure 22: qPCR confirmation of deregulated genes
qPCR (SYBR green) analysis was performed on 5 pooled control and Oct4 CKO embryos each

To confirm the differentially expressed genes found in the microarray analysis we performed qPCR analysis for several genes on pooled control and Oct4 CKO embryos at E7.5. We were able to confirm the misregulation of several genes like *Cdx1, Cdx2* and *Hoxb1* (Figure 22). As internal control qPCR showed a reduction of *Oct4* mRNA in CKO embryos by 50% compared to the control embryos as expected. This confirms the good quality of this analysis since Oct4 mutant embryos have one Oct4 FD allele and therefore only have half of the level of Oct4 in all tissues compared to control embryos.

Among the misregulated genes *Lefty2*, *Cripto* (*Tdgf1*) and *Nodal*, factors involved in Tgf-β/Nodal signaling, are within the most upregulated (Figure 21F). *Lefty2* is an inhibitor of nodal signaling (Meno et al. 1999) and plays an important role for LR asymmetry establishment and anterior-posterior (AP) patterning (Meno et al., 2001; Yamamoto et al., 2004). *Cripto* and *Nodal* are a co-receptor and ligand of the Tgf-β signaling pathway, respectively. This strengthens our observation that Oct4 is required for proper establishment of the LR axis during development.

We also observe down regulation of several Wnt genes, e.g. *Wnt4, Wnt5a/b, Wnt6, Wnt8a*, and *Wnt3a*. In conjunction with this, several Wnt target genes like *Grsf1, Fragilis2 (Ifitm1), Gbx2, Fgf4, Pitx2, Smarcd3, Cdx4* and *Cdx1* are down regulated in Oct4 CKO embryos. This shows that reduction of Wnt signaling also affects downstream target genes. Reduced Wnt signaling after depletion of Oct4 can explain the observed phenotypes like hindgut development defect or recruitment of cells to paraxial mesoderm and somites, processes which are dependent on Wnt/β-catenin signaling.

Among the most down regulated genes several members of the Hox family (*Hoxa1/3/5, Hoxb1/4/6/7*) were found in Oct4 CKO embryos (Figure 21D and Table 1). This family of genes plays an important role in axial extension and patterning of the developing embryo (Young & Deschamps 2009). This is in concordance with observed defects in formation of posterior endoderm in Oct4 CKO embryos (Figure 13).

Lineage tracing in mutant embryos indicated that Oct4 CKO cells have a higher contribution to the cardiac mesodermal lineage (Figure 11). For this we also looked at cardiac specific genes in our expression data. Comparing expression levels of Oct4 CKO vs. control we found several genes involved in cardiac development like *Mef2c, Nkx2.5, Hand1, αSMA, Tnnt2* and *Smarcd3* down regulated in Oct4 mutant embryos (Figure 21F and Table 1).

To investigate if differentially regulated genes could be direct targets of Oct4 we compared these genes to published Chromatin immunoprecipitation (ChIP) datasets of Oct4 bound genes in ES cells (Chen et al. 2008; Kim et al. 2008; Liu et al. 2008; Loh et al. 2006; Marson et al. 2008b; Mathur et al. 2008). 142 out of 522 (27,2%) differentially regulated genes were found as Oct4 targets in at least 2 of the published studies (Figure 21G, some examples are shown in Figure 21F right column). From 133 up regulated genes 30,1% are bound by Oct4 (40/133) whereas 25,7% (100/389) of down regulated genes are bound. This indicates that Oct4 could be involved in the regulation of these genes through directly binding to promoter or enhancer regions.

4.12 Analysis of expression domains of differentially regulated genes in embryos by whole mount in situ hybridization

To address possible changes of expression domains of differentially regulated genes found in the Microarray screen we performed whole-mount *in situ* hybridization (WISH) on embryos for selected genes at E8.5.

Cdx1 which is strongly reduced in Oct4 CKO embryos in the mRNA profile shows specific expression in the posterior part of the control embryos. Oct4 mutant embryos show expression of *Cdx1* in the posterior part of the embryo comparable to the control embryo (Figure 23C).

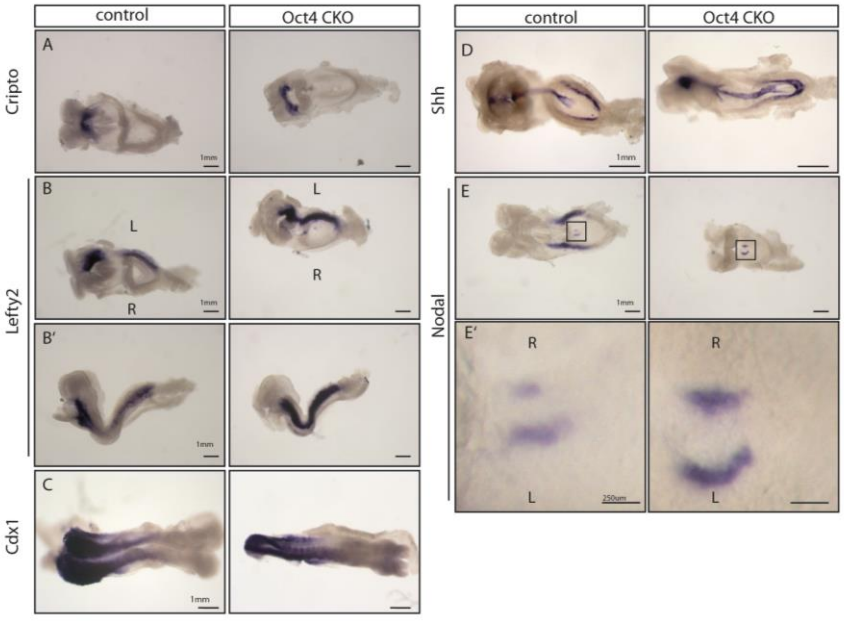

Figure 23: *In situ* hybridization analysis of mutant embryos
Control and Oct4 CKO embryos were dissected at E8.0 and stained by whole mount insitu staining for crypto (A), Lefty2 (B – view from ventral, B' – view from left), Cdx1 (C), Shh (D) and nodal (E, E' – enlarged view of node). Scale bars are 1mm and 250µm in E'.

Cripto, Lefty2 and *Nodal* are components of the Tgf-β signaling pathway and were all found to be upregulated in Oct4 CKO embryos (Table 1). *Cripto* expression was observed in the heart of control and Oct4 CKO embryos with no visible difference (Figure 23A). *Lefty2* was expressed in the left lateral plate mesoderm (LPM) in the control and showed a strongly increased expression in the Oct4 mutant embryo in the same domain (Figure 23B, B'). *Nodal* is expressed bilaterally in the LPM and asymmetrically in the lateral edges of the node with a higher expression on the left side (Figure 23E, E' left images). In the Oct4 mutant no *Nodal* expression in the LPM can be observed and expression in the node is more symmetrical

(Figure 23E, E' right images). Bilateral expression of *Nodal* in control embryos was unexpected since it is specifically expressed in the left LPM (Brennan et al. 2002a).

Sonic hedgehog (*Shh*) is the ligand of the hedgehog signaling pathway and involved in the induction of *Hox* genes during development of the chick hindgut (Roberts et al. 1995). Since *Shh* mRNA shows lower expression in Oct4 CKO embryos than in controls we were interested if the total expression level is lower or the *Shh* expression domain is changed. In control and CKO embryos *Shh* is expressed in the posterior endoderm and the axial mesoderm with no visible differences (Figure 23D). We were not able to see a reduction in *Shh* expression level in the mutant embryos.

In summary our analysis shows that expression domains of *Cdx1, Cripto and Shh* are not changed in CKO embryos although differential expression was detected by GeneChip analysis. For *Lefty2* we could confirm an increase in expression, but only in the left LPM. *Nodal* was expressed bilaterally in the LPM in control but no expression was detected in LPM of CKO embryos. However expression in the node was more symmetrically in CKO embryos. This indicates that deletion of Oct4 affects correct regulation of the Tgf-β/Nodal pathway.

4.13 **Generation of Oct4 ES cells for in vitro analysis**

In Oct4 CKO embryos we observed defects in endoderm formation, patterning and LR asymmetry establishment. To investigate the underlying defects on a molecular level we generated control and Oct4 CKO ESCs for *in vitro* analysis. One control (1F; Foxa2 $^{2AiCre/Venus\ fusion}$; Oct4 $^{wt/flox}$) and two CKO clones (1C and 2C; Foxa2 $^{2AiCre/Venus\ fusion}$; Oct4 $^{FD/flox}$) (see also Figure 6C) were isolated from outgrowths of the ICM. The Foxa2-Venus fusion allele specifically allows FACS sorting of Foxa2+ cells after differentiation, in which Oct4 has been deleted, for further analysis (Figure 24A). Using ES cells for *in vitro* analysis provides us with theoretically unlimited cell numbers for genetic and molecular analysis and also allows examination of isolated Foxa2+ endodermal cells without interfering cross signaling from other germ layers.

To confirm deletion of Oct4 invitro ES cells were differentiated to Epi stem cells (EpiSC) for 5 days and sorted for FVF expressing cells (Figure 24A). Genotyping of sorted FVF+ cells confirmed the recombination of the Oct4^{flox} allele in CKO ES cells (Figure 24 B). To demonstrate Oct4 deletion on a protein level we removed pluripotency promoting conditions by culturing ESCs in N2B27 medium without LIF and Serum to generate Foxa2+, Oct4+ co-expressing cells. With other differentiation protocols Foxa2+, Oct4+ cells were not found. After 5 days 34,5% of the Foxa2+ control cells coexpress Oct4+ whereas in the Oct4 CKO ESCs only 6,2% of Foxa2+ cells express Oct4 (Figure 24 C - F).

These results confirm that the Oct4flox allele is recombined in ESCs and the protein is not made.

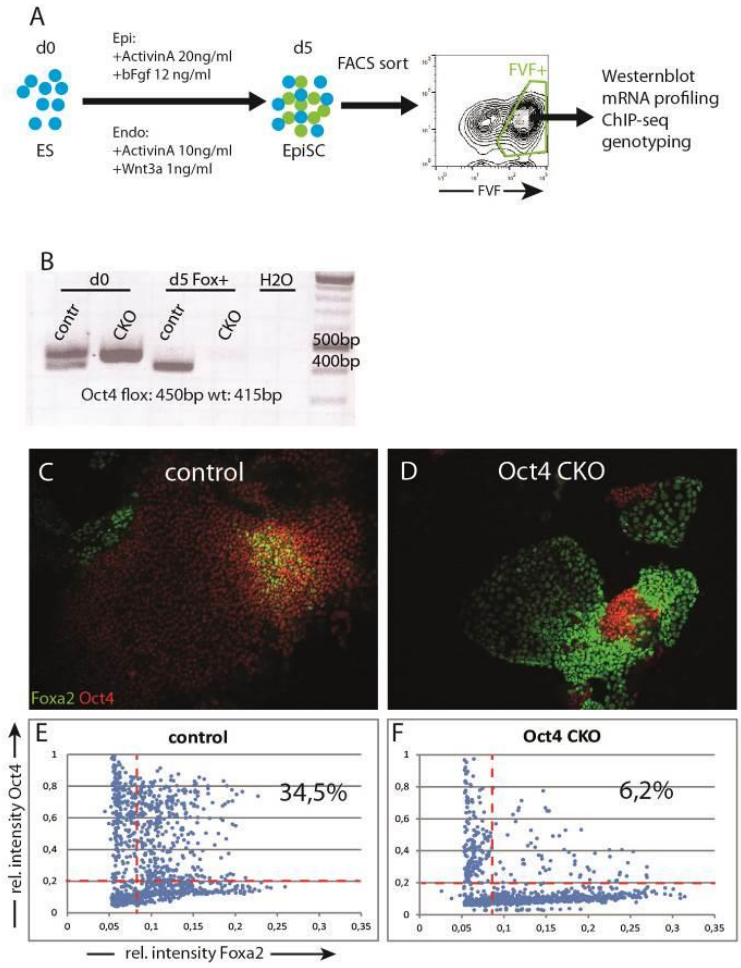

Figure 24: Generation and characterization of Oct4 CKO ES cells
(A) Scheme of differentiation of ES cells to endoderm or EpiSC. FVF+ cells were FACS sorted on d5 of differentiation and used for further analysis. (B) Genotyping of sorted control and Oct4 CKO ES cells differentiated to d5 endoderm (d5 F+) shows deletion of the Oct4 flox allele (450bp band) compared to pluripotent cells (d0). Control (C) and Oct4 CKO (D) ES cells were cultured under serum free conditions for 5 days and stained for Foxa2 (green) and Oct4 (red). Quantification of relative fluorescent intensities of Foxa2 and Oct4 in Foxa2 expressing cells of control (E) and Oct4 CKO (F) cells from C and D analyzed by cell profiler software. Percentages show cells with a relative Oct4 level >0,2 and Foxa2 >0,08.

4.14 Oct CKO ES cells show increased spontaneous differentiation into Foxa2+ cells under 2i conditions

Since it has been shown that low levels of Oct4 lead to a differentiation of ES cells into trophectoderm (TE) (Niwa et al. 2000) and ES cells can spontaneously differentiate into extra embryonic lineages (Figure 25A) investigated if conditional deletion of Oct4 has an effect on spontaneous differentiation. Morphologically pluripotent ESCs form dome shaped colonies

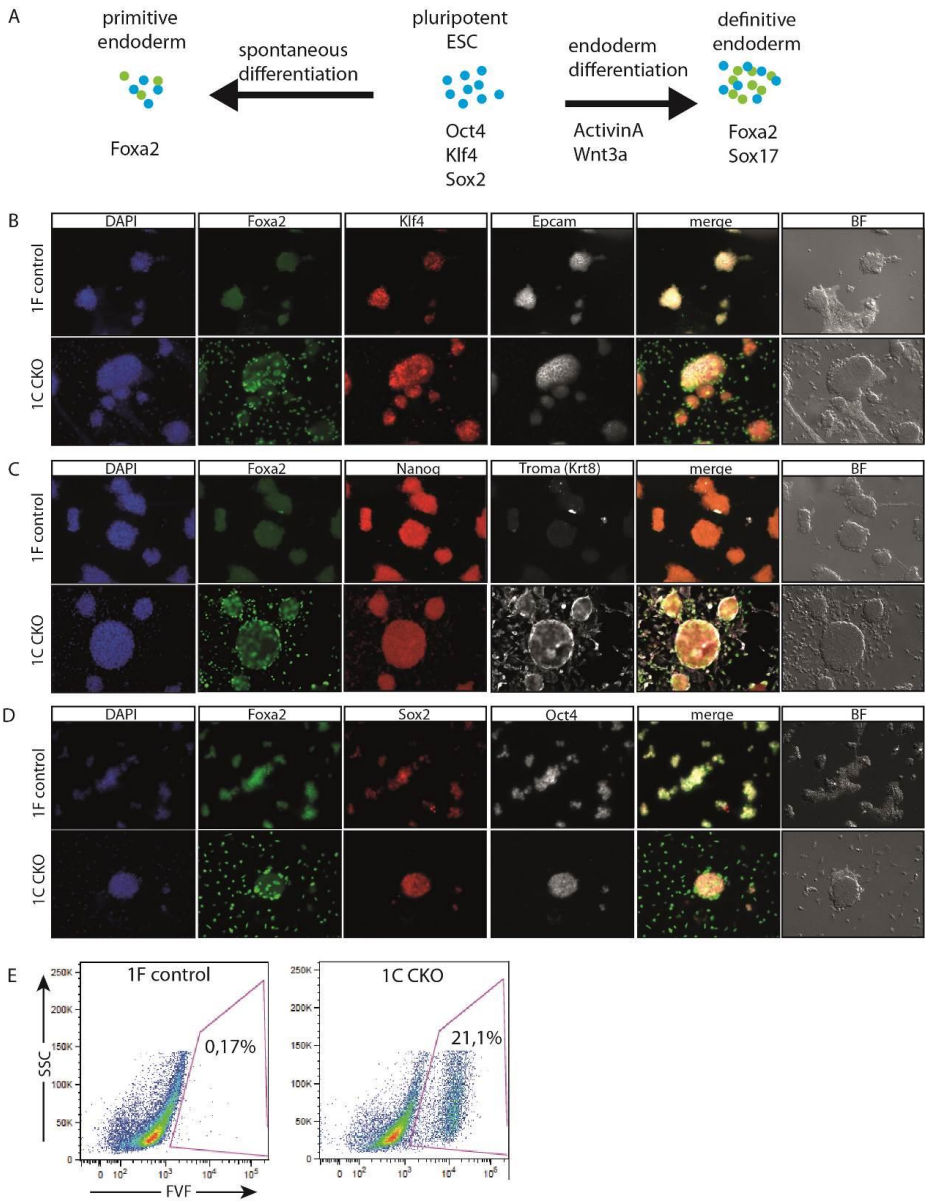

Figure 25: Increased spontaneous differentiation of CKO ES cells in 2i medium
(A) Scheme of ES cell differentiation; spontaneous differentiation to primitive endoderm or differentiation to definitive endoderm by Activin and Wnt. Control (clone 1F) or Oct4 CKO (clone 1C) ES cells were cultured under 2i conditions for 5 passages and stained for Foxa2 (green, B-D), Klf4 (red, B), EpCam (white, B), Nanog (red, C), Troma (=Krt8, white, C), Sox2 (red, D) and Oct4 (white, D). Counter staining with DAPI (blue). (E) FACS analysis of control and Oct4 CKO ES cells after 5 passages in 2i medium for FVF. SSC – side scatter, FVF – Foxa2-Venus fusion

whereas differentiated cells leave the colonies and acquire a flat shape (Figure 25B, BF). When we cultured control and Oct4 CKO ES cells in ground state conditions using inhibitors

for Gsk3β and MAPK (Erk1/2) signaling (2i medium) (Ying et al. 2008b) we observed an accumulation of cells with flat morphology outside of colonies only in the Oct4 CKO clone after 5 passages, resembling extraembryonic cells (Figure 25B-D right column, brightfield - BF).

To closer investigate the identity of these cells we performed immunostaining for the endodermal TF Foxa2, pluripotency TFs Oct4, Nanog, Klf4 and Sox2 and surface markers Epcam and Krt8/Troma which are expressed in pluripotent and differentiated cells respectively. Cells within colonies expressed the pluripotency markers Oct4, Nanog, Klf4, Sox2 and Epcam whereas cells with flatter morphology at the edge and outside of colonies expressed of Foxa2 and Troma (Figure 25B-D). Foxa2+, Troma+ cells were only found in Oct4 CKO ESCs and not in control ESCs. By FACS analysis we confirmed that 0,17% of the control and 21,1% of the Oct4 mutant ES cells were Foxa2+ positive in ground state conditions (Figure 25E).

This shows that Oct4 CKO ES cells have a higher propensity to undergo spontaneous differentiation towards Foxa2 and Krt8 expressing cells in ground state conditions (2i, LIF). These cells accumulate over time when cells are expanded under these conditions. The deletion of Oct4 in Foxa2+ CKO cells could then lock the cells in this differentiated state whereas in the control cells might revert back into the pluripotent state.

4.15 Oct4 CKO ES cells differentiate to mesendoderm at the expense of definitive endoderm

Oct4 is involved in the differentiation of ES cells into various lineages in vitro (Zeineddine et al. 2006; Yamada et al. 2013; Thomson et al. 2011; Teo, S. Arnold, et al. 2011; Stefanovic et al. 2009). Oct4 has also been shown to bind to the *T* promotor during endoderm differentiation (Thomson et al. 2011) which indicates a role of Oct4 during segregation of mesoderm and endoderm. It is however still unclear if Oct4 plays a role in lineage formation and segregation when deleted specifically in Foxa2 lineage cells.

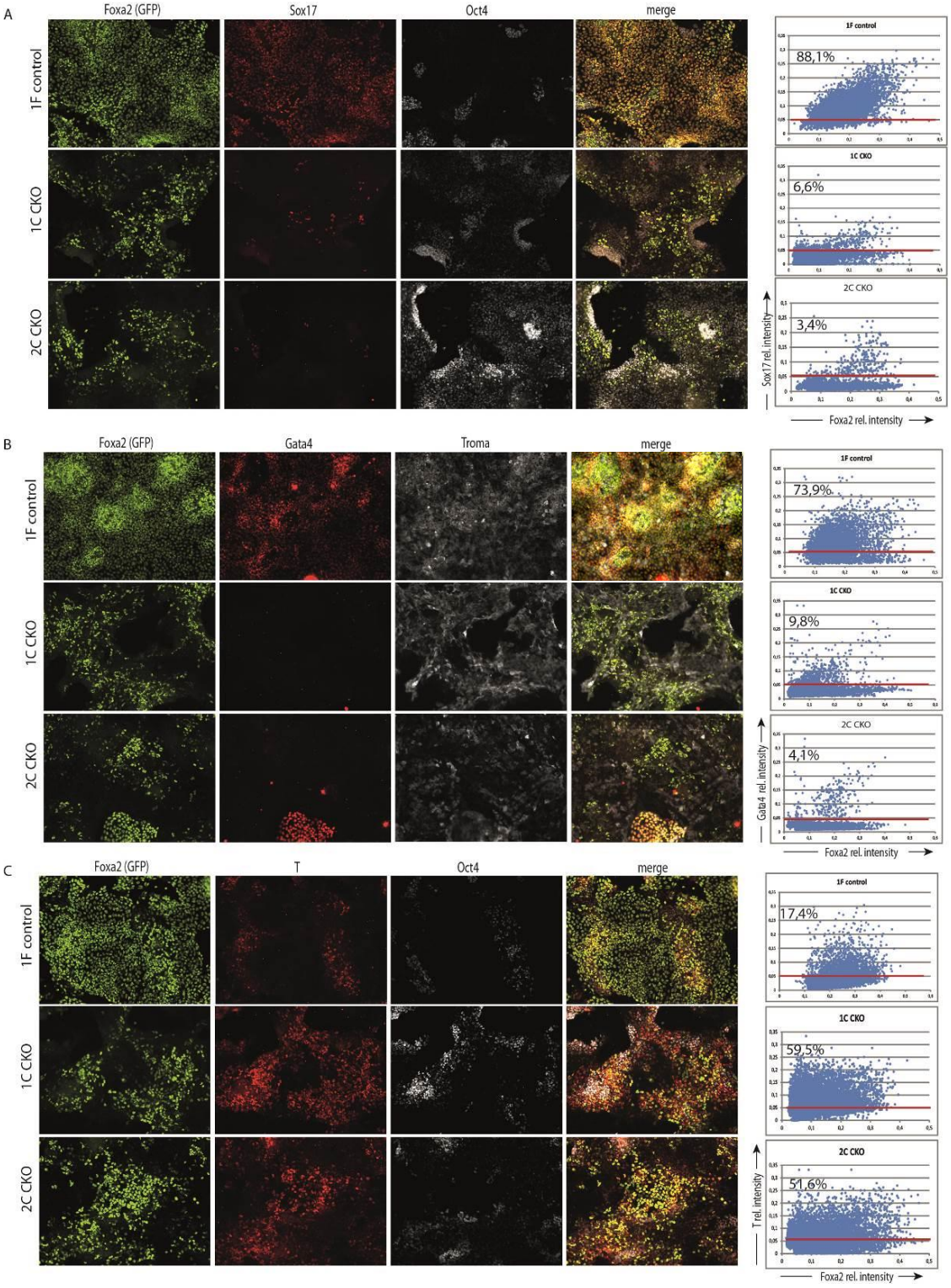

Figure 26: Oct4 CKO cells show defects in lineage segregation

Oct4 control (clone 1F) and CKO (clones 1C and 2C) ES cells were differentiated for 5d to EpiSC and stained for Foxa2 (green), Sox17 (red, A), Oct4 (white, A, C), Gata4 (red, B), Troma (=Krt8, white, B) and T (red, C). Merged images are shown in the right image column. The dotblot in the right column shows relative Sox17 (A), Gata4 (B) and T (C) fluorescent intensities of nuclei on the y-axis and relative fluorescent Foxa2 intensity (A-C) on the

x-axis. Analysis was done using cells profiler software, only Foxa2 positive cells were analyzed. Percentages of cells with a relative intensity >0,05 (red horizontal bar) for Sox17 (A), Gata4 (B) and T (C) are indicated.

To gain deeper insight into the role of Oct4 during endoderm lineage formation and segregation we differentiated control and Oct4 CKO ESCs to EpiSCs and analyzed cell populations by immunohistochemistry (IHC). Antibodies against Sox17 and Gata4 were used as endoderm markers and T (Brachyury) as mesendoderm or axial mesoderm marker.

After 5 days of differentiation 88,1% of Foxa2+ cells co-expressed Sox17 in the control clone. In the two Oct4 mutant clones only 6,6% and 3,4% of these cells showed co-expression of Foxa2 and Sox17 respectively (Figure 26A). Gata4 was expressed in 73,9% of Foxa2+ cells in the control whereas only 9,8% and 4,1% of the cells were double positive in the Oct4 CKO clones (Figure 26B). In contrast the mesendodermal marker T showed the opposite picture. In the control clone 17,4% of the Foxa2+ cells co-expressed T whereas 59,5% and 51,6% of the cells in the two mutant clones were double positive (Figure 26C).

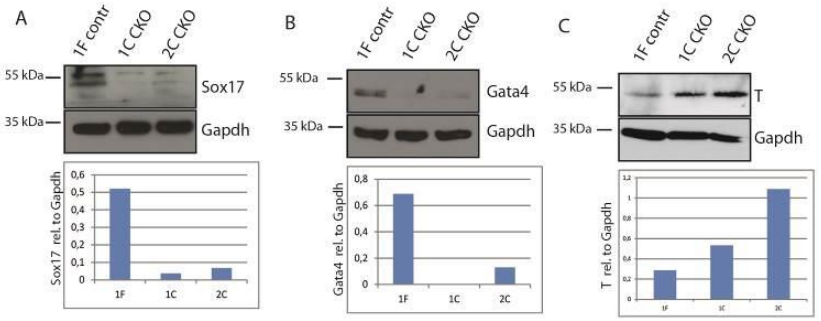

D

Gene	CKO/contr. (epi)	CKO/contr. (endo)
Sox17	N/A	0,34
Gata4	0,64	0,33
Brachyury	4,27	1,61

Figure 27: Confirmation of lineage switch by WB and mRNA analysis
d5 EpiSC or endoderm cells of control (clone 1F) and Oct4 CKO (clones 1C and 2C) were sorted for FVF and used for WB (only EpiSC) and mRNA microarray analysis. For WB antibody staining against T (A), Gata4 (B) and Sox17 (C) is shown. Gapdh was used as control. Graphs show quantification of expression levels relative to Gapdh. (D) Shows Affymetrix MicroArray results of sorted EpiSC (epi) and endoderm (endo) cells. Values show fold change (CKO/control) with a false discovery rate (FDR) <10%.

To confirm these results we performed western blot analysis on FACS sorted Foxa2+ (FVF+) EpiSC (scheme shown in Figure 24A) from control and Oct4 CKO cells. As shown in Figure 27C T protein levels were increased in Oct4 CKO cells compared to control whereas expression of

Gata4 and Sox17 proteins was strongly reduced in Foxa2 expressing cells (Figure 27B and A respectively).

Additionally mRNA expression of cells from 2 CKO clones (1C and 2C) and 2 replicates of the control clone (1F) was analyzed. Oct4 control and CKO ESCs were differentiated with the endoderm or EpiSC protocol and sorted on d5 of differentiation for FVF+ cells. From the sorted cells total RNA was isolated and analyzed by Affymetrix GeneChip.

Sox17 mRNA was reduced in Oct4 CKO cells compared to control only with the endoderm differentiation protocol and not under EpiSC conditions. *Gata4* mRNA levels were lower with both, EpiSC and endoderm differentiation protocols (0,28 and 0,33 respectively) (Figure 27D). In line with the WB results *T* mRNA is increased in the mutant cells with the EpiSC and endoderm differentiation protocol compared to the control (Figure 27D).

These results show that conditional deletion of Oct4 in the Foxa2 expressing cells during *in vitro* differentiation results in a fate switch towards Foxa2+, T+ axial mesoderm cells at the expense of Foxa2+, Sox17+ or Gata4+ definitive endoderm. This suggests that Oct4 is involved formation of DE, which we have also observed in embryos.

4.16 **Oct4 CKO embryoid bodies show aberrant differentiation**

Generation of embryoid bodies (EBs) from ESCs is a 3 dimensional differentiation approach to study lineage segregation *in vitro*. This system can also be used to mimic processes of early embryonic development, like symmetry breaking, axial organization and germ layer specification in cell culture (Warmflash et al. 2014; van den Brink et al. 2014).

To decipher differences in differentiation capacity upon Oct4 deletion we differentiated control and Oct4 CKO ES cells to embryoid bodies (EBs)(scheme in Figure 28A). After 5 days of differentiation EBs were harvested for analysis by IHC. In EBs from Oct4 CKO ES cells less Foxa2 and Sox17 expressing cells were observed compared to the control (Figure 28B). No significant difference in diameter of EBs was observed, indicating that Oct4 deletion does not interfere with cell proliferation (Figure 28D).

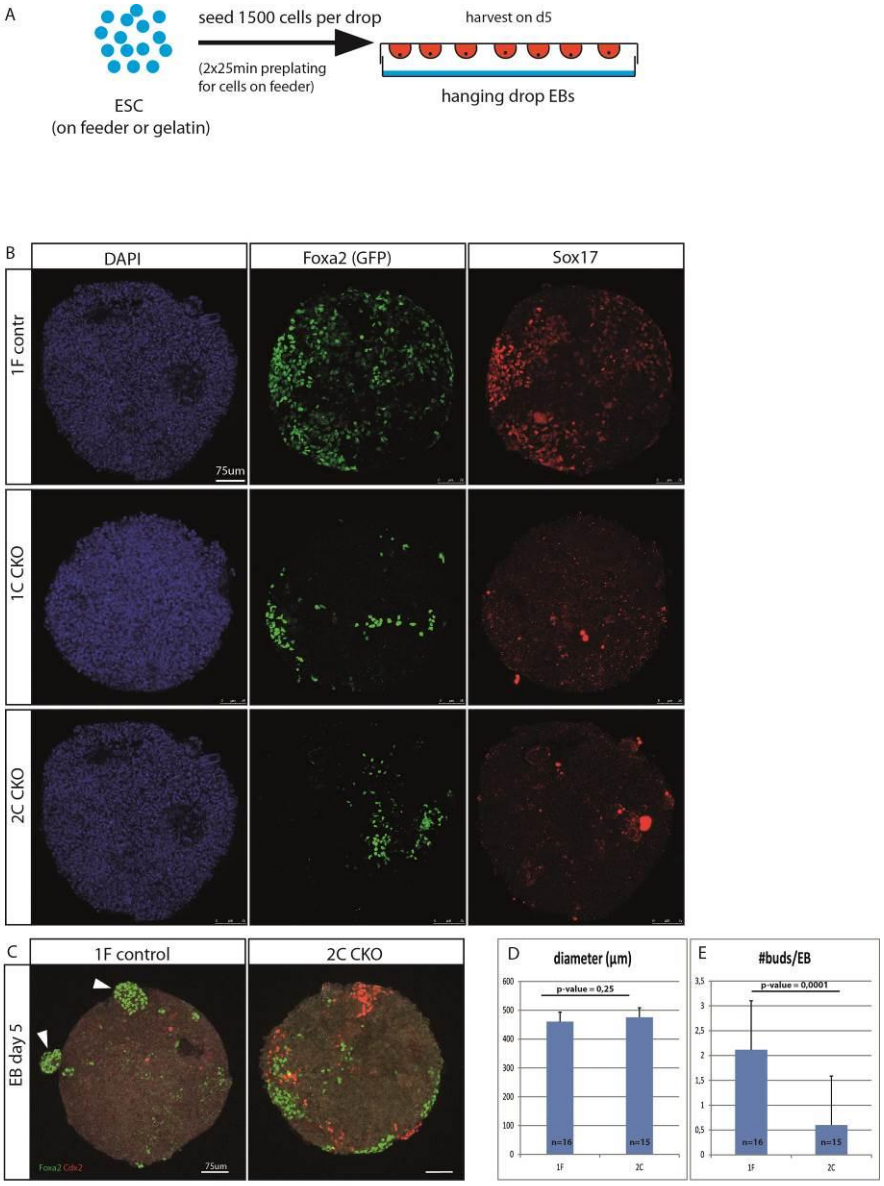

Figure 28: Analysis of Oct4 CKO differentiation by EB formation
(A) Scheme of EB differentiation from ESCs; feeder free ESCs are resuspended at 1500 cells per 25µl in serum free medium and placed as hanging drops on the lid of a tissue culture dish. (B) EBs are harvested after 5 days and stained for Foxa2 (green), Sox17 (red) and DAPI (blue). (C) Oct4 CKO EBs form less Foxa2+ buds than control cells (white arrow heads). Diagrams show quantification of diameter (D) and number of buds per EB (E).

Interestingly we noted a significantly lower number of Foxa2+ protrusions (buds) in Oct4 CKO compared to control EBs (Figure 28C and E). These protrusions might represent early organ buds but so far this has not been described in the literature.

It has been shown that low levels of Oct4 lead to differentiation of ES cells towards the TE lineage (Niwa et al. 2000). To analyze the effect of Oct4 deletion on TE differentiation we stained EBs for Cdx2 which, together with Oct4, is involved in trophectoderm lineagfe segregation (Niwa et al. 2005b). Quantification showed that in control 11,8 cells per EB are Cdx2+ whereas in the two Oct4 mutant clones 53,6 and 47 cells per EB are Cdx2+ respectively (Figure 29B). These cells also don't express the endodermal marker Foxa2 which could mean that it was never turned on or expression was only temporary in these cells. Since specific Cdx2+ hindgut differentiation has not been shown in EBs it is possible that the formed cells are TE. This suggests that reduced Oct4 levels result in differentiation of ESCs into TE.

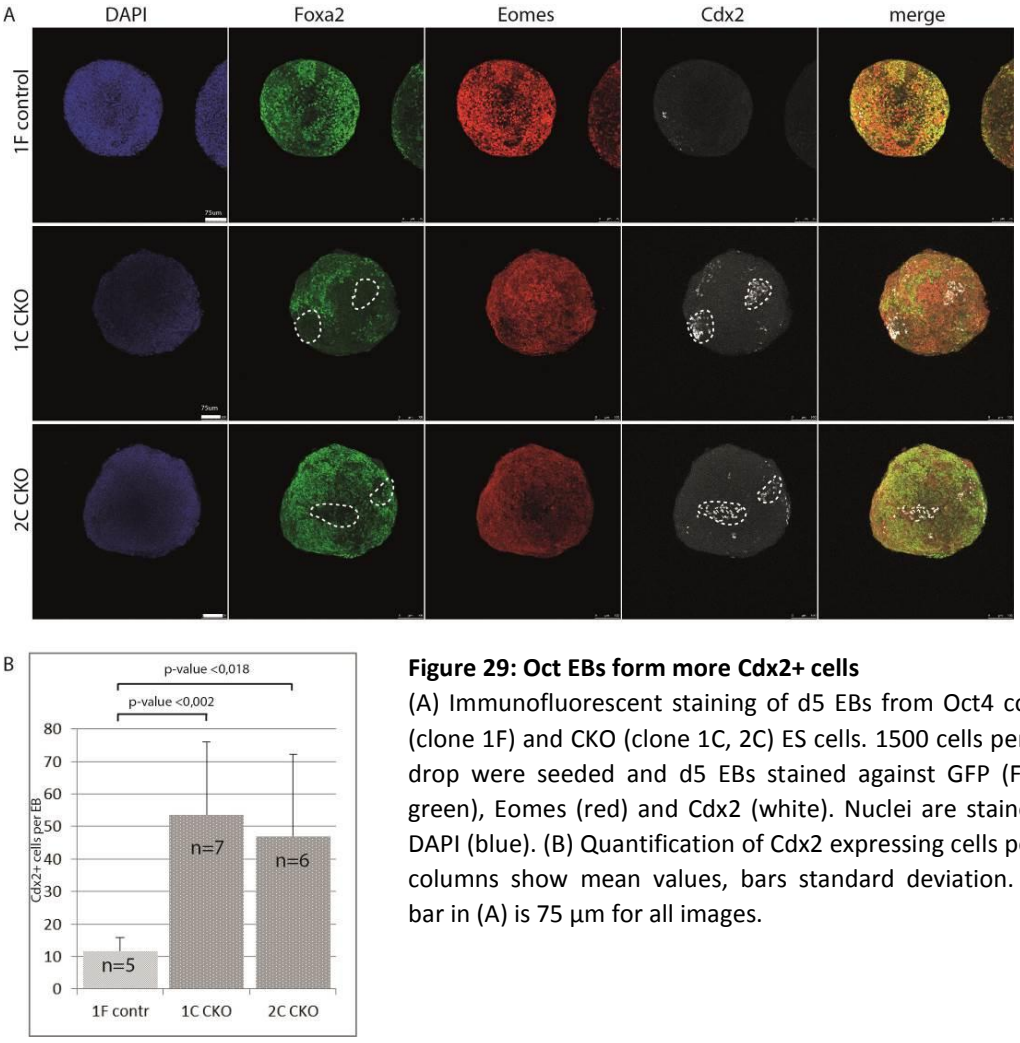

Figure 29: Oct EBs form more Cdx2+ cells
(A) Immunofluorescent staining of d5 EBs from Oct4 control (clone 1F) and CKO (clone 1C, 2C) ES cells. 1500 cells per 25ul drop were seeded and d5 EBs stained against GFP (Foxa2-green), Eomes (red) and Cdx2 (white). Nuclei are stained by DAPI (blue). (B) Quantification of Cdx2 expressing cells per EB, columns show mean values, bars standard deviation. Scale bar in (A) is 75 µm for all images.

4.17 **Oct4 is required for hindgut endoderm differentiation in vitro**

Since Oct4 mutant embryos have defects in hindgut development and patterning we wanted to investigate if these defects can be recapitulated in vitro. We adapted a hindgut specific differentiation protocol (Spence et al. 2010) to drive control and Oct4 CKO ES cells towards hindgut endoderm, monitored by expression of the endodermal markers Foxa2, Sox17 and the posterior marker Cdx2 (Sherwood et al. 2011).

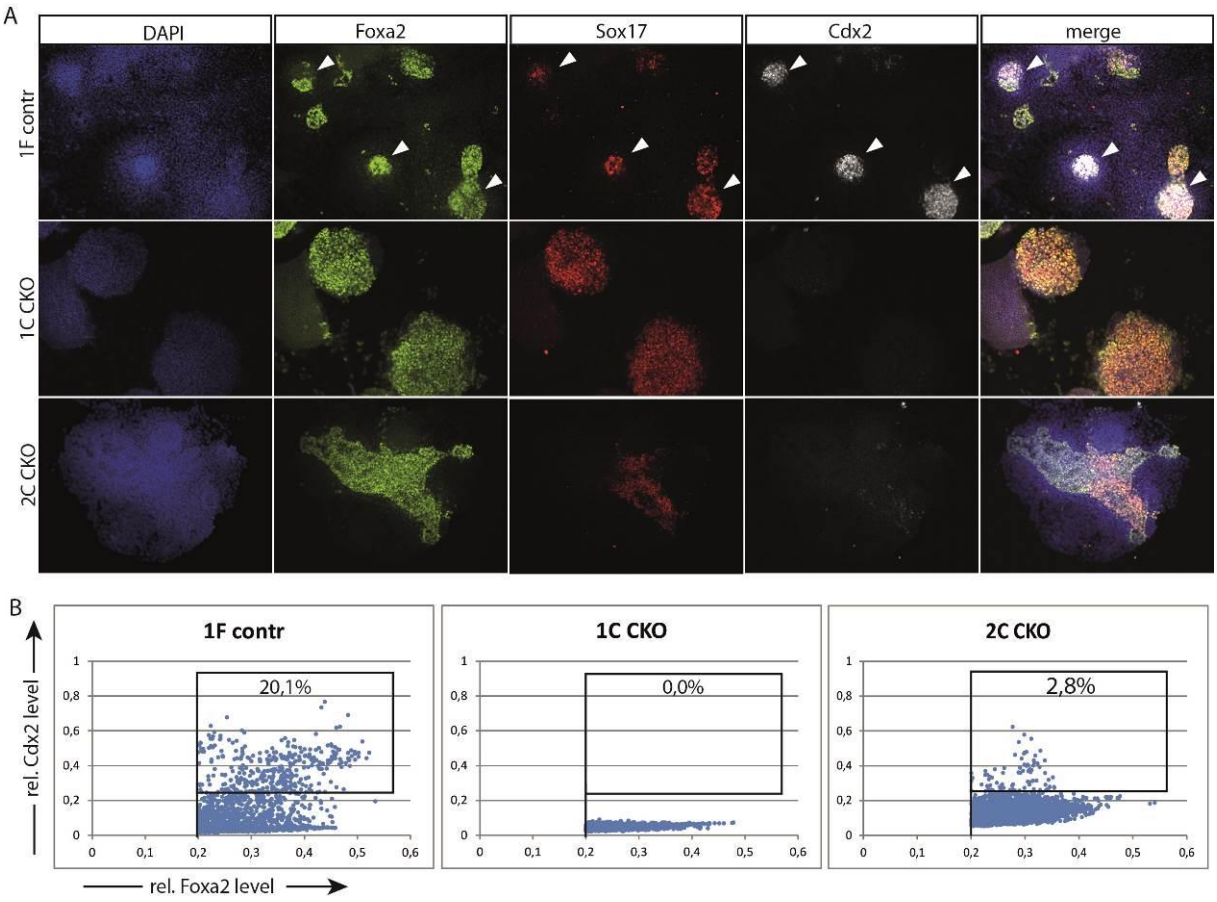

Figure 30: Oct4 CKO ES cells fail to form hindgut endoderm *in vitro*
Control (clone 1F) and Oct4 CKO (clone 1C, 2C) ES cells were differentiated to hindgut endoderm for 5 days in serum free N2B27 medium supplemented with 10ng/ml ActivinA and 20ng/ml Fgf4 (adapted from Spence et al., 2010). (A) shows representative images of control and CKO ES cells stained against Foxa2 (green), Sox17 (red) and Cdx2 (white). Nuclei are counterstained with DAPI (blue). White arrowheads show posterior endoderm colonies co-expressing Foxa2, Soxa17 and Cdx2 in control cells. (B) Quantification of relative Foxa2 and Cdx2 fluorescence intensity by Cell profiler software. Percentage of cells with a rel. Foxa2 level >0.2 and Cdx2 level >0.25 is shown.

After 5 days of differentiation ES cells have formed Foxa2, Sox17 and Cdx2 expressing hindgut endoderm (Figure 30A, first row white arrow heads). In control cells we observed

several colonies with cells co- expressing Cdx2, Sox17 and Foxa2 which resemble hindgut endoderm (Figure 30A, clone 1F). In the Oct4 CKO clones Foxa2+, Sox17+ colonies did not show co-expression of Cdx2 (Figure 301C and 2C). Quantification of fluorescent signals by Cellprofiler software revealed, that 20,1% of Foxa2+ cells in the control co-expressed Cdx2+ whereas 0% and 2,8% of the Oct4 CKO clones showed co-expression of Cdx2, respectively (Figure 30B).

These results support our observation in embryos, that conditional depletion of Oct4 results in the absence of posterior endoderm and reduced expression of the hindgut marker Cdx2 (Figure 21D and

Figure 13). Hindgut differentiation and patterning were shown to be regulated by Wnt/β-catenin signaling (Gregorieff et al. 2004; Lickert et al. 2000; Martin & Kimelman 2008; Pilon et al. 2006; Sherwood et al. 2011) which indicates that this pathway could be affected by Oct4 deletion.

4.18 Conditional deletion of Oct4 during differentiation results in a strong reduction of active Wnt and Tgf-β signaling

The most important pathways involved in early embryonic development include canonical Wnt signaling and Tgf-β/nodal signaling, which play important roles in formation of the primitive streak and endoderm development (Conlon et al. 1994, Lickert et al. 2002, Beddington & Robertson 1999). Since we have observed defects in endoderm formation in Oct4 mutant cells and embryos we asked if activation of these signaling pathways is affected by Oct4 deletion.

To analyze activation of these signaling pathways we differentiated one control and two Oct4 CKO ES cell lines to EpiSCs and sorted the FVF+ cells for WB analysis. Antibodies against active β-catenin (act β-cat) were used to monitor active canonical Wnt signaling and phospho-smad2/3 (p-smad2/3) for activated Tgf-β/Nodal signaling.

Protein levels of active β-catenin were strongly reduced in both mutant clones compared to the control, when normalized to the housekeeping gene Gapdh (Figure31B). Additionally a

strong reduction of p-smad2/3 levels in both Oct4 CKO clones was detected (Figure31A). From these results we conclude that the absence of Oct4 impairs the activation of two major endodermal signaling pathways, canonical Wnt and Tgf-β/nodal signaling.

The PI3K/Akt pathway has been linked to cell proliferation (Gesbert et al. 2000; Martelli et al. 2012). A potential cause of the endodermal phenotype we see *in vitro* could be defects in proliferation of differentiated cells upon deletion of Oct4. To analyze this we used an antibody against activated Akt phosphorylated at Ser473 (p-Akt) for WB analysis. In the two CKO clones p-Akt levels were moderately decreased compared to the control clone

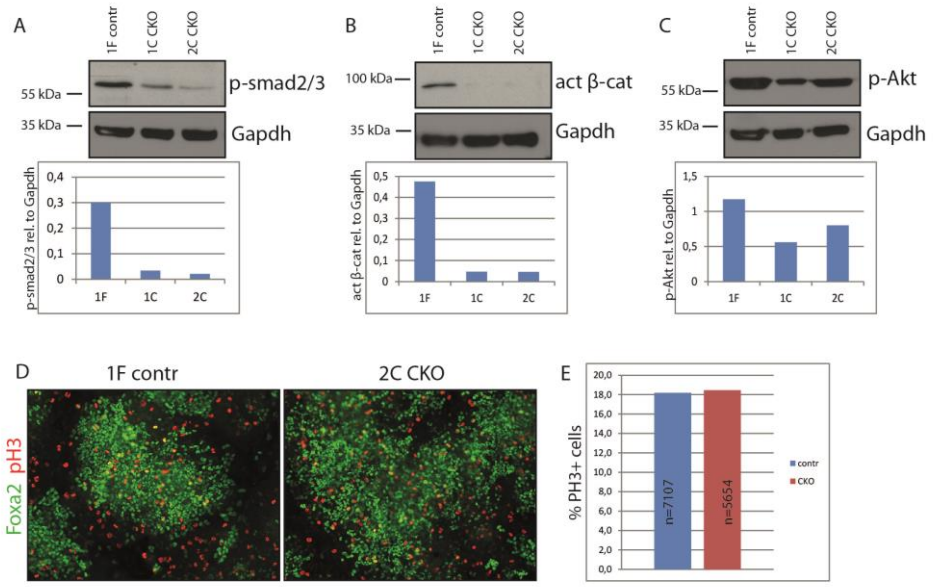

Figure 31: Oct4 depletion results in reduced Wnt, Tgf-β and Akt signaling.

Sorted control (1F) and Oct4 CKO (1C and 2C) EpiSCs were analyzed by WB for (A) Tgfβ signaling (p-Smad2/3), (B) Wnt signaling (act β-catenin), and (C) Akt signaling (p-Akt). Gapdh was used as loading control. Graphs show levels of protein relative to Gapdh. (D) d5 control and CKO cells were stained for Foxa2 (green) and phospho histone H3 (PH3, red) to monitor proliferation. (E) shows % of PH3 positive proliferating cells within the Foxa2+ cell population.

(Figure31C). To test if Oct4 depletion has have an effect on the number of proliferating cells during differentiation we stained control and mutant ES cells on d5 of EpiSC differentiation with the endodermal marker Foxa2 and phospho-histone H3 (PH3) which marks proliferating cells (Figure31D). Quantification of PH3 positive cells within the Foxa2+ cells showed that 18,2% of the control and 18,5% of the Oct4 CKO cells were proliferating (Figure31E).

This indicates that the conditional deletion of Oct4 has no effect on the proliferation of the differentiated Foxa2+ cell population but rather suggests a role in the activation of Wnt and Tgf-β/Nodal signaling pathways.

4.19 mRNA analysis shows differentially regulated genes in Oct4 mutant ES cells are associated with germ layers, Tgf-β and Wnt signaling

To gain more insight into the transcriptional changes resulting from the deletion of Oct4 we analyzed mRNA expression of differentiated control and Oct4 mutant ES cells. One control and two Oct4 CKO clones were differentiated to endoderm or EpiSCs for 5 days, FVF positive cells sorted by FACS and total RNA isolated for Affymetrix GeneChip analysis (scheme in Figure 24A). Comparison of control and Oct4 CKO EpiSCs showed differential regulation of 3970 genes with a ratio >1,3x and a false discovery rate (FDR) of <10%. Of these, 2187 were upregulated and 1783 down regulated and of the regulated genes 982 were changed by more than two fold. With the endoderm protocol 3750 genes were differentially regulated >1.3x, of which 1994 were upregulated and 1756 down regulated. From these regulated genes 660 are changed by more than two fold (heatmap overview shown in Figure 32A).

To identify potential direct effects of Oct4 on gene regulation we compared published datasets of Oct4 bound genes in ES cells to our expression data (Chen et al. 2008; Cole et al. 2008; Kim et al. 2008; Mathur et al. 2008; Marson et al. 2008b; Loh et al. 2006; Liu et al. 2008). Of the differentially regulated genes we found 24,5% (endoderm protocol) and 24,0% (EpiSC protocol) to be directly bound by Oct4 under pluripotent conditions in more than two studies (Figure 32F and G). This indicates that Oct4 might directly be involved in the regulation of these genes.

Genes down regulated in Oct4 CKO cells in EpiSC differentiation had an over representation of GO terms related to “endoderm”, “intestines”, “mesoderm”, “pancreas” and “cardiac” (Figure 32B). Among upregulated genes “mesoderm” and “primitive streak” are over

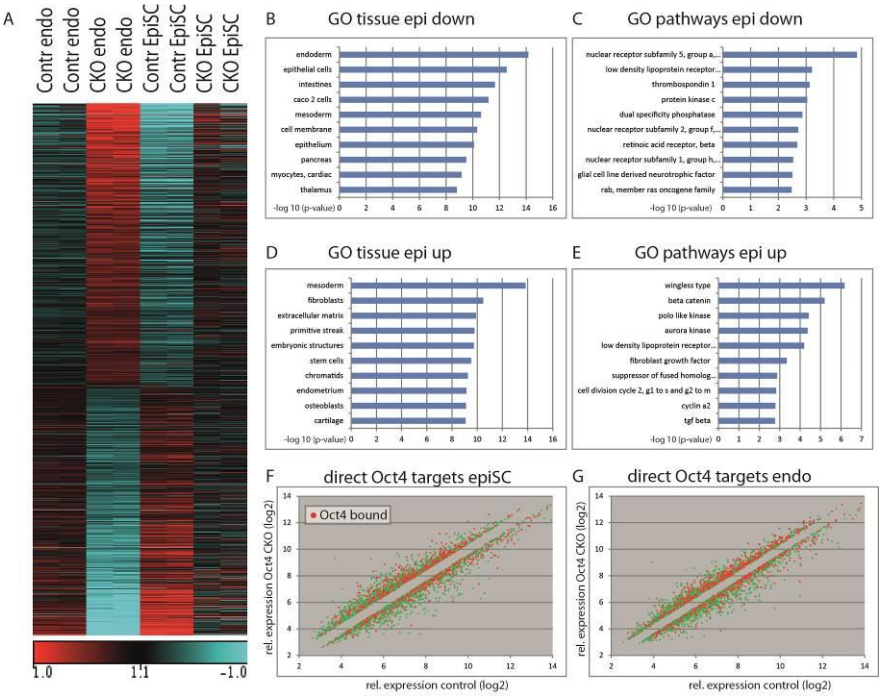

H

		epi	endo
known node/ notochord	Foxd4	2,29	0,33
	Foxa1	N/A	N/A
	T	4,27	1,61
	Foxa2	N/A	1,46
	Shh	3,15	0,64
	Car3	N/A	2,58
	Cthrc1	1,80	N/A
	Chrd	2,50	1,71
	Tmprss2	0,45	0,76
	Dynlrb2	N/A	0,58

novel node/ notochord	Gal	N/A	N/A
	Prnp	0,32	0,72
	Pim1	2,54	2,17
	Smoc1	N/A	N/A
	Gstm5	1,98	N/A
	Cyb561	N/A	N/A
	1700027A23	N/A	0,30
	Josd2	N/A	N/A
	Mif1	0,65	0,48
	1700009P17	N/A	0,39

I

		epi	endo
known DE	Sox17	N/A	0,34
	Cer1	0,89	0,22
	Foxa2	N/A	1,46
	Foxa1	N/A	N/A
	Trh	N/A	0,73
	Shh	3,15	0,64
	Gprc5c	N/A	N/A
	Cyp26a1	0,58	0,21
	Tmprss2	0,45	0,76
	Cpn1	0,32	N/A

novel DE	Cldn4	N/A	N/A
	Itga3	1,92	1,95
	Cpm	0,28	0,34
	Efhd2	N/A	N/A
	Ppp1r14a	N/A	N/A

J

gene	epi	endo
2810474O19Rik	1,45	N/A
Acin1	N/A	1,42
Amotl2	N/A	1,45
Atf2	N/A	1,32
Cad	1,99	N/A
Creb1	N/A	1,32
Ctbp2	N/A	1,55
Cul4b	N/A	1,34
Dnmt3a	1,59	1,71
Ep400	1,74	N/A
Frg1	1,35	N/A
Gatad2a	N/A	1,43
Hells	1,42	N/A
Hira	N/A	1,29
Ino80	1,66	N/A
L1td1	N/A	2,43
Mga	2,32	2,25
Mitf	1,38	N/A
Msh6	1,33	N/A
Mta3	1,51	1,72
Ogt	N/A	-1,58
P4ha1	N/A	-1,34
Phc1	1,67	1,37
Phf17	1,82	2,09
Pml	1,40	N/A
Rbm14	N/A	-1,36
Rbpj	-1,37	N/A
Rif1	N/A	1,55
Rpa1	1,65	1,44
Sall4	1,68	-1,35
Smarca5	1,33	1,48
Sox2	2,17	N/A
Sp1	1,36	N/A
Wdr5	1,42	1,35
Zfhx3	1,54	1,57
Zfp462	1,42	N/A
Zic2	2,45	1,46

Figure 32: Microarray analysis of differentiated Oct4 CKO ES cells

(A) Heatmap analysis of 2 biological replicates of one control clone and two Oct4 CKO clones which were differentiated to EpiSC or endoderm. (B) and (D) shows GO term analysis (tissues) for genes which are down or upregulated in Oct4 CKO cells compared to control during epiSC differentiation. (C) and (E) shows GO term analysis (pathways) for genes which are down or upregulated in Oct4 CKO cells compared to control during epiSC differentiation. (F) and (G) show differentially regulated genes which are found as direct targets in >2 published datasets in ES cells. Each dot shows the relative expression values in control and Oct4 CKO ES cells, red dots are genes bound by Oct4. Comparison of deregulated genes with known and novel notochord (H) and definitive endoderm (DE) (I) markers published in Tamplin et al. 2008. Ratios show mRNA expression of Oct4 CKO/control in epiSC and endoderm protocol (J) Shows Oct4 interacting proteins (van den Berg et al. 2010, Pardo et al. 2010) deregulated in differentiated Oct4 CKO ES cells. (red – downregulated, green – upregulated, N/A – no significant change).

represented (Figure 32D). We also identified signaling pathways important for embryonic development like Wnt, Fgf and Tgf-β within the deregulated genes (Figure 32E).

This suggests that deregulated genes in differentiated Oct4 CKO ES cells are involved in embryonic development.

Since Oct4 is depleted in node, notochord and definitive endoderm we more specifically looked at selected markers for these tissues (Tamplin et al. 2008). We observed that several genes involved in node and DE development, like *Cer1, T Sox17* and *Chordin* are misregulated in differentiated Oct4 CKO ESCs (Figure 32H and I).

A

gene	CKO/control epi	endo
2900092E17Rik	1,49	N/A
Adamts9	N/A	2,16
Ambp	0,34	N/A
Ang	0,44	0,35
Arhgef17	N/A	1,29
Asxl1	N/A	1,49
Cdkn1c	1,81	N/A
Commd3	N/A	0,73
Cpn1	0,32	0,64
Csrp1	0,41	0,77
Ctsz	0,70	0,75
Dlk1	0,57	N/A
Dll1	0,42	0,41
Dnahc2	N/A	N/A
Dynlt3	0,72	0,61
Ece1	N/A	1,42
Enc1	0,69	N/A
Flrt2	0,71	0,58
Flrt3	0,48	0,46
Foxa2	N/A	1,46
Gm98	0,54	0,63
Hhex	0,38	0,22
Hkdc1	0,53	N/A
Hnf1b	N/A	0,67
Hspg2	1,84	1,64
Id2	0,40	0,61
Krt8	0,59	0,58
Lcor	0,67	0,66
Meis1	N/A	N/A
Ncald	1,50	N/A
Plekha6	0,53	0,76
Pon2	0,72	0,63
Prss23	0,35	N/A
Rbp1	0,70	1,86
Rnase4	N/A	0,43
Sepp1	0,29	2,23
Serinc2	0,60	N/A
Sorbs2	2,15	N/A
Sox9	1,44	N/A
Spon1	3,11	N/A
Stard10	0,54	0,69
Tmc4	0,52	0,47
Tmem27	N/A	0,70
Tollip	N/A	1,36
Trak1	N/A	1,64
Vtn	3,37	N/A
Wls	1,75	N/A

B

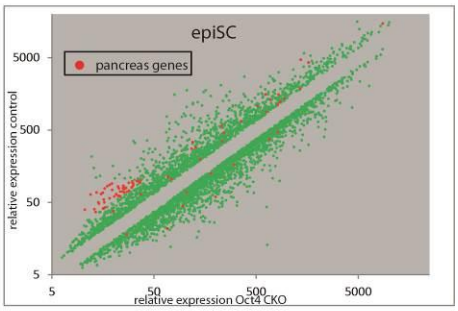

C

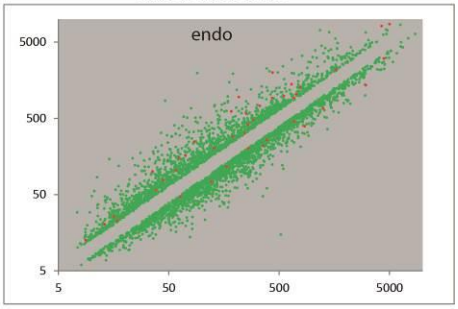

Figure 33: Pancreas specific genes are down regulated in Oct4 CKO epiSCs and endoderm
Genes specific for dorsal and ventral pancreas in mouse embryos (Rodríguez-Seguel et al. 2013) are compared with the mRNA expression profiles of EpiSC and endoderm differentiation of control and Oct4 CKO ES cells. (A) List of pancreas specific genes and the respective fold changes (FC, CKO/control) in EpiSC and endoderm differentiation with a false discovery rate (FDR) <10%. Green cells show upregulated genes and red cells down regulated genes (CKO vs. control). Dotblot analysis shows relative mRNA expression of CKO and control samples in EpiSC (B) and endoderm (C). Green dots mark individual genes, red dots show genes which are pancreas specific.

Interestingly we also noted that almost all genes which have been described to interact with Oct4 in two studies (van den Berg et al. 2010; Pardo et al. 2010) are upregulated in Oct4 CKO

cells (Figure 32J). This suggests that these genes are negatively regulated by Oct4 or might be upregulated as compensation for the loss of Oct4.

Since the GO term “pancreas” was amongst the most significant tissues in the down regulated geneset (Figure 32B) we compared our RNA expression data to published genes which are specifically expressed in E10.5 dorsal and ventral pancreatic progenitor cells (Rodríguez-Seguel et al. 2013). Expression data showed that the majority of pancreas specific genes are lower expressed in Oct4 CKO than in control cells during endoderm and EpiSC differentiation (67,7% and 73,5% of genes respectively)(Figure 33A-C). This might suggest that early patterning of the endoderm and initiation of organ formation is affected by Oct4 depletion.

These results show that genes misregulated upon Oct4 depletion are linked to gastrulation processes and signaling pathways important for embryonic development.

4.20 **Genes bound by Oct4 are linked to germlayers, primitive streak and signaling**

Since we have shown that conditional deletion of Oct4 leads to changes in expression of important developmental regulators, we were interested if these genes are direct Oct4 targets. We thus generated a chromatin immunoprecipitation-sequencing (ChIP-seq) dataset of Oct4 in pluripotent (d0) Foxa2-Venus-Fusion; Sox17-mCherry-Fusion (FVF;SCF) ESCs to identify genes which are directly bound by Oct4 (in collaboration with F. Cernilogar and G. Schotta, LMU). These ESCs harbor fluorescent reporters for Foxa2 (Foxa2-Venus fusion; FVF) and Sox17 (Sox17-mCherry fusion; SCF) which allow FACS sorting of pluripotent and endodermal cell populations (Burtscher et al. 2013; Burtscher et al. 2012).

We were able to identify 5456 Oct4 binding sites in d0 ESCs. These binding sites were correlated with 3904 know genes by ChIPseek software analysis (T.-W. Chen et al. 2014) (Figure 34). Oct4 binding sites are mostly found in intergenic regions (62,2% of target genes) but also in introns (28,2%), exons (0,9%) and in promoters (6,4%) (Figure 34A). We observed that binding sites of Oct4 peak around transcriptional start sites (TSS) (Figure 34A right graph) which indicates a regulatory function. For quality control we compared our results to

published Oct4 ChIP data on pluripotent mouse ESCs (Mathur et al. 2008; Marson et al. 2008b; Loh et al. 2006; Liu et al. 2008; Kim et al. 2008; Chen et al. 2008; Cole et al. 2008). 71,6% of the genes we identified as Oct4 targets were also described in at least one other study whereas 28,4% were novel Oct4 bound genes (Figure 34B).

Within Oct4 target genes GO terms related to Fgf, Wnt, Tgf-β signaling pathways and also cadherins were over represented (Figure 34C). These genes are also linked to tissues of all three germ layers (mesoderm, ectoderm and endoderm) and to rhombencephalon, prosencephalon and neurons (Figure 34D).

Our data indicate that genes bound by Oct4 in pluripotent ESCs are associated with embryonic tissues like mesoderm, PS and endoderm and also important signaling pathways like Wnt, Tgf-β and Fgf. In pluripotent cells this suggests that Oct4 represses germ layer specific factors and signaling pathways.

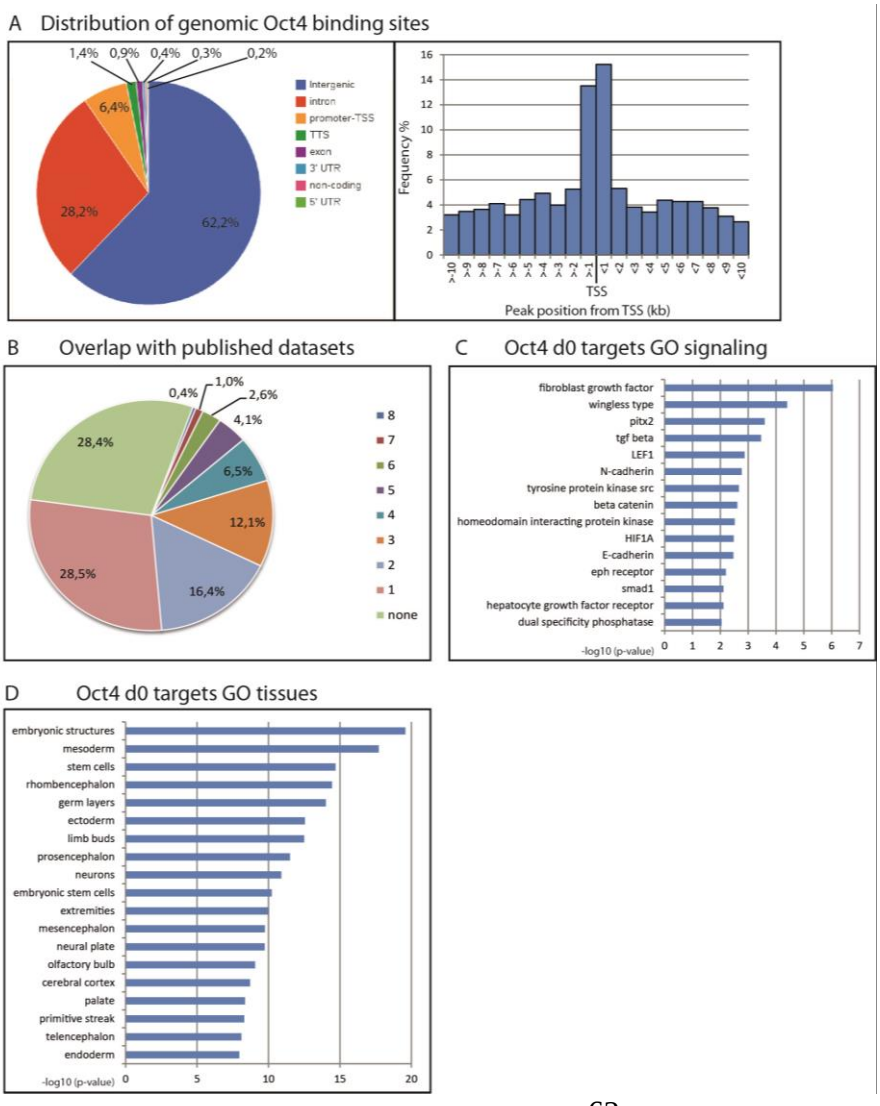

Figure 34: Oct4 targets in pluripotent mES cells
(A) Pie chart shows the distribution of Oct4 binding sites within the genome relative to transcriptional start sites (TSS), the bar graph on the right shows the distribution +/-10kb around TSS. (B) Shows the overlap of identified Oct4 bound genes with published datasets. GO terms for signaling pathways (C) and tissues (D) are shown with bars representing –log p-values.

4.21 **Oct4 bound genes in differentiated cells**

It has been demonstrated that Oct4 expression can still be detected at early time points of human ESC differentiation and diminishes thereafter (Teo, S. J. Arnold, et al. 2011).

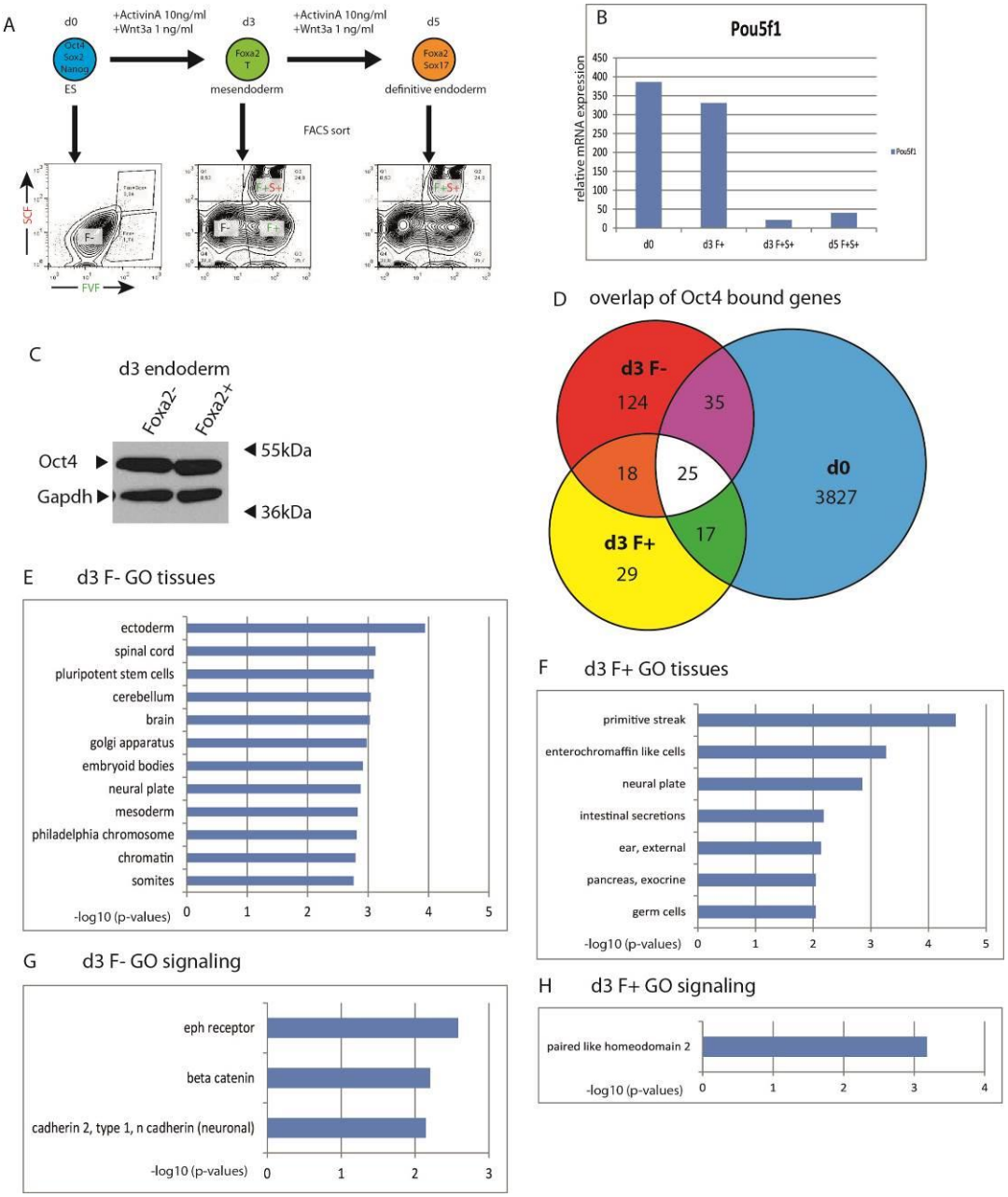

Figure 35: Oct4 ChIP-seq on d3 endodermal cells

(A) scheme of endoderm differentiation of FVF;SCF cells and sorting of cell populations for analysis: pluripotent (d0) mesendoderm (d3 F+) and definitive endoderm (d3 and d5 F+S+) cells were sorted. Foxa2- cells were sorted on d3 (d3 F-). (D) Venn diagram shows overlaps of Oct4 bound genes between d0, d3 F- and d3 F+ cells. Sizes are not to scale. GO term analysis in d3 F- cells for tissues (E) and signaling (G) and in d3 F+ cells for tissues (F) and signaling (H). Bars show –log10 p-values.

Our results show that Oct4 function is required during early endoderm commitment which suggests that Oct4 directly regulates activation of endodermal genes.

To analyze the expression of Oct4 during endoderm commitment we differentiated FVF;SCF ESCs using Activin A and Wnt3a, and sorted Foxa2+, resembling mesendoderm, and Foxa2+Sox17+ cell populations on d3 of differentiation (d3F+ and d3F+S+ respectively). We also sorted Foxa2 and Sox17 expressing cells at d5 (d5F+S+) of endoderm differentiation which represent definitive endoderm (Figure 35A). We then analyzed Oct4 expression by RNA-seq analysis. Our results confirm that in the d3F+ cells Oct4 is still expressed at a level comparable to pluripotent ESCs (d0) whereas in the cell populations expressing Foxa2 and Sox17 on d3 and d5 Oct4 expression is strongly reduced (Figure 35B).

We also wanted to demonstrate Oct4 expression in early endoderm on protein level. We thus sorted Foxa2 negative (F-) and positive (F+) cells at d3 of endoderm differentiation and examined Oct4 protein level by western blot analysis. Oct4 protein levels are comparable in F- and F+ cells which is consistent with mRNA expression (Figure 35C).

As we are interested in Oct4 function during early endoderm formation we asked if Oct4 bound genes change during the early endoderm differentiation compared to pluripotent cells. For this we performed ChIP-seq analysis for Oct4 on FACS sorted d3F- and F+ endoderm cells (Figure 35A). d3F- cells are an interesting population since they have been exposed to Activin and Wnt signaling but did not start expression of endodermal TF Foxa2 or Sox17. We thus speculate that these cells are primed for endodermal differentiation. For d3 F+ cells we combined the results of two independent experiments to compensate for variability in the results and to increase the amount of Oct4 target genes.

We identified 202 genes bound by Oct4 in d3 F- cells and 89 genes bound by Oct4 in d3 F+ cells. 124 genes were only found as Oct4 targets in F- cells, 29 only in F+ cells and 43 were bound in d3 F- and F+ cells (Figure 35D).

Oct4 bound genes in d3F- cells were associated with GO terms ectoderm, spinal cord and brain and also mesoderm and somites (Figure 35E). In these cells Oct4 bound genes are also associated with GO terms like β-catenin and n-cadherin which are important factors during

mesoderm and endoderm formation (Figure 35G). In in d3F+ cells Oct4 target genes are, amongst others, associated with the GO term primitive streak (Figure 35F) which fits well to the developmental states of these cells. We can also find paired-like homeodomain 2 (*Pitx2*) significantly enriched (Figure 35H), which plays an important role in LR patterning of the embryo (Ai et al. 2006; S. D. Bamforth et al. 2004).

These results show that the number of Oct4 bound genes is dramatically reduced upon differentiation, even in cells that still strongly express Oct4. The identified target genes are linked to germ layer formation and patterning which suggests that Oct4 is involved in early differentiation processes.

4.22 **Oct4 target genes show differences in active enhancer marks upon deletion of Oct4**

Core pluripotency factors like Oct4 associate with chromatin modifying complexes to silence developmental genes in pluripotent ESCs to prevent their differentiation (Kim et al. 2008; Chen et al. 2008; Marson et al. 2008, Wang et al. 2006). This repressive function is often carried out by the interaction of Oct4 with transcriptional repression complexes including NuRD and Polycomb (PRC1) (Liang et al. 2008; Ding et al. 2011). On the other hand an activating function of Oct4 on enhancers has also been demonstrated (Buecker et al. 2014; Yang et al 2014). We have shown that Oct4 function is involved in early embryonic development and ESC differentiation and also is bound to several developmental genes during differentiation. We thus asked whether Oct4 could induce a permissive epigenetic environment, e.g. active enhancer marks, which allows activation of developmental genes.

H3K27ac was used as active enhancer mark since it has been shown to discriminate active from poised enhancers (Creyghton et al. 2010b) and it was further demonstrated that Oct4, Sox2 and Nanog bind in the vicinity of H3K27ac marks in ESCs and drive expression of nearby genes (Göke et al. 2011).

Control and Oct4 CKO ESCs were differentiated to EpiSCs and Fox2+ (FVF+) cells were FACS sorted on d5 of differentiation. To analyze the distribution of active enhancer marks we performed histone 3 lysine 27 acetylation (H3K27ac) ChIP-seq analysis on this population.

For further analysis we focused on genes which are bound by Oct4 in pluripotent ES cells to decipher potential direct effects of Oct4.

A

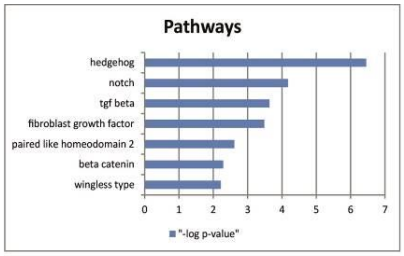

B

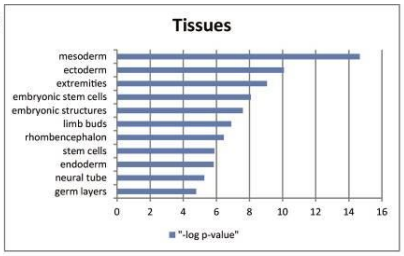

C

Gene Name	microarray epi CKO/contr	microarray endo CKO/contr	microarray E7.5 CKO/contr	Oct4 target in d3 Fox+	H3K27ac ChIP ratio CKO/contr	Gene.Description
Kif26b	0,69	0,66	0,54	X	0,71	kinesin family member 26B
Tcf12					0,68	transcription factor 12
Sox2	2,17				0,68	SRY (sex determining region Y)-box 2
Klf4					0,67	Kruppel-like factor 4 (gut)
Foxh1	0,60	0,71			0,59	forkhead box H1
Tcf7l1					0,55	transcription factor 7 like 1 (T cell specific, HMG box)
Fgfr2		0,63			0,55	fibroblast growth factor receptor 2
Lefty1				X	0,54	left right determination factor 1
Notch1	3,22	1,79			0,42	notch 1
Sema6d	0,59	0,53	1,96	X	0,42	sema domain, transmembrane domain (TM), and cytoplasmic domain, (semaphorin) 6D
Hoxb13					0,37	homeobox B13
Gadd45g	0,52	0,52	0,56		0,36	growth arrest and DNA-damage-inducible 45 gamma
Hoxd12					0,33	homeobox D12
Sox17		0,34			0,26	SRY (sex determining region Y)-box 17
Fzd8	0,72	0,32	1,64		0,23	frizzled homolog 8 (Drosophila)
Six3		0,54			0,15	sine oculis-related homeobox 3

D

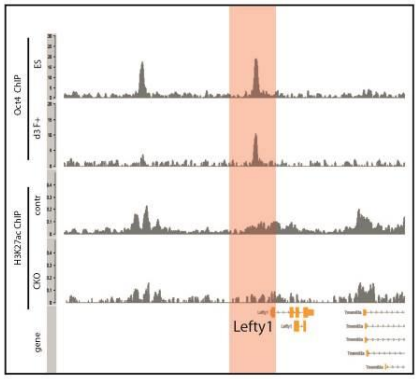

E

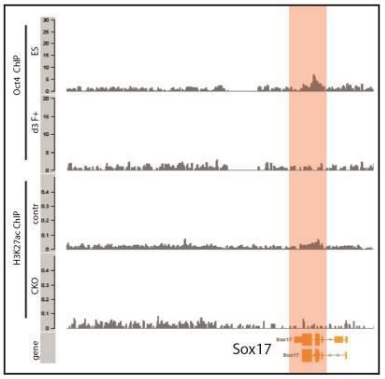

F

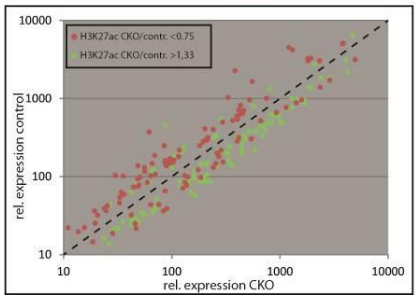

Figure 36: Changes in active enhancer mark H3K27ac in Oct4 CKO ES cells during differentiation

(A and B) GO term analysis of 300 genes with the strongest reduction in active enhancer mark H3K27ac in differentiated Oct4 CKO/control ESCs. Examples of binding sites on Lefty1 (D) and Sox17 (E) genomic loci. Top two plots show binding of Oct4 in FVF;SCF pluripotent (ES) and endodermal (d3F+) cells populations. Bottom two plots show peaks of H3K27ac in control and Oct4 CKO ESCs. Orange box marks the Oct4 bound region in both loci. (F) Shows correlation of mRNA expression of differentially expressed genes in Oct4 CKO and control ESCs compared to their change in active enhancer mark. Red dots mark genes with decreased and green dots with increased H3K27ac ratios in CKO/control cells.

We found 250 genes with an increase in H3K27ac in CKO cells compared to control and 651 genes with a decrease of more than 1.33 fold. *Lefty1*, a factor involved in LR asymmetry determination, had reduced H3K27ac levels in mutant cells but was not differentially expressed in differentiated CKO ESCs (Figure 36C and D). Also the endodermal TF *Sox17* showed a reduction in H3K27ac levels in Oct4 CKO cells and also mRNA expression was reduced in Oct4 CKO endodermal cells (Figure 36C and E).

Overall, our results show that genes with the strongest reduction in H3K27ac levels in Oct4 CKO cells are associated with GO terms like Hedgehog, Notch, Tgfβ and Wnt signaling pathways (Figure 36A). These genes are linked to tissues like mesoderm, ectoderm, endoderm and also neural structures like rhombencephalon and neural tube by GO term analysis (Figure 36B). When we look in more detail at genes with reduced H3K27ac levels upon Oct4 deletion we find factors like *Sox17, Sema6d and Foxh1* which are involved in endoderm formation, cardiac morphogenesis as well as Tgf-β signaling respectively (Figure 36C) (Kanai-Azuma et al. 2002; Toyofuku et al. 2004; Labbé et al. 1998).

Correlation of differentially regulated genes with active enhancer marks shows that genes with increased H3K27ac levels upon Oct4 deletion (Figure 36F red dots) are also higher expressed in Oct4 mutant cells whereas genes with reduced H3K27ac levels (Figure 36F green dots) also have a reduction in expression levels Oct4 CKO cells.

This indicates that expression of Oct4 target genes is correlated with their enhancer activation by H3K27ac which is dependent on the presence of Oct4 during early endoderm differentiation.

Taken together our analysis of Oct4 CKO embryos and ESC in vitro differentiation suggests that the function of Oct4 is required during early endoderm commitment for proper activation of Tgf-β and Wnt signaling but also the Shh pathway (Table 1A). Expression data also suggests that Oct4 is required for proper patterning of the embryos as seen by down regulation of *Hox* and *Cdx* genes (Table 1). Furthermore mRNA expression and ChIP-seq data indicates that Oct4 is also involved in processes like LR asymmetry, somite formation, cardiac

specification, PCP and EMT (Table 1B). We were able to demonstrate defects in somite formation and LR determination in Oct4 CKO embryos (Figure 12, Figure 16) which is in concordance with the observed transcriptional changes.

	mRNA expression (CKO/contr)			ChIP-seq for Oct4 on FVF;SCF cells			ChIP-seq for H3K27ac (CKO/contr)
Gene	E7.5	Endo	Epi	d0 target	d3 endo F- target	d3 endo F+ target	Epi
Tgfβ/nodal signaling							
Lefty1				1	X	X	0,55
Lefty2	15,48			5			0,94
Nodal	1,78	2,18		6			1,15
Tdgf1	13,56	1,96	4,67	7			0,87
Tgfb1	0,53		0,52	1			
Tgfb2	0,55	1,47	2,25				0,67
Tgfbr2		0,70	0,74				1,37
Tgfbr3	0,75						
Smad3	0,77	1,33					
Smad2			0,68				1,37
Smad6	0,60	0,73	0,71	3			
Foxh1		0,68	0,60	1			0,59
Wnt signaling							
Dkk1	1,62	0,42	1,66	5			
Dkk3	0,77						0,99
Dkk4	0,63						
Wnt3a	0,58			1			
Wnt4	0,66						
Wnt5a	0,61		0,33	3			
Wnt5b	0,60	2,41	1,85			X	0,91
Wnt6	0,59			2			
Wnt8a	0,46	1,47		5			1,41
Sfrp1		0,35	0,61				
Sfrp2		1,92	2,32				
Sfrp5		0,47	0,46				
Tcf15	0,44						
Tcf19		1,70					
Tcf21	0,44	0,28	0,36	1			
Tcf25		1,35					
Tcf4		1,36	1,47				
Tcf7		1,61		1			1,26
Tcf7l2	1,62	0,34	0,63	2			
Tcfcp2l1	0,61			5			
Fzd10	0,63			7			
Fzd3	0,80		0,75				
Fzd5		0,27	0,56	1			0,60
Fzd7		0,52	0,60	1			0,93
Fzd8	1,64	0,32	0,72	4			0,23
Hedgehog signaling							
Ptch1	0,55		2,23	7			1,03
Ptch2	0,72						
Shh	0,35	0,64	3,15				
Gli1	0,54		3,15	3			
Gli2	0,75	2,97	3,17	1			1,45
Gli3	0,76	1,66	3,45	1			

Table 1A: Overview of mRNA expression and ChIP-seq data of control and Oct4 CKO embryos and ES cells (signaling pathways)
Columns with blue headings show mRNA expression profiles comparing Oct4 CKO vs control of E7.5 embryos, ES cells differentiated with the endoderm or EpiSC protocol respectively (higher expression in CKO vs. control is marked in green, lower in red). Columns with orange headings show Oct4 ChIP-seq results in FVF;SCF ESCs in pluripotency (d0 target), Foxa2- d3 endoderm (d3 endo F- target) and Foxa2+ d3 endoderm (d3 endo F+ target). Numbers show overlap of studies which identified the indicated gene as target; red numbers indicate genes which were also found in our ChIP-seq data. Genes with a red "1" were only found in our data. For d3 endo F- and F+ targets "X" indicates genes found in our dataset as Oct4 target. No published ChIP-seq studies exist on these populations. Grey column shows ChIP-seq results of the active enhancer mark H3K27ac in Oct4 CKO vs. control ESCs differentiated to EpiSCs. Green fields show higher H3K27ac in CKO compared to control and red field show less. Genes are grouped according to signaling pathways and other categories. For empty fields no significant result was found or gene was not identified as Oct4 target. mRNA profiling and all ChIP-seq assays were performed on FACS sorted FVF+ cells except for E7.5 mRNA data.

	mRNA expression (CKO/contr)			ChIP-seq for Oct4 on FVF;SCF cells			ChIP-seq for H3K27ac (CKO/contr)
Gene	E7.5	Endo	Epi	d0 target	d3 endo F- target	d3 endo F+ target	Epi
Hox genes							
Hoxa1	0,17			2			
Hoxa2	0,60			1			
Hoxa3	0,45			3			
Hoxa5	0,28			2			
Hoxb1	0,38			4			
Hoxb13				1			0,37
Hoxb2	0,52		0,70	1			
Hoxb3	0,58			1			
Hoxb4	0,51			3			
Hoxb5	0,44			1			
Hoxb6	0,26			3			
Hoxb7	0,23			4			
Hoxb9	0,55	0,74		1			
Hoxc4	0,42						
Hoxc8	0,40			1			
Hoxd1	0,49			1			
Hoxd8	0,54						
Hoxd9	0,38						
Cdx genes							
Cdx1	0,07			6			0,86
Cdx2	0,48			1			1,80
Cdx4	0,37			5			
Mes/Endoderm							
Gata4			0,64				
Gata5	0,53						
Gata6	0,60	0,32	0,42	2			
Sox17		0,34		1			0,26
T		1,61	4,27	1		1	
Eomes	4,87			2			1,18
Otx2		0,61					
Foxd3	1,64						1,40
Mixl1		5,29					
Gsc			1,66				
LR asymmetry							
Smarcd3	0,42			1			
Lefty1				1	X	X	0,55
Lefty2	15,48			5			0,94
Cited2		1,79		1		X	1,21
Wnt3a	0,58			1			
Nodal	1,78	2,18		6			1,15
Pitx2	0,50			3			
Smad5		0,69		1			
Gja1			0,63	1			1,25
Somites							
Wnt3a	0,58			1			
Meox1	0,20						
Hes7	0,56			2			
Gbx2	0,32			1			
Cardiac genes							
Zfpm1		0,41	0,46			X	
Nkx2-5	0,63		0,67				
Mef2c	0,61	1,44		1			
Cited2		1,79		1		X	1,21
Sema6d	1,96	0,53	0,59	2	X	X	0,42
Gata4			0,64				
Gata5	0,53						
PCP							
Wnt5b	0,60	2,41	1,85			X	0,91
Celsr1	0,66						
Vangl1	0,67	0,72	0,68				
Vangl2			0,74				
Dvl2			1,34				
Prickle1		1,58		1			0,95
Prickle2	0,72						
Fzd3	0,80		0,75				
EMT							
Zeb1	0,61						
Acta2	0,29						
Vim	0,56		3,96				
Twist2	0,58						
Snai2	0,51		2,26				

Table 1B: Overview of mRNA expression and ChIP-seq data of control and Oct4 CKO embryos and ES cells (Hox and Cdx, endoderm, somites, cardiac, PCP, EMT genes); details as described in table 1A.

4.23 Analysis of mRNA expression and epigenetic changes during the exit of pluripotency and endoderm commitment

Pluripotent ES cells are defined by their capacity to self-renew and differentiate into all cells of an organism. When ESCs differentiate into a distinct lineage they have to switch from a pluripotency regulatory network to a network promoting differentiation. During this exit of pluripotency a stable epigenetic repression of lineage inappropriate genes has to be established in a precise manner (Xie et al. 2013; Zhu et al. 2013).

To gain insight into transcriptional regulation and epigenetic changes during endoderm differentiation FVF;SCF ESCs were differentiated for 3 days under endoderm promoting conditions using Activin A and Wnt3a. mRNA expression was analyzed by microarray and epigenetic marks by ChIP qPCR in pluripotent (d0) and bulk differentiated endoderm cells (d1-d3) (in collaboration with S. Dulev and G. Schotta, LMU). We focused our analysis of epigenetic marks on H3K4me3, which marks actively transcribed genes as well as on the suppressive marks H3K27me3 and H3K9me3. Additionally DNA methylation (5mC) and hydroxymethylation (5hmC) were analyzed by 5-methylcytosine DNA IP (meDIP) and 5-hydroxymethylcytosine DNA IP (hmeDIP), respectively. DNA methylation correlates with gene repression whereas 5hmC is enriched in euchromatic regions of the genome and associated with increased transcription (Cedar 1988, Ficz et al. 2011).

During differentiation transcription of pluripotency-related genes *Oct4, Sox2* and *Nanog* was repressed. In parallel these gens showed enrichment of the repressive histone mark H3K27me3 and an increase in DNA methylation. On the other hand the active histone mark H3K4me3 was lost in *Oct4, Sox2* and *Nanog* and for *Sox2* and *Nanog* we observed decreasing levels of DNA hydroxymethylation (

Figure 37A-C).

In the course of differentiation transcription of the endodermal genes *Foxa2, Sox17, Gata6*, *Cer1* and *Eomes* increased. Gain of H3K4me3 levels was observed in all genes while H3K27me3 is largely lost. Low levels of H3K9me3 are only found for *Sox17, Gata6* and *Cer1* at d0 and are lost during differentiation.

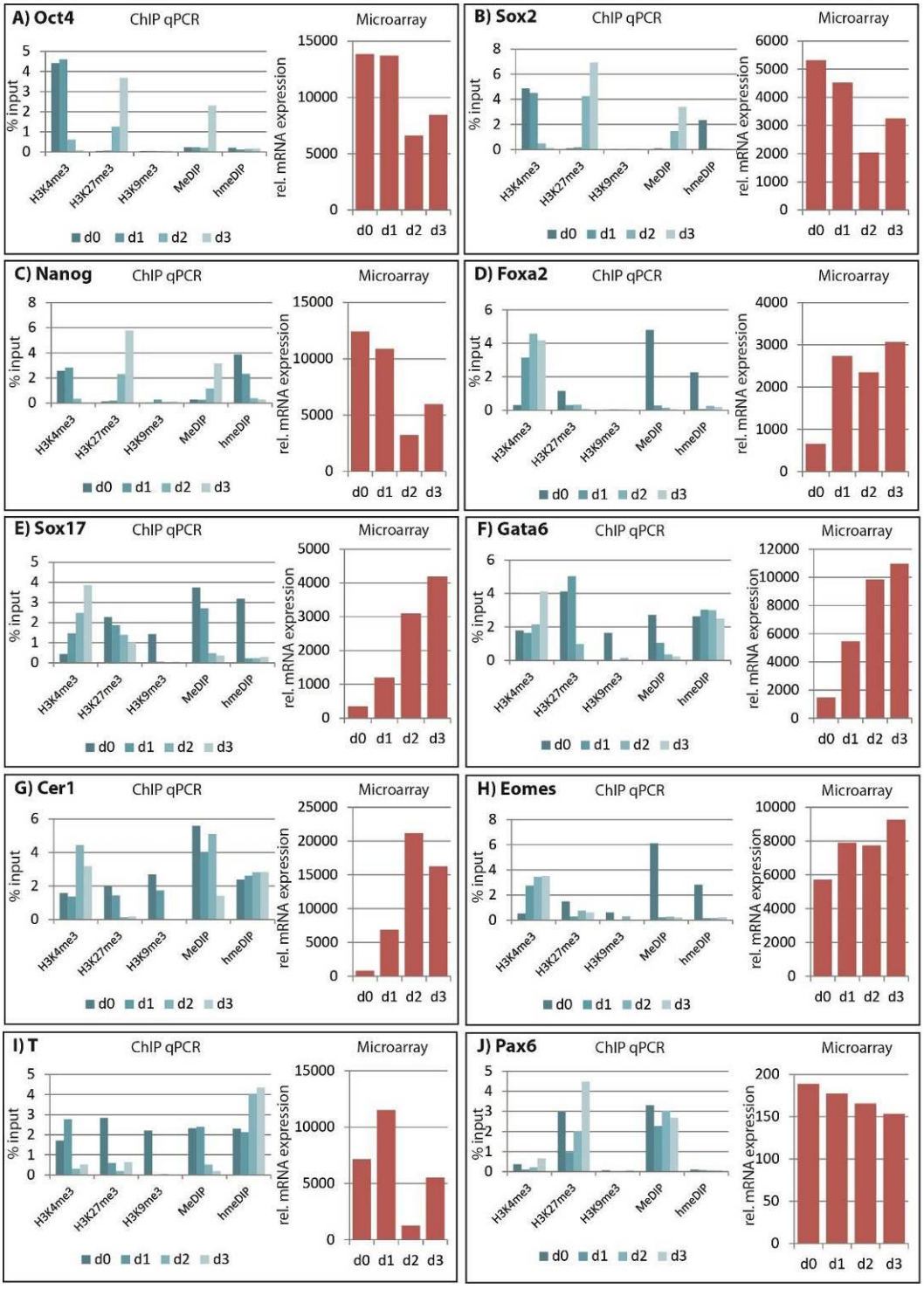

Figure 37: Correlation of expression with epigenetic marks

Blue bars show level of histone marks (H3K3me3, H3K27me3, H3K9me3) and DNA methylation and hydroxymethylation (MeDIP and hmeDIP respectively) at the indicated genes for pluripotent (d0) and endoderm differentiated (d1, d2, d3)FVF;SCF cells. Red bars show relative mRNA expression of the genes. Representative genes for pluripotency (A-C), mesendoderm (D-I) and ectoderm (J) were analyzed during differentiation.

This suggests that this DNA modification has a repressive function for these genes (

Figure **37**D-G).

DNA methylation levels decreased during differentiation but for *Cer1* showed delayed kinetics compared to *Foxa2, Gata6* and *Eomes*. Surprisingly high levels of 5hmC were detected at d0 for *Foxa2, Sox17* and *Eomes* which were strongly reduced from d1. Expression of the axial mesoderm marker *T* increased on d1 of differentiation and dropped thereafter. On d0 the promoter of *T* was marked by the bivalent chromatin mark H3K4me3 and H3K27me3 (Bernstein et al. 2006) which was lost during differentiation. DNA methylation was reduced after d1 of differentiation whereas hydroxymethylation increased. (Figure37I).

The ectoderm specific gene *Pax6* was expressed at very low levels and did not change over time. The repressive mark H3K27me3 was transiently reduced but increased until d3 whereas promoter DNA remained highly methylated (Figure37J).

These results indicate that transcriptional changes in several important pluripotency and endodermal TFs correlate with a transition in epigenetic signatures during endoderm differentiation. DNA hydroxy methylation can be associated with active transcription for some pluripotency genes (*Sox2, Nanog*) but could have repressive function in other developmental genes (*Foxa2, Sox17, Eomes*).

4.24 Genome wide analysis of transcriptional and epigenetic changes during endoderm differentiation

To gain a genome-wide information on transcriptional and epigentic processes during the loss of pluripotency and differentiation towards mesendoderm and endoderm we used FVF;SCF reporter ESCs to isolate mesendoderm and DE cells at specific time points during differentiation by FACS sorting (schematically shown in Figure 35A). First we analyzed and compared gene expression in pluripotent ESCs (d0), mesendoderm (d3 Foxa2+ = F+) and DE at earlier and later stages (d3 and d5 Foxa2+, Sox17+ = F+S+) by RNA sequencing (RNA-seq). A published marker set was used to characterize the obtained populations (Loh et al. 2014).

D0 cells expressed distinct pluripotency markers, and also the d3F+ populations still expressed pluripotency markers but also primitive streak and endoderm markers whereas d3 and d5 F+S+ cells have a distinct definitive endoderm signature with some expression of mesodermal markers (Figure 38A). Moreover, cells expressing *Foxa2* and *Sox17* showed an expression profile resembling foregut endoderm while posterior markers were not detected. (Figure 38B).

Several important pluripotency genes like *Sox2, Klf4* and *Rex1* were highly expressed in d0 cells and down regulated in all populations expressing Foxa2. Surprisingly, core pluripotency genes like *Oct4, Nanog* and *Myc* are still expressed in d3F+ cells at similar levels compared to d0 (Figure 38C). Genes characteristic for PS and node (*T, chordin*) and the key factor for ciliogenesis (*Foxj1*) were only expressed in d3F+ cells (Figure 38D). This indicates that d3F+ cells are correlate to PS and node cell populations in vivo. Endodermal specific genes *Sox17, Cer1, Gata4/6* and *Cxcr4* are strongly expressed in cell populations positive for Foxa2 and Sox17.

This data shows that with our differentiation protocol we generated well characterized cell populations which resemble axial mesoderm (d3F+) and definitive endoderm (d3 and d5 F+S+).

Epigenetic modification	Function	Enzyme
H3K27ac	active enhancer	Ep300
H3K4me3	active promoter	Mll proteins (Set1 complex)
H4K20me3	gene silencing	Suv4-20h1/2
H3K9me3	gene silencing	Suv39h1/2, G9a, Setdb1
H3K27me3	silencing developmental Regulators	Ezh1/2
DNA methylation	gene silencing	Dnmt3a/b (de novo)
DNA methylation	gene silencing	Dnmt1 (maintenance)
DNA methylation	gene silencing	Dnmt3l (co-factor)
DNA hydroxy methylation	increased transcription	Tet proteins

Table 2: Epigenetic modifications, their function and enzymes for their establishment
Epigenetic histone and DNA modifications, their major function and the enzymes involved in generating the epigenetic marks are shown.

Silencing of pluripotency genes and lineage inappropriate genes and activation of lineage specific genes by epigenetic mechanisms are critical events during mammalian development and differentiation of ESCs (Smith & Meissner 2013; Gifford et al. 2013; Xie et al. 2013, Dixon et al. 2015).

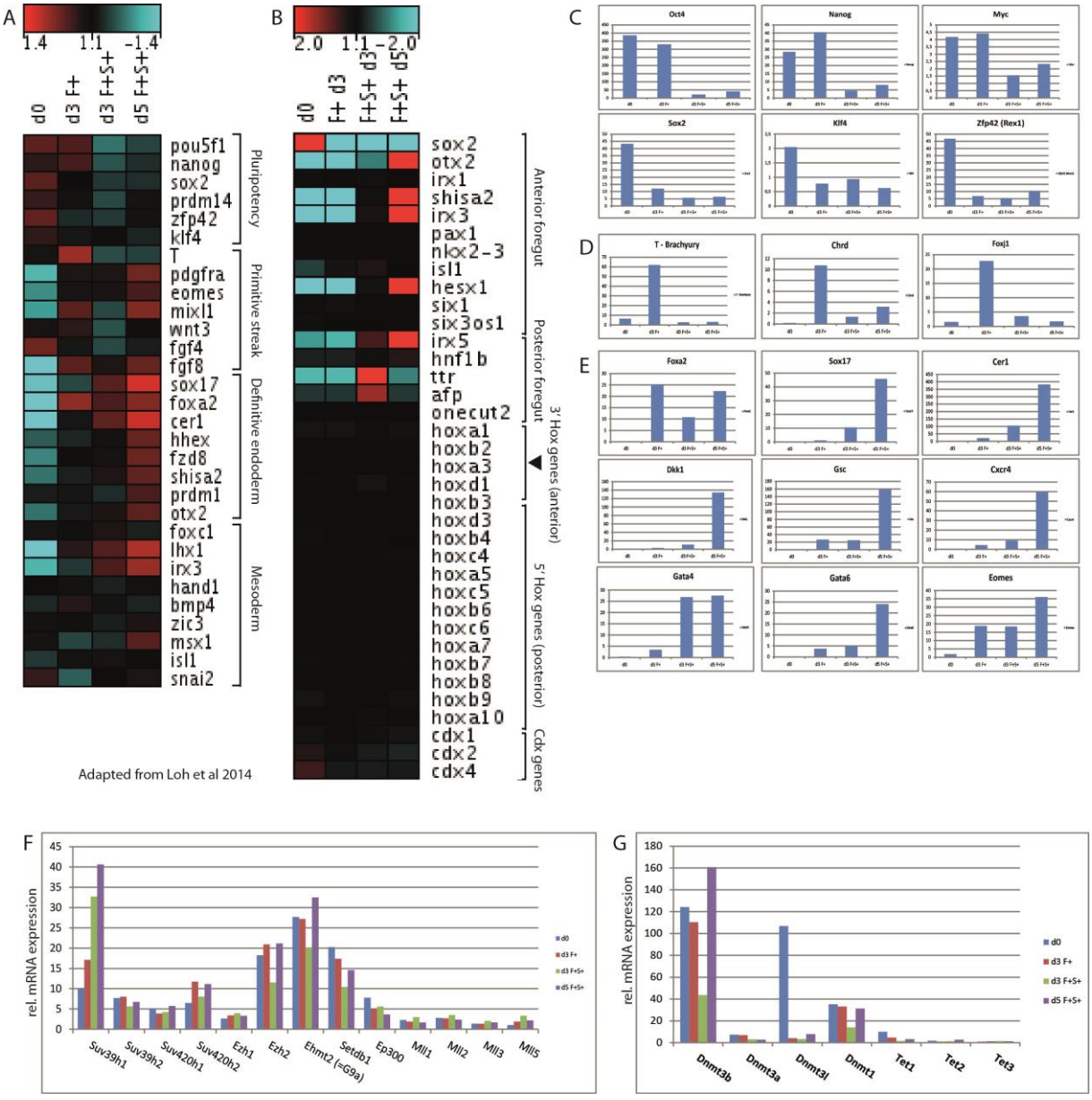

Figure 38: Characterization of sorted endoderm cells

(A) mRNA expression values of sorted d0, d3F+, d3/d5 F+S+ cells are shown in a heat map of selected genes characteristic for pluripotency, primitive streak, definitive endoderm and mesoderm (adapted from Loh et al. 2014). (B) Shows characterization of sorted cells populations according to genes specific for anterior and posterior foregut, 3' and 5' Hox genes and Cdx genes (adapted from Loh et al. 2014). Relative mRNA expression levels from RNA-seq are shown for selected pluripotency (C), organizer (D) and endodermal (E) genes. (F) Shows mRNA expression for histone modifying enzymes and (G) for DNA methyltransferases and Tet enzymes.

To gain deeper insight into epigenetic processes during differentiation we analyzed transcriptional changes of factors which are important for establishing epigenetic marks in the genome. An overview of these factors and their respective epigenetic modifications is shown in Table 2.

Among the histone modifying enzymes analyzed only the H3K9 methyltransferase *Suv39h*1 showed increased expression in differentiated cell populations whereas all others did not change significantly (Figure 38F). Among the factors responsible for DNA modifications *Dnmt3l* expression was lost upon differentiation whereas *Dnmt3b* and *Dnmt1* transcription dropped in d3F+S+ cells and reached comparable levels as in d0 in the d5 population(Figure 38G).

These results suggest that changes in epigenetic profiles upon differentiation do not result from transcriptional changes of chromatin modifying factors but might be dependent on lineage specific TFs which could guide these enzymes to their target sites.

For detailed characterization changes in the epigenetic landscape during endoderm differentiation we are currently performing ChIP-seq analysis for histone modifying factors and meDIP and hmeDIP for DNA methylation and hydroxymethylation, respectively (in collaboration with F. Cernilogar and G. Schotta). These experiments are ongoing and will give us a more detailed insight into genome-wide epigenetic changes during the exit of pluripotency and endoderm differentiation.

To generate β-cells from ESCs for cell transplantation therapies it is necessary to produce large amounts of pure tissue specific cells with high efficiency. To achieve this it would be of great advantage to start differentiation into organ specific cells from a pure self-renewing source of endodermal cells. This step would reduce heterogeneity and increase the yield of the differentiated cell population.

We therefore examined if we can sort differentiated Foxa2+ endoderm cells and propagate them in a endodermal stem cell state (Cheng et al. 2012). FVF;SCF mESCs were differentiated for 3 days using Activin and Wnt3a and sorted for F-S-, F+ and F+S+ cell populations by FACS

and reseeded on fibronectin coated cell culture plates (sorting scheme in Figure 35A). As media for reseeding we used ES medium (ES), ES medium without serum (ES – serum), ES medium with 50 µg/ml ascorbic acid (ES+VitC), N2B27 medium with Gsk3β inhibitor and Mek inhibitor and LIF (2i LIF) and serum free endoderm differentiation medium with 10 µg/ml ActivinA and 1µg/ml Wnt3a (EDM 10/1) to decipher the optimal culture conditions. After 5 days of culture we counted the number of colonies per well.

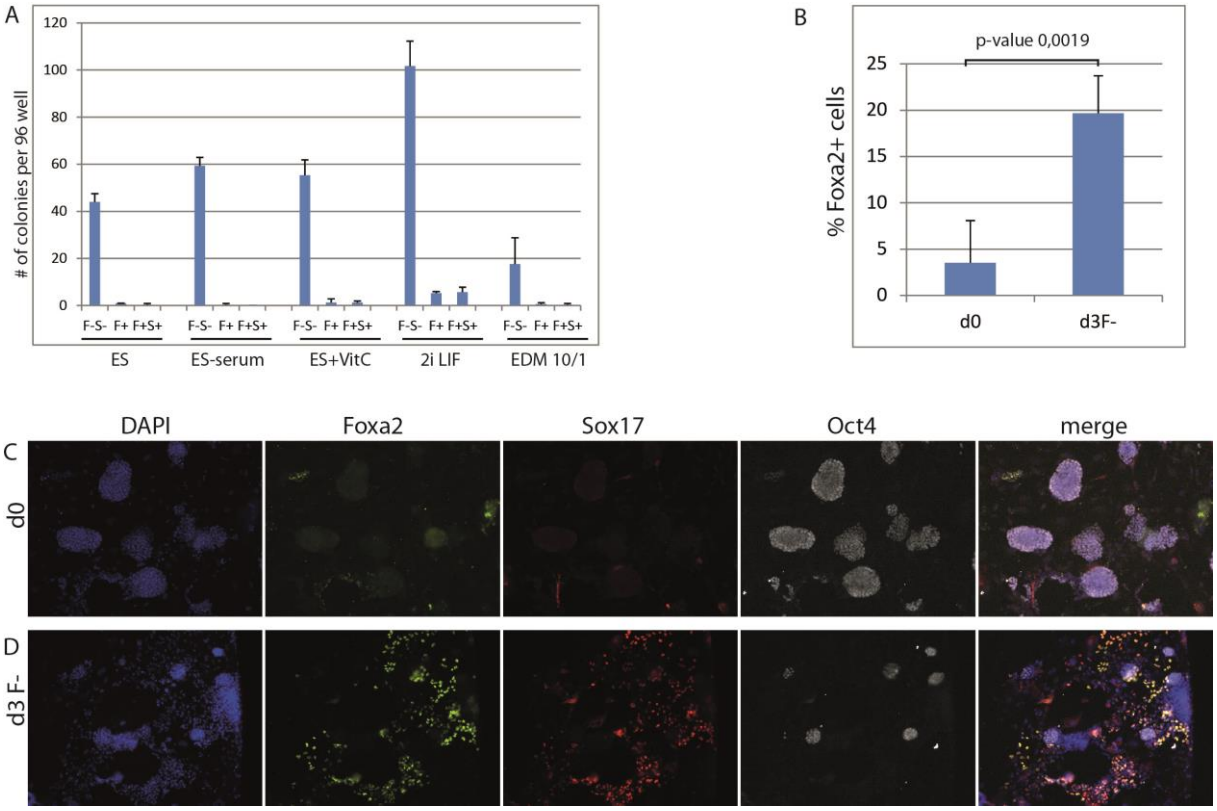

Figure 39: D3 F-S- cells show different response to Wnt signaling (under 2i conditions) than pluripotent ES cells

(A) FVF;SCF ES cells were differentiated to endoderm for 3 days, FACS sorted for FVF-SCF-(F-S-), Foxa2+Sox17- (F+) and Foxa+Sox17+ (F+S+) and reseeded on fibronectin coated 96w plates at 10.000cell per well. Cells were reseeded in standard ES medium (ES), ES medium without serum (ES-serum), ES medium with 50ug/ml Vitamin C (ES VitC), N2B27 medium containing 1uM Mek inhibitor PD0325901 and 3uM Gsk3b inhibitor CHIR99021 and LIF (2i LIF) or serum free differentiation medium containing 10ug/ml Acitvin A and 1ug/ml Wnt3a (EDM10/1). After 5 days of growth cells were fixed and number of colonies per well counted. Graphs show mean values of 3 experiments, bars show standard deviation. (B) Quantification of Foxa2+ cells from (C). Graphs show mean values of 3 experiments, bars show standard deviation. (C) Shows FVF;SCF differentiated to endoderm and FACS sorted on d3 for Foxa2- (d3 F-) cells or under pluripotent conditions (d0) and reseeded in 2i LIF on MMC treated embryonic fibroblasts. Cells were fixed after 5 days and stained for GFP (Foxa2), RFP (Sox17) and Oct4.

In all conditions we only observed colonies from F-S- cells whereas colonies from F+ and F+S+ cells were hardly found. For the F-S- cells 2i LIF medium resulted in the highest number of colonies whereas EDM 10/1 gave the lowest (Figure 39A).

These result indicated that with the medium and culture conditions used we cannot sort and culture cells expressing Foxa2. For further experiments different culture media and plate coatings need to be tested. For human endodermal progenitors matrigel and feeders were used as matrix and medium containing Bmp4, bFGF, EGF and VEGF (Cheng et al. 2012). However, since human ESCs are more similar to mouse EpiSCs it would likely be necessary to adapt these conditions.

In this experiment we noted that d3F-S- endoderm cells showed increased flattened morphology after culture in ground state (2i LIF) conditions, indicating a differentiated state, even though these cells still expressed the pluripotency marker Oct4. We speculate that Oct4+, Foxa2-, Sox17- cells after 3 days of endoderm differentiation are in a primed state since they have been exposed to Activin and Wnt signaling but did not initiate a differentiation program. In contrast, pluripotent d0 ESCs show flattened morphology and retain a colony shape in ground state conditions. The 2i LIF medium contains the Gsk3β inhibitor to activate canonical Wnt signaling by blocking β-catenin degradation (Ying et al. 2008b). Since it has been shown that the Wnt/β-catenin pathway has a dual function in ESCs (Lyashenko et al. 2011; Cole et al. 2008; Wray et al. 2011; Lindsley et al. 2006; Gadue et al. 2006b; Berge et al. 2011) we asked at which stage cellular response to Wnt switches from maintenance of pluripotency to triggering differentiation.

Pluripotent (d0) and d3 F-S- primed cells were FACS sorted and reseeded onto fibronectin coated dishes under 2i LIF conditions. After culture for 5 days we fixed and stained the cells for GFP (Foxa2), RFP (Sox17) and Oct4 (Figure 39C). 3,5% of the reseeded d0 cells expressed Foxa2 whereas in the d3F-S- cells 19,7% expressed Foxa2 after 5days in 2I LIF (Figure 39B and D). A large proportion of the Foxa2+ cells also expressed Sox17 (Figure 39D).

These results suggest that primed Oct4+, Foxa2-, Sox17- cells respond to induction of Wnt signaling by starting an endoderm differentiation program whereas ESCs remain pluripotent. These results also suggest that activation of Wnt signaling alone in primed cells can override

blocking Erk signaling (Mek inhibitor in 2i medium) and drive cells towards endoderm. It might be possible that the dual role of Wnt/β-cat signaling results from association with cell state specific TFs which allows activation of pluripotency or endodermal target genes within a permissive environment.

5 Discussion

5.1 Short summary of results

Oct4 is the key transcription factor for pluripotency and incorporated in a network together with Nanog and Sox2. Recent studies have shown that Oct4 function reaches beyond the maintenance of pluripotency and plays a role during early development (Deveale et al. 2013; Morrison & Brickman 2006; Reim et al. 2004). Because of this we were interested in the function of Oct4 specifically in mesendoderm and endoderm formation during early mouse embryonic development. Since the full KO of Oct4 is lethal before implantation (Nichols et al. 1998), we developed a system for conditional deletion of Oct4 in Foxa2 expressing mesendodermal progenitors during gastrulation in mouse embryos.

In Oct4 CKO embryos we observe malformation of the hindgut endoderm and some neural developmental defects. Furthermore, the formation of LR asymmetry was perturbed in Oct4 CKO embryos. The likely cause was the malformation and morphological defects at the node, including ciliation problems, which cause impaired nodal flow. These defects are supported by mRNA profiling, which showed misregulation of genes important for posterior development, patterning and LR asymmetry formation.

This also includes several important signaling pathways like Tgf-β and Wnt. For further experiments we used Oct4 CKO ES cells for *in vitro* analysis of the defects caused by Oct4 deletion. With this we showed that Oct4 conditional deletion results in a cell fate switch from definitive endoderm to mesendoderm during EpiSC differentiation and a reduced activation of the Wnt and Tgf-β signaling pathway. In concordance with the embryonic hindgut defect we can also show that Oct4 CKO ES cells fail to form $Cdx2^{+}$ hindgut endoderm *in vitro*. mRNA expression profiling in Oct4 mutant cells shows misregulation of genes involved in germ layer formation and Wnt and Tgf-β signaling. We could also show that several misregulated genes are bound by Oct4 in pluripotent and endoderm cells. Several of these misregulated genes could be affected by changes in active enhancer mark H3K27ac observed in differentiated Oct4 mutant cells.

5.2 Generation of Oct4 CKO embryos

Studies which have looked at the effect of Oct4 function during embryonic development have depleted Oct4 in all germ layers (Morrison & Brickman 2006; Reim et al. 2004; Deveale et al. 2013). Since Oct4 expression is still detected in cells of the definitive endoderm we were interested in its function in the formation of mesendoderm and definitive endoderm.

Since the complete KO of Oct4 is early embryonic lethal (Nichols et al. 1998) we generated a CKO to delete Oct4 only in Foxa2 expressing cells and their descendants by Cre recombinase. The conditional deletion of Oct4 in Foxa2 expressing cells allows us to specifically analyze the role of Oct4 in Foxa2 lineage cells axial mesoderm (node, notochord), definitive endoderm and endoderm derived organs like liver, lung and pancreas.

Mice homozygous for Oct4 ^{flox} are fertile and don't show any obvious phenotype. This shows that this allele does not interfere with the function of the Oct4 gene. Mice with the Foxa2 $^{2AiCre/wt}$; Oct4 $^{FD/wt}$ alleles are also viable and do not show any obvious phenotype which suggests that heterozygosity of Oct4 does not visibly affect development. However, we observed a reduced number of male offspring from matings with Oct4 heterozygous mice. This indicates that the lower level of Oct4 could affect survival of male embryos or interfere with fertilization.

One has to keep in mind, that all cells in Oct4 CKO embryos and all CKO ES cells are heterozygous for Oct4, even when Foxa2 ^{2AiCre} is not expressed . Since Oct4 function has been shown to be dose dependent (Niwa et al. 2000; Radzisheuskaya et al. 2013; Karwacki-Neisius et al. 2013), is possible that some observed effects are also due to the reduced dose of Oct4 in cells not expressing Foxa2. These cells might influence endodermal cell populations but do not effect viability.

5.3 Oct4 expression in definitive endoderm and conditional deletion

Oct4 is expressed from the fertilized zygote to the ICM and the epiblast. During development expression decreases in an anterior to posterior manner (Yeom et al. 1996) and after E9.25 can only be found in primordial germ cells (PGC). In adult mice Oct4 expression is confined to germ cells but can also be detected in several somatic human cancers in which an impact of

Oct4 levels on clinical outcome has been proposed (Ezeh et al. 2005; Wen et al. 2010; X. Zhang et al. 2010).

At the LS stage cells in the anterior epiblast are specified to become neuroectoderm. In the posterior epiblast where the PS forms, Foxa2+ cells in the anterior PS will give rise to endoderm, T+ cells to posterior mesoderm and Foxa2+ and T+ cells form the axial mesoderm (Burtscher & Lickert 2009). All of these populations in the epiblast and the PS express Oct4. Furthermore we also find some cells in the definitive endoderm layer which still express Oct4. Thus Oct4 is deleted in the endoderm and axial mesoderm and their progeny. An effect on the node and notochord are not surprising and can explain morphological defects in node formation in CKO embryos. As the lineage separation between endoderm and mesoderm progenitors starts in the epiblast, deletion of Oct4 in Foxa2 expressing cells influences proper lineage segregation. This we observe *in vitro* where Oct4 depletion directs cells into a T positive axial mesoderm state at the expense of Sox17 and Gata4 expressing DE cells.

Sustained expression of Oct4 in Sox17 expressing DE cells might specify hindgut endoderm. This is strongly supported by the absence of hindgut endoderm in Oct4 CKO embryos. In these cells Oct4 could interact with Sox17 for proper expression of endodermal genes (Aksoy et al. 2013). However staining of ESCs differentiated *in vitro* to endoderm did not reveal co-localization of Oct4 and Sox17. Thus it is questionable if the overlap in expression is long enough. It is also possible that expression level of Oct4 in Sox17+ cells is below the immunological detection level or differences in the ESC line or differentiation protocols are permissive for this Oct4+/Sox17+ state.

5.4 **Perinatal death of CKO embryos**

Oct4 CKO embryos show an expected Mendelian ratio of 50% until E12.5. Thereafter the ratio decreases and Oct4 deletion leads to prenatal or neonatal lethality. This shows that the conditional deletion of Oct4 causes abortion or death of embryos or pups at various time points. Even though embryos show defects in patterning, LR asymmetry or neural development, none of these could clearly be associated with embryonic death. A cause for

the broad range of time points when Oct4 CKO embryos die could be differences in the exact time point of Cre mediated recombination of Oct4. A later deletion could result in milder defects and embryos survive longer. Since Oct4 is only expressed in PGCs after E9.5 (Downs 2008), it is likely that lethality thereafter results from secondary effects of Oct4 deletion in mesendoderm-derived lineages, such as axial mesoderm, cardiac mesoderm, and endoderm.

Oct4 CKO pups which died neonatally were normally developed. The functionality of all organs was not assessed but no gross morphological defects besides pulmonary left isomerism were observed. The presence of only 2 lung lobes, in our mutants caused by pulmonary left isomerism, has been shown to interfere with breathing and lead to poor oxygenation of the blood (Chuang et al. 2003). In some neonatal pups we noted cyanosis. This would argue for a lack of oxygen as cause of death after birth. Another cause of death could be congenital heart defects. Abnormal looping of the heart or defects in development of the second heart field can underlie these defects (Francou et al. 2012; I S Kathiriya & Srivastava 2000). Signaling pathways like Wnt and Shh, which are affected by Oct4 depletion, can be a potential cause for congenital heart defects (Rochais et al. 2009). Taken together congenital heart and lung defects might cause neonatal death in Oct4 mutant animals.

5.5 **Open brain phenotype, neural tube patterning**

Although Foxa2 is a key factor for endoderm development (Ang et al. 1993; Ang & Rossant 1994b) we also see some defects in neuronal development. This can be explained by the fact that the Foxa2 lineage contributes to the floor plate of the neural tube, which is essential for DV patterning and neural tube closure (Briscoe & Novitch 2008, Sasaki & Hogan 1994). Oct4 deletion in frog or zebrafish also showed neural tube patterning and mid/hindbrain formation defects (Morrison & Brickman 2006; Lunde et al. 2004; Burgess et al. 2002). However, these studies have knocked down Oct4 or its homologues in all germ layers which can explain the stronger effects with a higher penetrance compared to our study.

In concordance with this phenotype Hoxa1, which is involved in hindbrain patterning (Martinez-Ceballos & Gudas 2008; Barrow et al. 2000; Gavalas et al. 2003) is down regulated in E7.5 Oct4 CKO embryos. Interestingly we also find the neural regulator Meis1 expression

reduced in Oct4 mutant embryos. Oct4 was shown to regulate this gene through direct binding to its promoter which affects neural differentiation (Yamada et al. 2013). Additionally, Shh signaling which is reduced in Oct4 CKO embryos has been demonstrated to be essential for neural tube patterning (Briscoe & Novitch 2008; Ericson et al. 1995). These observations support our observation that deletion of Oct4 results in neuronal development defects.

5.6 **Contribution of Oct4 CKO cells to organs**

Oct4 CKO cells can contribute to organizer structures, all endodermal organs and Foxa2 lineages in the heart and the floorplate of the neural tube. It has been shown by others that Oct4 function in somatic stem cells is not required (Lengner et al. 2007). However in this study Oct4 was deleted in mice only after birth in somatic stem cells. In our study we deleted Oct4 during formation of the axial mesoderm and endoderm during gastrulation. These cells can still contribute to all endodermal organs, including the colon epithelium, which is derived from hindgut endoderm. One interesting observation is an increase in contribution of Oct4 CKO cells to the heart. Cells in the heart develop from the primary and secondary heartfield (Buckingham et al. 2005) and are partially derived from Foxa2 expressing epiblast progenitors, most likely cells from the mid gastrula organizer (Eon et al. 2008, Horn et al. 2012, Kinder et al. 2001). The increase of Oct4 CKO cells in the heart would argue that some endodermal cells are undergoing a fate switch towards mesodermal cells when Oct4 is deleted. This observation is also supported by *in vitro* results where Oct4 CKO ES cells differentiate more to Foxa2+/T+ axial mesoderm cells at the expense of Foxa2+/Sox17+ endoderm cells. The commitment of cells to the DE lineage (Foxa2+/Sox17+) or the cardiac mesoderm lineage (Foxa2+/T+) is strongly dependent on Wnt/β-catenin signaling (Lickert et al. 2002) which indicates an involvement of Oct4 in the regulation of this signaling pathway.

Due to the neonatal lethality we are not able to examine potential effects of conditional Oct4 deletion in adult organs using our Foxa2 ^{2AiCre} deletion strategy. To dissect effects of Oct4 in DE or axial mesoderm deletion in the Sox17 lineage by Sox17 ^{iCre} (Engert et al. 2009) could be used to give more insight. However, in this approach it would be questionable if the

overlap of Sox17 and Oct4 expression would be long enough to see an effect. Sox17 expressing DE cells are already determined and it would be questionable if deletion of Oct4 at this stage can change the cell fate.

5.7 **Foxa2 lineage contribution to somites**

Oct4 depleted cells are not able to contribute to posterior somites in embryos. It has been shown that Oct4 can induce EMT programs in cancers (Chiou et al. 2010; Hu et al. 2012, Luo et al. 2013, Tsai et al. 2014). It is thus possible that in the absence of Oct4 specific cells which contribute to somites cannot properly initiate their EMT program and thus do not end up in their prospective tissue. Also the finding that Oct4 function is linked to cell adhesion (Livigni et al. 2013) supports the role Oct4 might play in EMT and sorting cells into the right lineage. The reduced mRNA expression of EMT regulators like Snail2, Twist2 and Zeb1 in Oct4 CKO embryos additionally supports this observation. Since Oct4 expression in the embryo during development is down regulated from anterior to posterior it is possible that extended expression plays a role in morphogenesis particularly of the posterior somites. It has been shown that Wnt signaling is required for posterior mesoderm formation, segmentation and somite organization (Linker et al. 2005, Dunty et al. 2008, Aulehla et al. 2003). We observe down regulation of several Wnt genes and a general defect in Wnt signaling in our Oct4 mutants which could also be a cause for this phenotype (Kemler et al. 2004, Martin & Kimelman 2008). Thus it is likely, that reduced Wnt signaling in Oct4 CKO embryos results in decreased activation of the EMT program

Other studies have also described a severe defect in somitogenesis upon deletion of Oct4 in Xenopus and mouse (Morrison & Brickman 2006; Deveale et al. 2013). Compared to our approach these two papers delete Oct4 in all germ layers and thus probably observe a much stronger phenotype. However, the defects in Xenopus clearly show that the function of Oct4 is conserved across species.

5.8 **Absent hindgut in Oct4 CKO embryos**

Conditional deletion of Oct4 in Foxa2 expressing cells results in defective hindgut formation. Our first results showed a complete absence of the hindgut endoderm in post-gastrulation embryos at E8.5 and E9.5. Since our Oct4 $^{flox/flox}$ R26R mice died out we regenerated them by crossing Oct flox with R26R mice. In these mice we could not observe a complete absence of hindgut endoderm but Oct4 CKO embryos still had a curly tail phenotype and thus defects in correct hindgut morphogenesis.

Expression of Oct4 can be detected in Foxa2 expressing endoderm at E7.5 and also in hindgut endoderm up to the 5-s state (Downs 2008). It has also been shown that Oct4 expression decreases from anterior to posterior during early embryonic development (Yeom et al. 1996; Downs 2008) which indicates a specific role in in the hindgut region. Oct4 function in hindgut formation could act in two ways. First Oct4 might directly act in the endodermal epithelium to trigger a hindgut specific transcriptional program. On the other hand development of the endoderm is also regulated by signaling from neighboring tissues like mesodermal structures (Wells & Melton 2000). It has been shown that signals from the adjacent notochord are important for pancreas development and patterning of the endoderm (Fausett et al. 2014; Cleaver & Krieg 2001; Kim et al. 1997, Wells & Melton 2000). It would thus be possible that, due to the defects in axial mesoderm formation inductive signals for hindgut formation and patterning are missing or reduced. mRNA expression profiling of Oct4 CKO embryos shows lower expression of Wnt4 and Wnt3a, which induce the posterior gene *Cdx1* (Lickert et al. 2000). On the other hand the Wnt effector molecule *Tcf7l2 (Tcf4)* is upregulated in mutant embryos. This could mean that upon Oct4 deletion less Wnt from posterior mesoderm is signaling to the adjacent endoderm which, as compensation upregulates *Tcf7l1*. The low Wnt signaling activity then could result in reduced induction of *Cdx1* and *Cdx2* and subsequently in defective posterior development.

Other studies in frog, zebrafish and mice have shown that deletion of Oct4 in all germ layers also results in disturbed posterior development, although the defects are more severe, e.g. posterior truncations (Morrison & Brickman 2006; Deveale et al. 2013, Lunde et al. 2004). This proves that Oct4 is involved in posterior development and the mechanism in conserved

between several species; our data can specifically confine the function of Oct4 to cells of the Foxa2 lineage, axial mesoderm and endoderm.

5.9 Contribution of Oct4 CKO cells to the intestinal stem cell compartment

It has been proven that Oct4 is dispensable for adult stem cell function (Lengner et al. 2007), however expression in adult somatic cells has been reported but is questionable (Lengner et al. 2007, TableS1). By using Foxa2 ^{2AiCre} Oct4 is depleted a much earlier state, during gastrulation, and thus might have a function to prime future somatic stem cells. The intestinal stem cell compartment is thus interesting since Oct4 CKO embryos show an absence of hindgut endoderm which form the colon. Furthermore overexpression of Oct4 in adult mice resulted in dysplasia in the intestine (Hochedlinger et al. 2005). By generating chimeras we could show that Oct4 depleted cells are still able to contribute to the intestinal stem cell compartment postnatally. Since we observed posterior defects in Oct4 CKO embryos at earlier stages the possibility remains that in cases with a less severe early phenotype a later effect on intestinal morphology or function could have been observed. Yet in Oct4 CKO embryos the colon, which is derived from hindgut endoderm, was formed at E18.5. Analysis of CKO animals at later time points is not possible because of the 100% lethality shortly after birth. In the diploid aggregation approach animals can survive but potentially fatal effects of the conditional deletion of Oct4 can be compensated by WT cells in these chimeric animals. Thus it is unclear if Oct4 CKO cells in the intestine are fully functional.

5.10 Defects in LR asymmetry upon Oct4 deletion

After specific deletion of Oct4 in Foxa2 expressing cells mutant mice show characteristic defects in LR asymmetry formation like pulmonary left isomerism and cardiac looping defects. We also observed malformation of the node and defects in cilia formation. This defect is a plausible explanation for the LR patterning defect we observe.

There could be several ways how Oct4 influences correct node and cilia formation. First, it directly activates Wnt and Tgf-β/Nodal signaling, two pathways which play important roles in LR axis determination (Brennan et al. 2002a; Kitajima et al. 2013; Nakaya et al. 2005). Oct4 also binds to promoters of several Wnt genes under pluripotent conditions; this suggests that it might directly be involved in their transcriptional control. Wnt and Tgf-β/Nodal signaling pathways have been shown to be involved in LR asymmetry establishment (Brennan et al. 2002b; Nakaya et al. 2005; Kitajima et al. 2013) and expression is reduced in Oct4 CKO embryos and differentiated ES cells. Because of reduced signaling it is possible that downstream target genes are not activated. This could then lead to the observed LR asymmetry defects.

Another possibility is that Oct4 regulates planar cell polarity (PCP) in cells of the node. PCP has been shown to be important for correct positioning of motile cilia in the node and LR asymmetry establishment (Song et al. 2010). Conditional deletion of Oct4 leads to reduced expression of several PCP components like Celsr1, Vangl1 and Prickle2. Members of the Wnt family, like Wnt5, have also been shown to be involved in PCP and regulation of LR asymmetry (Kitajima et al. 2013; Kilian et al. 2003; Qian et al. 2007). Wnt5a and Wnt5b, which are both involved in PCP (Qian et al. 2007; Nishita et al. 2010, Tada & Kai 2009), showed reduced expression in Oct4 CKO embryos. Wnt5b was also bound by Oct4 in Foxa2+ endodermal cells which suggests a direct involvement of Oct4 in its activation. These observations indicate that Oct4 is involved in the activation of the Wnt/PCP pathway and establishment of correct positioning to node cells and cilia.

We also speculate that Oct4 could be responsible for correct specification of node cells. In the node of Oct4 CKO embryos we observed cells which express neither Foxa2 nor T. It has been demonstrated that Oct4 binds to the T promoter in endodermal cells but a direct activation has not been proven (Thomson et al. 2011). As we showed that Oct4 plays a role in lineage segregation during *in vitro* endoderm differentiation it is possible that correct cell lineage specification in the node is dependent on Oct4 function. The lack of properly specified node cells might influence node function and thus establishment of the LR axis.

In this context it is also possible that Oct4 acts as survival factor for cells in the node and its absence causes apoptosis of some node cells. It has been shown by others that deletion of Oct4 increases apoptosis in the PS and that Oct4 can promote cell survival (Deveale et al. 2013; Kotkamp et al. 2014). We did not observe a reduction in node size, but absence of ciliated pit cells in the node could result from apoptosis of this cell population due to the absence of Oct4. Missing cells could have been replaced by cells from the definitive endoderm. To confirm this, staining with apoptosis markers, like activated caspase3, are required to test if conditional Oct4 depletion in causes apoptosis of node cells.

5.11 **Transcriptional changes in Oct4 CKO embryos**

To investigate the phenotype on a molecular level in Oct4 CKO embryos we compared mRNA expression of E7.5 Oct4 Mutant and control embryos by micro array analysis.

Interestingly we observe down regulation of several Wnt genes, e.g. Wnt4, Wnt5a/b, Wnt6, Wnt8a. Wnt signaling has been shown to play an important role in mesendoderm induction (Liu et al. 1999) and Wnt3a is also important for somite and tail bud formation (Takada et al. 1994; Ikeya M 2001). Wnt signaling is also known to dose-dependently play an important role in AP patterning where high Wnt signaling induces posterior fates. In this context Wnt5a was demonstrated to influence intestinal elongation (Cervantes et al. 2010, Gregorieff et al. 2004, Kiecker & Niehrs 2001). Wnt signaling also directly activates the posterior gene Cdx1, which is strongly down regulated in Oct4 CKO embryos (Lickert et al. 2000). Cdx4 and Cdx2, which have been shown to regulate posterior development, are both regulated by Wnt signaling and are also down regulated in Oct4 Mutants (Savory et al. 2009, Zhao et al. 2014; Pilon et al. 2006, van den Akker et al. 2002). These mRNA expression differences explain the observed absence of hindgut endoderm in Oct4 mutant embryos. This defect indicates that Oct4 activates components of the Wnt signaling pathway which in turn regulate hindgut formation and also contribution of cells to somites. These functions of Wnt signaling in the hindgut could also be the reason why Oct4 expression remains longer in the posterior embryo and is down regulated in an anterior to posterior fashion (Yeom et al. 1996). Also the down regulation of Wnt target genes like Grsf1, Fragilis2 (Ifitm1) and Smarcd3 in Oct4

CKO embryos confirms the defects observed in the Wnt signaling pathway. These targets genes have also been shown to play a role in (par) axial mesoderm formation, embryo patterning and axial elongation (Lickert et al. 2005, Lickert & Kemler 2002).

One interesting aspect is, that the segregation of ICM and TE involves reciprocal repression of Oct4 and Cdx2 (Niwa et al. 2005a). In this context Oct4 has a repressive effect on Cdx2 expression whereas our data indicate an activating effect on Cdx2 during endoderm formation. Since it has been shown that Oct4 interacts with the histone methyltransferase Setdb1 (ESET) to silence TE genes (Yuan et al. 2009a) it is possible that in a different environment other cofactors are present which result in the activation of Cdx2. Association of Oct4 with various TFs and epigenetic complexes has been demonstrated (Pardo et al. 2010; van den Berg et al. 2010), however this data is only limited to pluripotent ES cells. It is thus possible that Oct4 interacts with different cofactors depending on the tissue or developmental state and guides its interacting partners to different target genes. This mechanism could explain that Oct4 can have different effects in different tissues.

The family of Hox genes is known to regulate morphologies along the AP axis during development (Lewis 1978; Forlani 2003, Mallo et al. 2011). In conjunction with patterning defects in Oct4 mutant embryos we also find genes of the Hox cluster, like *Hoxa1/a2/a3/c8/d1/d8/d9* and others, down regulated in Oct4 mutant embryos. Several of these genes are also directly bound by Oct4 in ES cells. These differences could also be downstream effects of the general down regulation of Wnt effector genes which are important for embryonic patterning (Lengerke et al. 2008; Nordström et al. 2006; Maloof et al. 1999).

Genes like *Hes7, Meox1 and Gbx2* which play a role in somite formation showed reduced expression in Oct4 mutant embryos (Bessho et al. 2003; Jukkola et al. 2005; Carapuço M, Nóvoa A, Bobola N 2005). This supports our observation in the embryo where we see less contribution of Foxa2 lineage cells to somites in the absence of Oct4.

5.12 Involvement of Oct4 in lineage segregation

We demonstrated that conditional deletion of Oct4 results in a fate switch from DE (Foxa2+. Sox17+) to axial mesoderm (Foxa2+, T+) during ESC differentiation. This argues that Oct4 is involved in the fate decision between these lineages *in vitro*, driving cells towards DE. It has been demonstrated that Oct4 is blocking neuronal differentiation and driving cells in to mesendoderm (Thomson et al. 2011). Our data can more precisely restrict the function of Oct4 after endoderm differentiation has been initiated. From our data we can conclude that Oct4 is involved in the lineage segregation between axial mesoderm and DE, directing cells into the latter. Interaction of Oct4 with Sox17 has been shown to be involved in expression endodermal genes (Aksoy et al. 2013). However, since Sox17 expression is strongly reduced after Oct4 deletion it is likely that Oct4 is already required for its activation during endoderm differentiation *in vitro*. This could also be an indirect effect of the Wnt/β-cat signaling pathway. Sox17 and Wnt/β-cat have been demonstrated to drive endodermal gene expression (Sinner et al. 2004, Engert et al. 2013a). Reduced Wnt signaling could result in lower Sox17 expression and impaired endoderm differentiation which we observe in Oct4 CKO cells.

5.13 Specification of hindgut endoderm by Oct4 in vitro

In vitro differentiation towards hindgut endoderm showed that Oct4 CKO ES cells have a reduced potential to form Foxa2+/Cdx2+ hindgut cells. This supports our observation of malformation in embryonic hindgut endoderm and reduction in Cdx1, Cdx2 and Cdx4 mRNA expression.

Fgf4 plays important roles in axial elongation and posterior fate specification in a concentration dependent manner. Interestingly Oct4 and Sox2 have been shown to activate the Fgf4 enhancer. (Ambrosetti et al. 1997; Boulet & Capecchi 2012; Wells & Melton 2000). Since we add Fgf4 to our hindgut differentiation system it is possible that Oct4 is involved in activation of downstream target genes to specify hindgut endoderm.

Reduced Wnt signaling, which we observed in Oct4 CKO embryos could also be responsible for hindgut defects since Wnt signaling is important for activation of the hindgut genes Cdx2

and 1 (Benahmed et al. 2008; Lickert et al. 2000). It has been shown that synergistic action of Oct4 and Wnt signaling activates the Cardiac gene Mesp1 (Li et al. 2013b). Thus it is possible that a similar mechanism also activates posterior genes like Cdx1 since Wnt is highly expressed in the posterior part of the embryo and Oct4 expression remains longest in the posterior part of the embryo (Yeom et al. 1996).

5.14 **Activation of signaling pathways by Oct4**

Signaling pathways like Wnt and Tgf-β/Nodal are crucial for embryonic development and formation of the germ layers. Upon conditional deletion of Oct4 in embryos or ES cells both of these pathways show reduced activation and misregulation of their components.

Wnt signaling

Our results strongly suggest that Oct4 is involved in proper activation of the Wnt pathway since we see a down regulation of several Wnt genes in Oct4 CKO embryos and a strong reduction in active β-catenin during endoderm differentiation. Conversely it has been shown that Oct4 forms a complex with β-catenin at the membrane, acts as negative regulator of Wnt signaling and facilitates degradation of the effector molecule β-catenin (Abu-Remaileh et al. 2010; Davidson et al. 2012; Marikawa et al. 2011, Faunes et al. 2013). From these results we would expect that deletion of Oct4 causes an increase in β-catenin. In the system used in these studies Oct4 was not depleted during endoderm development, as in our approach, but under pluripotent conditions, which could explain the observed differences. On the other hand Oct4 overexpression was also shown to increase activated β-cat in intestinal cells (Hochedlinger et al. 2005). Our findings suggest that Oct4 is involved in activation of the canonical Wnt pathway during early endoderm formation.

It has also been demonstrated that Oct4 together with Wnt signaling activates the cardiac TF Mesp1 in ES cells (Li et al. 2013b). Interestingly Mesp1 is upregulated in Oct4 CKO embryos, which indicates that these mechanisms are more complex in embryos due to the interaction of all germ layers.

The combined action of Oct4 and canonical Wnt signaling could also be a potential direct mechanism for activation of the Wnt target genes Cdx1 and Cdx4 (Lickert et al. 2000, Pilon et al. 2006), which are strongly down regulated in Oct4 CKO embryos. In these embryos we can also observe an upregulation of Tcf7l2 (Tcf4) which has been shown to be important for Cdx1 activation (Lickert et al. 2000). This could potentially be a compensation for the reduced Wnt signaling observed in Oct4 CKO embryos.

Another involvement of Oct4 and β-catenin could be cell adhesion and EMT. For the most part involvement of Oct4 in EMT processes has been demonstrated in the context of cancer (Chen et al. 2014; Chiou et al. 2010; Hu et al. 2012; Hu et al. 2011; Luo et al. 2013; Tsai et al. 2014) but also in cell adhesion in mouse embryos (Livigni et al. 2013). During pluripotency Oct4, β-cat and E-cad are associated in a complex at the cell membrane (Faunes et al. 2013). Upon differentiation Oct4 levels decrease and β-cat can shuttle to the nucleus to activate, together with Tcf4 an EMT program (Sánchez-tilló et al. 2011). In our Oct4 CKO embryos we see a reduction in Wnt signaling and in EMT specific markers like Twist2, Zeb1 and Snail2. This could mean that premature decrease of Oct4 results in an improper activation of the EMT program. Thus, some cells in the epiblast might undergo faulty EMT and fail to form their progeny in a correct spatiotemporal manner. This could explain the observation of cells in the node, which do not express Foxa2 and T in CKO embryos.

Tgf-β/Nodal signaling

The nodal signaling pathway is necessary and sufficient to initiate mesendodermal development. Separation of mesoderm and endoderm results from low or high levels of Nodal signaling, respectively (Zorn & Wells 2009). In Oct4 CKO ES cells we can see a strong reduction of activated Tgf-β/Nodal signaling upon differentiation. This can explain the shift from definitive endoderm towards axial mesoderm during differentiation of Oct4 CKO ESCs.

Oct4 has been shown to interact with Smad3 and is involved in its recruitment to co-occupied target genes, like Lefty1. This co-occupation results in the recruitment of the coactivator histone acetyltransferase p300 to target genes (Mullen et al. 2011). Our observation that differentiated Oct4 CKO ES cells show a reduction in phospho-smad2/3 indicates, that Oct4 is involved in proper activation of this pathway. The reported interaction

of Oct4 and Smad3 supports a direct role of Oct4 in this process (Mullen et al. 2011). This could mean that Oct4 is regulating activation of the Tgf-β pathway downstream of the receptors. It is possible that the observed upregulation of the ligand Nodal and the co-receptor Crypto is a countermeasure in Oct4 CKO embryos and ES cells to compensate for the reduced activation of the signaling pathway. Downstream of the receptor we can also find the Smad2 interacting TF Foxh1 down regulated in differentiated ES cells. Interestingly the combinatorial action of Foxh1 and PouV proteins is required for proper expression of some mesendodermal genes during development (Chiu et al. 2014). These results show that Oct4 is involved in activation of the Tgf-β pathway and target gene activation during early endodermal development.

Akt signaling

It has been demonstrated that Oct4 is involved in regulation of Akt signaling (Lin et al. 2014; Campbell & Rudnicki 2013). Since we can see a reduction in p-Akt in differentiated Oct4 CKO ES cells it is likely that Oct4 plays a role in activating this signaling pathway. How and if this might influence differentiation and lineage decisions in ES cells has to be determined. So far Akt signaling has been shown to maintain pluripotency and block differentiation signals (Singh et al. 2014; Watanabe et al. 2006) which would suggest that reduced Akt signaling after Oct4 deletion results in differentiation. Since we delete Oct4 in differentiated cells we would not expect an impact of reduced Akt signaling on differentiation.

Fgf4

Fgf4 has been shown to drive hindgut endoderm development and is activated by Oct4 and Sox2 in pluripotent ES cells (Jason R. Spence et al. 2010c; Yuan et al. 1995). In Oct4 CKO embryos we can see a reduction of Fgf4 levels which indicates that Oct4 is involved in its activation. Since it has been shown that Oct4 binds to Fgf4 in pluripotent ES cells it is possible that the activation through a direct mechanism. The reduction of Fgf4 could explain the defects observed in posterior embryonic development.

5.15 Transcriptional changes during endoderm differentiation upon Oct4 depletion

mRNA expression analysis of *in vitro* differentiated and sorted control and Oct4 CKO cells only shows very limited overlap with our data from embryos. The embryo consists of three germ layers which interact in a complex manner; this cannot be recapitulated in its full complexity by *in vitro* differentiation. Still, analysis of isolated Foxa2 expressing Oct4 CKO cells can give important insights into role of Oct4 for the process of endoderm formation and lineage segregation. The *in vitro* system allows us to analyze specifically endodermal cells to gain a more mechanistic insight into Oct4 function during endoderm differentiation. For further analysis it would be interesting to differentiate the DE population into more specialized organ specific cells and look for potential defects of the Oct4 deletion. Even though we did not observe organ defects which are directly caused by Oct4 deletion it might still be possible to identify changes *in vitro*.

5.16 Direct Oct4 targets during pluripotency and early endoderm differentiation

To elucidate direct effects of Oct4 on activation or repression of target genes, we identified Oct4 binding sites by ChIP-seq in mES cells during pluripotency and in early Foxa2- and + endodermal cells. Oct4 ChIP-seq in pluripotent ES cells has been performed by others and comparison with our results showed a strong overlap (Mathur et al. 2008; Marson et al. 2008b; Loh et al. 2006; Liu et al. 2008; Kim et al. 2008; Chen et al. 2008). This proves the quality of our dataset. However, observed differences could result from the use of different ESC lines or slight differences in the pluripotency status due to differences in cell culture. Compared to the pluripotent state we can see a strong reduction in the number of Oct4 bound genes in Foxa2- cells on d3 of endoderm differentiation, even though Oct4 is still expressed at comparable levels. This indicates that differentiation inducing signaling from Tgf-β/Nodal or Wnt pathways results in displacement of Oct4 from its pluripotency target genes. The genes which are still bound by Oct4 are associated with GO terms like ectoderm, mesoderm, somites and primitive streak which supports the involvement of Oct4 in early commitment of cells into these lineages. Among the genes bound by Oct4 in Foxa2+ endodermal cells we can find Sema6d, Cited2 and Lefty1 which are involved in cardiac

morphogenesis and LR asymmetry formation respectively (Toyofuku et al. 2004, Meno et al. 1998, Bamforth, Braganca, et al. 2004). Even though we did not find misexpression of Lefty1 in our CKO embryos it is still possible that potential expression changes are too little to be detected in a whole embryo by mRNA expression profile. A very interesting Oct4 target in Foxa2 expressing ES cells is also Wnt5b, which shows reduced expression in Oct4 CKO embryos and has been shown to be involved in PCP (Bradley & Drissi 2011). PCP plays a role in positioning of cilia in the node and thus makes a good candidate to explain the node defect in CKO embryos (Mahaffey et al. 2013; Song et al. 2010).

Our data is the first ChIP-seq data of Oct4 on endodermal cells. It was shown by others that Oct4 binds to the Brachyury promoter in endodermal cells (Thomson et al. 2011) which we could not confirm in our approach. This could be explained by differences in ES cell culture and cell line but also by the use of Gsk3β inhibitor for endodermal differentiation without Activin in this study (Thomson et al. 2011).

Our dataset is very valuable to address the function of Oct4 during early endoderm commitment. Due to the limited number of cells in embryos it is very challenging to identify for Oct4 targets in the gastrulating epiblast on a global scale. The information on Oct4 targets in vivo would be very useful and increase our knowledge of the role of Oct4 in early embryonic development.

5.17 **Changes in enhancer activation after Oct4 depletion**

Since Oct4 is down regulated during embryonic development and ESC differentiation it is also plausible that signaling and transcriptional changes in CKO cells are affected by epigenetic regulation. Interaction of Oct4 with components of chromatin modifying complexes has been demonstrated by others, which demonstrates the involvement of Oct4 in epigenetic gene regulation (Liang et al. 2008; Pardo et al. 2010; Ding et al. 2011; Yuan et al. 2009b). It has further been demonstrated the during transition from naïve to primed pluripotency Oct4 is involved in rearrangement and establishment of new enhancer sites (Buecker et al. 2014; Yang et al. 2014). We decided to look at changes of the active enhancer

mark H3K27ac upon deletion of Oct4 since this mark is characteristic for active enhancers (Creyghton et al. 2010a).

Our results show that a lot of genes have a reduction in active enhancer mark upon Oct4 deletion which for several genes also correlates with lower mRNA expression in CKO cells. From this data we can conclude that Oct4 is involved in the epigenetic activation of several of its target genes. Other studies have only looked at Oct4 relocation during early exit of pluripotency towards primed pluripotent cells (Buecker et al. 2014; Yang et al. 2014). With our results we can add an extra layer of information by extending the existing data to early endoderm commitment.

Even though published data does not show direct interaction of Oct4 with p300, which deposits the H3k27ac mark, the association of Oct4 with a complex containing p300 has been demonstrated in human ES cells (Lu et al. 2014). This suggests that Oct4 plays a role in recruiting epigenetic machinery to enhancer sequences during early endodermal commitment for proper activation of gene expression.

5.18 **Analysis of transcriptional and epigenetic changes during the exit of pluripotency**

To gain more insight into transcriptional and epigenetic changes during differentiation of mES cells towards DE we sorted Foxa2+ and FOxa2+,Sox17+ endodermal populations and analyzed them by RNA-seq and ChIP-seq. Compared to published studies our results refine the analysis to defined cell populations at specific stages over bulk cells (Gifford et al. 2013; Xie et al. 2013). The insights gained from the transcriptional and epigenetic dynamics during endoderm formation are an important basis for further applications. Since different cell types contain the same DNA sequence but differ in their epigenetic landscape it is very important to understand epigenetic changes to be able to differentiate or transdifferentiate cells into the desired populations.

The DNA modification 5-hydroxymethylcytosine (5hmC) has gained increased attention in the last few years (Ficz et al. 2011; Ito et al. 2010, Koh et al. 2011; Cimmino et al. 2011). 5hmC is generated by hydroxylation of 5mC, shows enrichment in CpG islands and

promoters, generally marks euchromatic regions and is associated with increased transcription (Ficz et al. 2011). Our results show that on the promoters of definitive endoderm TFs Foxa2, Eomes and Sox17 hmC increases with the expression of these genes. However, hmC is enriched in the promoter region of Nanog and Sox2 in pluripotent ES cells and decreases when these pluripotency factors are turned off. This contrary observation might be explained by the use of directed endoderm over EB differentiation (Ficz et al. 2011), which produces a more heterogeneous cell population. It is also possible that for a set of genes other activating mechanisms are more important and hmC has a different function for these factors.

6 Material and Methods

6.1 Material

6.1.1 Equipment

Agarose gel chamber	Midi 450 (Harnischmacher, Kassel)
	Typ Mini (neoLab, Heidelberg)
Balances	ScoutTM Pro (OHAUS)
	Sartorius
Cameras	AxioCam MRc5 (Carl Zeiss AG, Göttingen)
	AxioCam HRm (Carl Zeiss AG, Göttingen)
Centrifuges	5417 R (Eppendorf AG, Hamburg)
	5417 C (Eppendorf AG, Hamburg)
	5804 R (Eppendorf AG, Hamburg)
	Haereus Rotanta 460R (Thermo Fisher Scientific Inc., Waltham)
	Hettich Universal 30F (Andreas Hettich GmbH & Co. KG, Tuttlingen)
	1-14 (Sigma Laborzentrifugen GmbH, Osterode am Harz)
	Galaxy Mini (VWR International GmbH, Darmstadt)
Counting chamber (cells)	Neubauer (LO-Laboroptik GmbH, Friedrichsdorf)
Cryotome	Leica CM 3050S
Developing machine	AGFA Curix 60 developing machine (AGFA HealthCare GmbH, Bonn)

FACS	FACS AriaIII (BD Biosciences, San Jose USA)
Film cassettes	Hypercassette (Amersham, GE Healthcare GmbH, München)
Freezer	-20 °C (Liebherr Hausgeräte Ochsenhausen GmbH, Ochsenhausen)
	-80 °C (New Brunswick Scientific)
Fridge	4 °C (Liebherr Hausgeräte Ochsenhausen GmbH, Ochsenhausen)
Gel documentation system	UV-Transilluminator (Biorad, München)
	Gene Flash (Syngene Bio Imaging, Synoptics Ltd, Cambridge)
Glassware	Schott-Duran (Schott, Mainz)
Heating plate	RCT basic (IKA® -Werke GmbH, Staufen)
Hybridisation tubes	Hybridizer HB 100 (ThermoHybaid, Thermo Fisher Scientific Inc., Waltham)
Incubation systems/ovens	Shaking incubator; 37 °C bacteria (Shel Lab, Sheldon Manufacturing, Cornelius)
	TH-30 and SM-30; 32 °C bacteria (Edmund Bühler GmbH, Hechingen)
	65 °C Southern Blot (Thermo Electron Corporation)
	Thermomixer comfort (Eppendorf AG, Hamburg)
	Shake'n'Stack (ThermoHybaid, Thermo Fisher Scientific Inc., Waltham)
Microscopes	Axiovert 200 M (Carl Zeiss AG, Göttingen)

	Lumar.V12 (Carl Zeiss AG, Göttingen)
	MS5, $MZ7_5$(Leica Microsystems GmbH, Wetzlar)
	TCS SP5 (Leica Microsystems GmbH, Wetzlar)
Microtome	Microm HM 355 S rotation microtome (Thermo Fisher Scientific Inc., Waltham)
PCR machines	Personal Thermocycler (Biometra, Goettingen)
	Px2 ThermoHybaid (Thermo Fisher Scientific Inc., Waltham)
	PXE0.2 Thermo Cycler (Thermo Fisher Scientific Inc. Waltham)
pH meter	pH211 Microprocessor pH Meter (HANNA instruments Deutschland GmbH, Kehl am Rhein)
Photometer	BioPhotometer (Eppendorf)
	ND-1000 Spectrophotometer NanoDrop, (Thermo Fisher Scientific Inc., Waltham)
Pipettboy	accu-jet and accu-jet® pro (Brand GmbH & Co. KG, Wertheim)
Polyacrylamid gel chamber	Mini Trans-Blot® Cell (BioRad GmbH, Heidelberg)
Polyacrylamid gel preparation	BioRad
Power suppliers	Power Pack Basic (BioRad Laboratories, München)
	EC105 (Thermo Electron Corporation)
Pumps	LABOPORT ® (neoLab Migge Laborbedarf-Vertriebs GmbH, Heidelberg)
Roller Mixer	SRT1 (Bibby Scientific (Stuart), Staffordshire, GB)

Rotator/tumbler	VSR 23 (Grant BOEKEL, VWR international GmbH,Darmstadt)
	SHAKER DOS-10L (neoLab, Heidelberg)
Sonificator	Elmasonic
	UW 2070 (Bandelin electronics, Berlin)
Stirrer	STIR (VWR international GmbH, Darmstadt)
Water bath	VWR
	GFL, Burgwedel
Western Blot semi-dry system	Trans-Blot® SD, Semi-Dry Transfer cell (Biorad, Heidelberg)
	Trans-Blot Turbo (Biorad)
Vortexer	Vortexer (VWR international GmbH, Darmstadt)

6.1.2 Consumables

Pipettes (2 ml /5 ml/10 ml)	Greiner Bio-One GmbH, Frickenhausen
Pipette tips	Eppendorf AG, Hamburg
Pipette Filtertips	TipOne (Starlab GmbH, Hamburg)
14 ml tubes	BD Labware (Becton Dickinson GmbH, Heidelberg)
safe-lock reaction tubes	Eppendorf AG, Hamburg
dishes tissue culture	nunc (Thermo Scientific Fisher, Wiesbaden)
6-/ 12-/ 24-/ 48-well plates	Falcon
96-well plates (straight/conical)	nunc (Thermo Scientific Fisher, Wiesbaden)
10 cm bacterial plates	BD FalconTM (Becton Dickinson GmbH, Heidelberg)
Cover slips	VWR

Cell scraper	Starstedt
DNA Ladder (100 bp)	NEB
Embedding cassettes	Carl Roth GmbH & Co. KG, Karlsruhe
Embedding moulds	Carl Roth GmbH & Co. KG, Karlsruhe
Plastic pipettes	Greiner bio-one, Frickenhausen
Glas slide, Superfrost Plus	Thermo Scientific
Glas vials (ISH)	A. Hartenstein
Pasteur pipettes, plastic	transfer pipettes (Carl Roth GmbH & Co. KG, Karlsruhe)
Pasteur pipettes, glass	15cm/23cm (LABOR-BRAND, Gießen; Hirschmann Laborgeräte GmbH & Co. KG, Eberstadt)
Parafilm	Parafilm (Pechiney Plastic Packaging, Menasha)
PCR Tubes	Eppendorf AG, Hamburg
PVDF membrane	Immun-Blot PVDF-Membrane (BioRad Laboratories, Hercules)
Nitrocellulose membrane	GE Healthcare Buchler GmbH & Co. KG, München
Blotting paper	Whatman paper (GE Healthcare Buchler GmbH & Co. KG, München)
Scalpels	surgical disposable scalpels B/Braun (Aesculap AG & Co. KG,Tuttlingen)
Films	Kodak BioMax MS (Sigma-Aldrich GmbH, Hamburg)
	Amersham

Hyperfilm ECL (GE Healthcare Buchler GmbH & Co. KG, München)

6.1.3 Kits

miRNeasy Mini Kit (Qiagen Holding, Hilden)

ECL Detection Kit (Millipore Cooperation, Billerica, MA)

RNA to cDNA kit (Invitrogen)

iQ SYBR green supermix (Biorad)

6.1.4 Chemicals

(Sigma-Aldrich GmbH, Hamburg, Merck KGaA, Darmstadt, Carl Roth GmbH & Co. KG, Karlsruhe):

A

Acetic acid (glacial; Merck KGaA, Darmstadt)

Activin A, human (R&D Systems, Minneapolis)

Acrylamide/bisacrylamide (Rotiphorese® Gel 30 (37,5:1), Roth 3029.2)

Agarose (Biozym Scientific GmbH, Hess. Oldendorf)

Ampicillin (Roche 10835269001)

Ammonium peroxodisulfate (APS; Roth A3678-25G)

Anti-Digoxigenin-AP Fab fragments (Roche Diagnostics, Mannheim)

Antifade (Invitrogen P36930, Oregon)

Aqua Poly/Mount (Polyscience Inc., Warrington)

B

Blocking reagent (Roche Diagnostics, 11096176001, Mannheim)

Big Dye/ Big Dye Buffer (Life Technologies 4337457 or Lager 5000986)

BM purple AP Substrate (Roche Diagnostics, Mannheim)

BSA (Sigma-Aldrich)

Bradford reagent (Sigma-Aldrich)

Bromophenol Blue (Roth A512.1)

C

Calcium chloride (Roth CN93.1)

Chemiluminescent HRP Substrate (Millipore, WBKLS0500)

Chloroform, 99+ % (Sigma-Aldrich)

CI (Chloroform-Isoamylalcohol: 24:1)

Citric acid monohydrate (Roth)

CT 99021 (Gsk3β, 1386; Axon Medchem BV, Groningen)

D

D-EMEM (+) 4.5 Glucose (+) Pyrovate (Gibco®, Invitrogen™ Cooperation,

Carlsbad, CA)

DMEM/F12 (Invitrogen)

Diethylpyrocarbonate (DEPC), approx. 97 % (Sigma-Aldrich)

Dimethylsulfoxide (DMSO), >99.9 % (Sigma-Aldrich D5879-100ML)

Disodium phosphate dehydrate (Roth)

Dithiothreitol (DTT**;** Sigma D0632-10G)

dNTPs (Fermentas GmbH, St. Leon-Rot)

DPBS (-)$MgCl_2$, (-) $CaCl_2$ (Gibco®, Invitrogen™ Cooperation, Carlsbad, CA)

E

EDTA (Roth 8043.2)

EGTA (Roth)

Enhanced chemiluminescence (ECL) solution (Millipore Corporation)

Ethanol 100 % (Merck KGaA, Darmstadt)

Ethidiumbromide (Roth)

FBS (heat inactivated, Gibco®, Invitrogen™ Cooperation, Carlsbad, CA)

Formaldehyde (>37 %; Roth 7398.1)

Formamide (>99,5 %; Roth 6749.1)

G

Gelatine (Applichem A1693,0500)

Glutaraldehyde (25 %; Sigma-Aldrich G6257-1L)

Glycerol (Sigma G9891-25G)

Glycine (Sigma G8898-1KG)

H

HCl (2 M; Roth T134.1)

HEPES (200 mM, Gibco, InvitrogenTM Cooperation, Carlsbad, CA)

H_2O_2 30 % (Roth)

I

Isopropanol, 100 % (Merck KGaA, Darmstadt)

L

Levamisole hydrochloride (AppliChem)

L-glutamine (200 mM, Gibco, InvitrogenTM Cooperation, Carlsbad, CA)

LIF (produced at Helmholtz Zentrum München)

M

Magnesium chloride (VWR Prolabo 25108.260)

Magnesium Sulphate 7 hydrate (Roth)

Maleic acid (Sigma-Aldrich M0375-250G)

MEM non essential amino acids (100x, Gibco, InvitrogenTM Cooperation,

Carlsbad, CA)

Methanol, 100 % (Merck 1.06009.2500)

Mek1 (PD98059, Cell Signalling Technology, Frankfurt am Main)

Milk powder (Roth)

Mitomycin C (Sigma-Aldrich)

β-mercaptoethanol (50 mM, Gibco, InvitrogenTM Cooperation, Carlsbad, CA)

N

N-laurolysarcosine sodium salt (Sigma-Aldrich L5777-50G)

Neurobasal medium (Invitrogen)

Nitrogen(l) (Linde AG, München)

NP-40 (Roche Diagnostics, Mannheim)

Nuclear Fast Red (NFR; Fluka 60700)

O

Oligo-dT-primer (Promega GmbH, Mannheim)

Orange G (AppliChem, Darmstadt)

P

PAA FBS(PAA Laboratories GmbH/GE Healthcare, Pasching)

PAN FBS (PAN-Biotech GmbH „Pansera ES“)

Paraformaldehyde (Sigma-Aldrich)

Paraplast X-Tra (Sigma-Aldrich)

PBS (Gibco, InvitrogenTM Cooperation, Carlsbad, CA)

PCI (Phenol-Chloroform-Isoamylalcohol: 25:24:1; Carl Roth GmbH + Co. KG, Karlsruhe)

Penicillin/Streptomycin (Gibco, InvitrogenTM Cooperation, Carlsbad, CA)

Polyacrylamide/Rotiphorese Gel 30 (Roth)

Ponceau S solution (Sigma P7170-1L)

Potassium acetate (Roth)

Potassium chloride (Roth)

Potassium hexacyanoferrate(III) (Sigma-Aldrich)

Protease Inhibitor (Sigma, P8340)

Proteinase K (Roche)

Proteinmarker (Fermentas SM1811)

R

RNaseZAP (Sigma-Aldrich)

Rotihistol (Roth 6640.1)

Roti-Phenol/C/I (Roth)

Sheep serum (ISH, Sigma Aldrich S-2263)

S

Sodium chloride (Merck 1.06404.1000)

Sodium desoxycholate (97 %; Sigma D6750-100G)

Sodiumdodecylsulphate (SDS) (Roth N071.1)

Sodium Dihydogen Phosphate (Roth)

Sodium hydrogenic phosphate (Roth)

Sodium hydroxide (Roth)

Sodium acetate trihydrate (Roth)

T

TEMED (Roth, 2367.3)

Triethanolamine (Sigma T1377-500ML), (>99 %; Roth 6300.1)

Tris (Merck 1.08382.2500)

Tri-sodium-citrat (>99 %, Roth 3580.2)

Triton X-100 (Roth)

Trizol Reagent (Gibco, InvitrogenTM Cooperation, Karlsruhe)

Trypsin/EDTA (Gibco, InvitrogenTM Cooperation, Carlsbad, CA)

Tryptone (Roth 8952.2)

TWEEN-20 (Sigma P2287-500ML; Karl Roth GmbH, Karlsruhe)

V

Vectashield (Vector Laboratories, Burlingame)

X

Xylene (Merck 8.08691.2500)

6.1.5 Buffers and solutions

Isolation of genomic DNA

Tail clip (TC) lysis buffer: 100 mM Tris, pH 8.0-8.5, 5 mM EDTA, pH 8.0; 0,2 % SDS, 200 mM Sodium chloride

Yolk sac lysis buffer:50 mM KCl, 10 mM Tris-HCl, pH 8.3, 2 mM MgCl2, 0.45 % NP-40, 0.45 % Tween-20

DNA/RNA agarose gels

TAE buffer (50x stock): 2 M Tris, 50 mM Glacial acetic acid, 50 mM EDTA

Loading buffer DNA: 100 mM EDTA, 2 % SDS, 60 % Glycerol, 0.2 % Bromophenol blue

Loading buffer RNA (2x): 95 % Formamide, 0.025 % SDS, 0.025 % Bromophenol blue, 0.025 % Xylene cyanol FF, 0.025 % Ethidium bromide, 0.5 mM EDTA

Western blot

4x SDS-loading dye: 200 mM Tris-HCl, pH 6.8, 8 % SDS, 40 % Glycerol, 0.4 % Bromophenol blue, store aliquots à 320 µl at -20 °C, add 80 µl 2 DTT before use

2 M DTT: dissolve 3,085 g DTT powder in 10 ml H_2O, store aliquots à 80 µl at -20 °C, add 320 µl 4x SDS loading buffer before use

10 % APS: dissolve 5 g Ammonium peroxodisulfate powder in 45 ml H2O, store aliquots à 2 ml at -20 °C

Lysisbuffer (RIPA): 50 mM Tris-HCl, pH 7.4, 150 mM Sodium chloride, 0.5 % sodium deoxycholate, 1 % Nonidet P-40, 0.1 % SDS, filtrate sterile and add Proteinase Inhibitor 1:200 before use

4x Tri.HCl/SDS buffer: 100 ml: 6.05 g Tris, add 40 ml H_2O, adjust pH to 6.8 withconc. HCl, add H_2O to a total volume of 100 ml, filter sterile through a 0.45 µm filter, add 0.4 g SDS, store at RT

4x Tris-HCl/SDS buffer: 500 ml: 91 g Tris base, add 300 ml H_2O, adjust pH to 8.8 with conc. HCl, add H_2O to total volume of 500 ml, filter sterile through a 0.45 µm filter, add 2 g SDS, store at RT

10x Running Buffer:	60.6 g Tris, 288.2 g Glycine, 100 ml 20 %SDS, add H_2O up to a volume of 2 l, store at RT
10xTBS:	171.4 g NaCl (final conc. 150 mM),150,0 g Tris (final conc. 50 mM), dissolve in 1 l H_2O, adjust pH 7.5, add H_2O up to a volume of 2 l, autoclave, store at RT
KP-Buffer:	3 g Tris-HCl, 3 g Glycine, 100 ml Methanol, add H_2O to a final volume of 1 l, store at RT
AP I –Buffer:	36.3 g Tris-HCL, 100 ml Methanol, add H_2O to a final volume of 1 l, store at RT
AP II-Buffer:	3 g Tris-HCL, 100 ml Methanol, add H_2O to a final volume of 1 l, store at RT
Ponceau-solution:	0.2 % PonceauS, 3 % TCA
Blocking solution:	milk powder 1:10 in 1x TBST
ECL-solution:	directly before use mix Solution A and B 1:1

Immunostaining

Permeabilisation:	0.1 % TritonX-100, 100 mM Glycine in H_2O
Blocking solution:	10 % FCS, 1 % BSA, 3 % serum (donkey) in PBST (0.1 % Tween-20 in PBS)
DAPI solution	1mg/ml DAPI in H2O

LacZ staining

Fixation solution:	0.02 % NP-40, 5 mM EGTA, pH 8.0, 2 mM $MgCl_2$ x $6H_2O$, 1 % Formaldehyde, 0.2 % Glutaraldehyde in PBS
Washing buffer:	0.02 % NP-40 in PBS

Staining solution: 0.02 % NP-40, 2 mM $MgCl_2$ x $6H_2O$, 5 mM $K_3[Fe(CN)_6]$, 5 mM $K_4[Fe(CN)_6]$ x $6H_2O$, 0.01% Sodium desoxycholat, 1 mg/ml X-Gal (add freshly before use) in PBS

***In situ* hybridization**

DEPC-H_2O: add DEPC 1:1000 to H_2O, stir overnight, autoclave

PBS: 1.15 g Disodium Phosphate, 8 g Sodium Chloride, 0.2 g Monopotassium Phosphate, 0.2 g KCl in 1 l DEPC-H_2O, add 0.1 g $MgCl_2$ x $6H_2O$ and 0.1 g $CaCl_2$ x $2H_2O$, adjust pH to 7.2-7.3, filtrate sterile

PBT: 0.1 % Tween-20 in PBS

Heparin: 50 mg/ml in DEPC-H_2O

tRNA: 20 mg/ml in DEPC-H_2O

SDS: dissolve 10 g SDS in DEPC-H_2O

20 x SSC: 175 g Sodium Chloride, 88.2 g Sodium citrate in 1 l DEPC-H_2O, adjust pH to 4.5 with citric acid

Hybridisation buffer: 1 µg RNA probe per ml prehybridisation buffer

Prehybridisation buffer: 50 % Formamide, 5 x SSC, pH 5.4, 1 % SDS, 50 µg/ml yeast tRNA, 50 µg/ml Heparine, store at -20 °C

Solution I: 50 % Formamide, 5 x SSC, pH 5.4, 1 % SDS in MiliQ H_2O, store at -20 °C

Solution II: 50 % Formamide, 2 x SSC, pH 5.4, 0.2 % SDS in MiliQ H_2O, store at -20 °C

MAB: 100 mM Maleic acid, 150 mM Sodium Chloride, 2 mM Levamisole; 0.1 % Tween-20 in MiliQ H_2O, adjust pH to 7.5 with sodiumhydroxide, prepare solution fresh

MAB/Block	2 % Boerhinger Manheim blocking reagent in MAB
Antibody solution:	dissolve 10 mg embryo powder in 5 ml MAB/Block in a 50 ml falcon tube, vortex and incubate at 70 °C for 30 min, cool down on ice. Add 50 µl sheep serum, 4 µl α-Dig Alkaline Phosphatase (1:5000) and incubate at 4°C for 1 h. Centrifuge at 5000 rpm for 10 min at 4 °C. Decant supernatant to new falcon, add 154 µl sheep serum and dilute to 20 ml with MAB/Block. Prepare solution fresh.
TNT:	10 mM Tris pH 7.5, 0.5 M Sodium Chloride, 0.1 % Tween-20 in MiliQ H_2O
NTMT:	100 mM Tris, pH 9.5, 50 mM $MgCl_2$, 100 mM Sodium Chloride, 0.1 % Tween-20, 100 µl Levamisole in MiliQ H_2O

Nuclear fast red staining

NFR:	25 g Aluminum sulphate in 500 ml dH_2O, add 0.5 g NFR, heat up to dissolve, cool down and filter

6.1.6 Enzymes

Proteinase inhibitors	Sigma-Aldrich GmbH, Seelze
Superscript II	Fermentas GmbH, St. Leon-Rot
RNase inhibitors	Fermentas GmbH, St. Leon-Rot
Restriction enzymes	NEB GmbH, Frankfurt a. M.; Fermentas GmbH, St. Leon-Rot
DNA-Polymerases	*Taq* DNA Polymerase recombinant (Fermentas GmbH, St. Leon-Rot)
	Taq DNA Polymerase (Qiagen, Hilden)
RNA-Polymerases	Sp6 (Roche Diagnostics, Mannheim)
	T7 (Roche Diagnostics, Mannheim)
	T3 (Roche Diagnostics, Mannheim)
RNase A	Qiagen Holding, Hilden

RNase A Roche Diagnostics, Mannheim

RNase-free DNase I Promega GmbH, Mannheim

6.1.7 Antibodies and sera

Primary antibodies

ID	Antigen	Species	Dilution	Company	Order Number
29	a tubulin	mouse monocl.	IF 1:250 WB 1:5000	Sigma	T6199
30	Acetylated tubulin	mouse monocl.	IF 1:250	Sigma	T7451
3	Active-ß-Catenin	mouse monocl.	WB 1:1000	upstate/Millipore	05-665
184	Alpha Fetoprotein Ab2	rabbit polycl.	WB 1:100 IF 1:200	Thermo Schientific	RB-365-A1
206	Anti-GAPDH	mouse monocl.	WB 1:6000	Merck Biosciences	CB1001
22	beta-catenin	rabbit antiserum	IC:2000	Sigma	C2206
121	beta-Catenin	mouse monocl.	WB 1:2000	BD	610154
25	Brachyury (N-19)	goat polycl.	IF 1:500	Santa Cruz	sc17743
290	Cdx2	mouse	IF 1:500	Biogenex	Cdx2-88
5	E-Cadherin	mouse IgG2a	WB 1:2500, IF 1:2000	BD	610181
111	E-Cadherin (24E10)	rabbit polycl.	IC1:100	NEB	3195
84	Ep-CAM (G8.8-c)	rat hybridoma	IF 1:500	DSHB Hybridoma	4G1
23	Foxa2 M-20	goat polycl.	WB 1:800 IC 1:1000	Santa Cruz	sc-6554
56	Foxa2	rabbit polycl.	IF 1:500	abcam	ab40874
173	Gamma-Tubulin	mouse monocl.	WB 1:10.000	abcam	ab11316
103	GATA-4 (C-20)	goat polycl.	IF 1:100	Santa Cruz	sc-1237
189	GATA-4 (C-20)	goat polycl.	WB 1:200-1:1000 IF 1:50	Santa Cruz	sc-1237
104	GATA-6	goat polycl.	IF 1:100	R+D	AF1700
48	GFP	chicken	IF1:1000	Aves Labs	GFP-1020
23	HNf-3ß (Foxa2) M-20	goat polycl.	WB 1:800 IC 1:1000	Santa Cruz	sc-6554
125	Ki67	rabbit polycl.	IC Paraffin 1:2000	Menarini/Novocastra	NCL-ki67p
216	Ki67	rabbit polycl.	IF 1:500	abcam	ab15580
127	KRT8 TROMA-I	rat monocl.	IC 1:500	DSHB Hybridoma	TROMA-I
255	N-Cadherin	mouse	IF 1:500	BD	610920
59	Oct-3/4 (C-10)	mouse monocl.	WB 1:500, IC 1:1000	Santa Cruz	sc-5279
102	Oct-3/4 (N-19)	goat polycl.	IF 1:500	Santa Cruz	sc-8628
174	Pericentrin	rabbit polycl.	WB 1:300 IF 1:500	covance/HISS Diagn.	PRB-432C
146	phospho Histone H3	rabbit polycl.	IHC 1:500	Millipore	06-570
270	Phospho-Akt (Ser473) (D9E)	Rabbit	WB 1:2000 IP 1:50	Cell signaling	4060
58	p-Smad 2/3	goat polyclonal	WB 1:500 IC 1:100	Santa Cruz	sc-11769
192	RFP antibody (5F8)	rat	WB 1:1000 IF 1:1000	chromotek	ORD003515
99	Sox17	goat polycl.	IF 1:500	Acris/Novus	GT15094
74	Sox-2 (Y-17)	goat polycl.	IF 1:500	Santa Cruz	sc-17320
164	Tbr2/Eomes	rabbit polycl.	IC 1:300	Millipore	AB2283
165	Tbr2/Eomes	rabbit polycl.	IF 1:250	abcam	ab23345
37	ZO1	mouse IgG1	IF 1:200	Invitrogen	33-9100

Secondary antibodies

ID	Fluor	antigen species	Dilution	company	Order Number
25	488	goat	IC 1:800	Invitrogen	A11055
26	488	rabbit	IC 1:800	Invitrogen	A21206
12	546	mouse	IC 1:800	Invitrogen	A11030
24	555	rabbit	IC 1:800	Invitrogen	A31572
32	555	mouse	IC 1:800	Invitrogen	A31570
35	555	goat	IC 1:800	Invitrogen	A21432
58	564	rabbit	IC 1:800	Invitrogen	A11010
61	564	guinea pig	IC 1:800	Invitrogen	A11074
9	594	rat	IC 1:800	Invitrogen	A11007
56	594	mouse	IC 1:800	Invitrogen	A21203
63	594	goat	IC 1:800	Invitrogen	A-11058
64	594	rabbit	IC 1:800	Invitrogen	A-21207
18	633	goat	IC 1:800	Invitrogen	A21082
33	633	guinea pig	IC 1:800	Invitrogen	A21105
34	633	mouse	IC 1:800	Invitrogen	A21052
60	647	rabbit	IC 1:500	Invitrogen	A31573
62	647	rat	IC 1:800	Dianova	712-605-150
44	649	rabbit	IC 1:400	Dianova	711-605-152
45	649	rat	IC 1:400	Dianova	712-495-150
46	649	guinea pig	IC 1:400	Dianova	706-495-148
59	660	mouse	IC 1:800	Invitrogen	A21055
28	Cy2	chicken	IC 1:400	Dianova	703-225-155
27	Cy3	chicken	IC 1:400	Dianova	703-165-155
20	Cy5	chicken	IC 1:800	Dianova	703-175-155
29	Cy5	rabbit	IC 1:400	Dianova	111-175-144
37	Cy5	mouse	IC 1:800	Dianova	715-175-151
30	DyLight 488	chicken	IC 1:400	Dianova	103-485-155
41	DyLight 549	rat	IC 1:400	Dianova	712-505-153
16	HRP	goat	WB 1:20.000	Dianova	305-035-045
15	HRP	mouse	WB 1:20.000	Dianova	115-036-062
19	HRP	rabbit	WB 1:20.000	Dianova	111-036-045
38	HRP	rat	WB 1:20.000	"Kremmer" IMI	N/A

Sera:

Sheep serum (Sigma-Aldrich GmbH, Hamburg)

Goat serum (Sigma-Aldrich GmbH, Hamburg)

Donkey serum (Sigma-Aldrich GmbH, Hamburg)

6.1.8 Oligonucleotides for genotyping

Oligonucleotides used for genotyping mice, embryos and ES cells, All shown in 5' to 3'.

Name	Sequence (all 5' – 3')
EP408	TTGTTACTGAAGAAGTTGGGTGTG
EP409	GGGGACTCCTGCTACAACAATCGC
EP410	AACTGGTTTGTGAGGTGTCCG
EP411	GTATCCACTCGCACCTTGTTC
EP397	CTACTACCAAGGAGTGTACTCC
EP398	CTGTGGCCCATCTATTTAGGG
EP564	GATCTATGGTGCCAAGGATGAC
EP308	AAAGTCGCTCTGAGTTGTTAT
EP309	GCGAAGAGTTTGTCCTCAACC
EP310	GGAGCGGGAGAAATGGATATG
EP038	CAAGATCCGCCACAACATCG

6.1.9 Oligonucleotides for qPCR with SYBGREEN

Gene	Fwd primer (all 5' – 3')	Rev primer (all 5' – 3')
Cdx1	CCGAACCAAGGACAAGTACC	GATCTTTACCTGCCGCTCTG
Hoxb1	ACCTAAGACAGCGAAGGTG	ACGGCTCAGGTATTTGTTG
Aldh1a2	ACCATTCCTGTAGATGGAGAC	TTTGATGACCACGGTGTTAC
Dkk1	GAGGGGAAATTGAGGAAAGC	TTGGTGCACACCTGACCTTC
Cdx2	GGAAGCCAAGTGAAAACCAG	CCAGCTCACTTTTCCTCCTG
Fzd10	GGTGGCCGGACTCCCTGGAT	TGGGGCCTGAAGAGCGGAGG
Wnt8a	AACGGTGGAATTGTCCTGAG	GGTGACTGCGTACATGATGG
Grsf1	ACAGCTGCAATGAAAAGGAC	GCTTTAGAAGCGCTTGGTTG
Cdx4	GTGCCCATGAATGACATGAC	GCCGTTGATGATCTGTGTAG
Oct4	TGGAGACTTTGCAGCCTGAG	GCTTCAGCAGCTTGGCAAAC

6.1.10 Cell Culture media

MEF	DMEM (Gibco, Invitrogen™ Cooperation, Carlsbad, CA), supplemented with 2 mM L-glutamine (200 mM Gibco, Invitrogen™ Cooperation, Carlsbad, CA), 15 % FCS (PAN Biotech GmbH, Aidenbach), 0.1 mM β-mercaptoethanol (50 mM, Gibco, Invitrogen™ Cooperation, Carlsbad, CA), 1x MEM (non-essentiell amino acids, 100x; Gibco, Invitrogen™ Cooperation, Carlsbad, CA)
Freezing Medium:	5ml FCS (PAN/PAA), 4 ml D-MEM (or ESC medium), 1 ml DMSO (1x)
ESC lines	DMEM (Gibco, Invitrogen™ Cooperation, Carlsbad, CA), supplemented with 2 mM L-glutamine (200x, Gibco, Invitrogen™ Cooperation, Carlsbad, CA), 15 % FCS (PAN Biotech GmbH, Aidenbach), 0.1 mM β-mercaptoethanol (50 mM, Gibco, Invitrogen™ Cooperation, Carlsbad, CA), ESGRO® (LIF) (107 U/ml; Chemicon, Millipore, Schwalbach), 1x MEM (non-essential amino acids, 100x; Gibco, Invitrogen™ Cooperation, Carlsbad, CA), 2 mM HEPES (200 mM, Gibco, Invitrogen™ Cooperation, Carlsbad, CA)
EDM	Endoderm differentiation medium: DMEMF12/RPMI1640 1:1 supplemented with Glutamax100x, Albumax 100x, HEPES, cytidine, b-mercapto ethanol, Insulin-sodium selenite-transferrin (IST), ActivinA 10ng/ml, Wnt3a 1 ug/ml (=EDM 10/1) or other concentrations where stated
Epi	Epi stem cell differentiation medium: DMEM/F12 / neurobasal medium 1:1 supplemented with N2 supplement, B27 supplement without RA, glutamax, Pen/Strep, b-mercapto ethanol, ActivinA 20ng/ml, bFGF 12ng/ml

6.1.11 Reagents for cell culture

Reagent	Company	order #
DPBS	Invitrogen	14040133
DMEM	Invitrogen	41966029
DMEM/F12	Invitrogen	11320074
Neurobasal medium	Invitrogen	21103049
L-glutamine	Invitrogen	25030081
Pen/Strep	Invitrogen	15140122
Trypsin	Invitrogen	25300054
DMSO	Sigma Aldrich	D4540
N2 supplement	R&D Systems	A1370701
B27 supplement	R&D Systems	12587010
AcitvinA	R&D Systems	338-AC-050
Wnt3a	R&D Systems	1324-WN-010
bFgf	R&D Systems	233-FB-025
Fgf4	R&D Systems	5846-F4-025

6.2 Methods

6.2.1 Expansion of mouse embryonic fibroblasts (MEF) and treatment with mitomycin C (MMC)

One 15cm plate (frozen in 1 vial) of passage 2 (P2) MEFs is thawed onto 5x15cm tissue culture plates in 20 ml feeder medium. Cells are fed every other day. When cells are confluent they are split 1:5 onto 15 cm plates grown again to confluence. For splitting cells

are washed 2 times with DPBS and 4ml 0.05% trypsin/EDTA is added per plate. When the cells have detached after ca. 4 min at 37°C 6ml of medium is added and cells are spun down 4 min at 1200rpm. The pellet is resuspended in fresh medium and cells are plated onto new plates. Cells are passaged once more as described above to obtain P4 cells.

To generate mitotically inactive feeder cells for ES cell culture P4 MEFs are trypsinized as described above. The pellet is the resuspended in 20 ml feeder medium containing 10µg/ml mitomycin C (MMC) and cells are incubated for 1h at 37°C, mixing the cells by inverting the tube after 20 and 40 min, with a loose cap. Afterwards the cells are washed 3 times with 20ml DPBS.

6.2.2 Freezing and thawing of MEFs

For cryopreservation cells are spun down and the pellet is resuspended in freezing medium at 1x15cm plate per 1ml. 1ml is frozen in 1 cryovial in a precooled freezing container at -80°C. After at least 4 hours cells are transferred to liquid nitrogen.

For thawing the cells, vials are defrosted in a37°C waterbath and pipetted into 5ml of medium. Cells are spun down, resuspended in medium and seeded onto tissue culture dishes of the desired size.

6.2.3 Establishment of ES cell lines from mouse blastocysts

For blastocyst generation males are mated with superovulated females and are checked for vaginal plugs every morning.

One day before dissection MMC feeders are seeded in a 96-well plate and ES medium is supplemented with MEK1 inhibitor (50µM) and Gsk3β inhibitor (3µM).

From pregnant mice uteri are dissected at embryonic day 3.5 (E3.5) and collected in Sterile PBS. Uteri are washed with PBS and flushed with 0.5ml ESC medium in a 6cm dish to collect the non-implanted blastocysts.

The blastocysts are washed with ESC medium under a laminar flow hood an each placed into a well of a 96-well plate with ESC medium containing MEK1 and GSK3b inhibitors on feeders.

Blastocysts are cultures for 3 days without disturbance at 6% CO2 and 37°C. When the embryos have attached to the feeder layer medium is changed and culture is continued until d5-6.

To dissociate the ICM after 5-6 days the cells are passage onto a new 96-well feeder plate. For this, wells are washed with 100µl DPBS each and 30µl of 0.05% trypsin is added per well. After 10min incubation at 37°C the outgrowth are disaggregated by pipetting up and down. 100µl ES medium is added and the disaggregation is continued. The cells are then transferred to the new well with 30µl Medium with inhibitors. Cells are fed the next day.

After about 6 days ESC colonies have formed and well are fed with normal ES medium without inhibitors. At this stage cells are P1.

For expansion cells are split as above onto 48 well plates with feeders and afterwards depending on density and growth rate on larger dishes. For genotyping some cells are split onto 0.1% gelatin coated dishes.

6.2.4 Freezing and thawing of ES cells

For long-term storage, ESCs were trypsinized as described above and the cell pellet was resuspended in 500 µl cooled 1 x ESC freezing medium. Cells were transferred to cryovials which were put into pre-cooled freezing boxes. Freezing boxes were kept at -80 °C for at least 4 h to cool the cells slowly down to -80 °C before vials were transferred to N2 tank.

ESCs were defrosted in a water bath for 1 min at 37 °C and re transferred to a 15 ml falcon tube prefilled with ESC medium. Cells were centrifuged at 1200 rpm for 4 min and the cell pellet was resuspended in the according amount of ESC medium. ESCs were cultured on MMC-treated MEFs at 5-7 % CO2 in a humidified incubator.

6.2.5 Endoderm differentiation of mouse ES cells

For all differentiation experiments ES cells were cultured for 2 passages in ES medium with PAA serum on 0.1% gelatin coated dishes to remove feeder cells. Each 10cm plate of these cells is frozen per vial to increase reproducibility of experiments (g3 stocks).

ES cell gelatin stocks are thawed onto 0.1% gelatin coated dished and let recover. For differentiation plates are coated with 0.1% gelatin one day before differentiation at 37°C.

Cells are trypsinized, spun down and washed once with PBS. The pellet is resuspended in EDM and cells are counted in a Neubauer chamber. Cells are seeded in EDM containing ActivinA and wnt3a at a density of 30000 to 60000 per cm^2. Cells are harvested on d1-5 of differentiation for analysis.

6.2.6 Epi stem cell differentiation of mouse ES cells

For Epi stem cell differentiation passage3 gelatin cells are used. Cells are trypsinized like for endoderm differentiation, washed once with PBS and resuspended in EpiSC medium. Cells are counted at a dilution of 1:10 on a Neubauer chamber and plated at15000-30000 per cm2 on fibronectin or gelatin coated dishes or plates. Harvesting/analysis of cells is done on d1-5 of differentiation.

6.2.7 Embryoid body (EB) formation from ES cells

Mouse ES cells are cultured on feeders, trypsinized and preplated 2x25min on non-coated tissue culture plates in ES medium to remove feeders. Cells are then resuspended in ES medium without LIF, counted and drops of 25µl containing 1500 cells each are put on the lid of a 15cm tissue culture plate. To prevent drying out 10ml PBS is put into the dish. The lid is put on the dish and EBs are differentiated for 4-5 days without changing medium.

6.2.8 FACS sorting of ES cells

Before sorting or analysis, cells are filtered through a70µm filter.

ES cells are FACS sorted on a BD FACS Aria III. Nozzle size 70µm or 85µm is used for sorts and the Venus signal is detected by the 530/30 I A filter set and cherry in the 610/20 A filter. Data is analyzed with the Tree Star FlowJo software

6.2.9 Chromatin immunoprecipitation (ChIP) of FACS sorted cells

To crosslink proteins and DNA ES cells are harvested from 10cm plates by washing 2 times with 5ml PBS and adding 1ml of 0.05% trypsin for 3min at 37°C. After adding 5ml ES medium cells are spun down 4min at 1200rpm and the pellet is resuspended in 15ml medium. Crosslinking is done by adding 5ml 4% formaldehyde to a final concentration of 1% and incubation for 10min at RT. To stop the crosslinking 6.66ml of 0.5M glycine is added to a final concentration of 0.125M for 5min at RT. Cells are spun down and the pellet is washed 2 times with 50ml cold PBS containing 10% FBS. The cells are resuspended in PBS and used for FACS sorting. Sorted cells are spun dow with the addition of FCS and pellets are snap frozen in lN2. Samples are stored at -80°C until further processing. ChIP was performed by Stanimir Dulev and Filippo Cernilogar, Gunnar Schotta lab, LMU.

6.2.10 RNA extraction

RNA from cells embryos is extracted with the Qiagen RNAeasy mini kit according to the manufacturer's protocol.

RNA extraction was also performed without the use of a commercial kit:

For this cells/embryos are collected in a clean 1.5ml tube and 250µl of Trizol® is added. Cells are homogenized by pipetting up and down until no tissue/ cells are visible. The lysate is incubated for 5min at RT, then 50 µl of chloroform is added and the tube is mixed vigorously. After 2-3min incubation at RT the tube is spun at 14000rpm for 15min at 4°C in a phase lock gel tube. Now the organic and aqueous phases have separated. The upper aqueous phase is transferred to a new tube without taking the white interphase containing proteins. 125µl of isopropanol is added and the solution is incubated 10min at RT after mixing. The solution is spun down 15min at 14000rpm at 4°C, the pellet washed with 70% EtOH/DEPC H2O and

spun again. All liquid is removed from the tube and the pellet air dried for 5-10min. When no liquid is left the pellet is resuspended in DEPC H2O and frozen at -80°C.

6.2.11 Measuring of DNA and RNA concentration

For determining DNA and RNA concentrations the absorptions at 260nm measured on a Nanodrop was used.

6.2.12 Analysis of RNA quality for qPCR

To check the integrity of the isolated RNA for following applications ca 200-500ng of the isolated RNA are loaded onto a 1% TAE gel made with DEPC H2O. All items used are cleaned thoroughly before use and TAE buffer is set up with DEPC H2O. The gel is run at 135V for 10-15min and presence of the 28s and 18s bands without a smear indicates good RNA integrity.

6.2.13 Reverse transcription from RNA to cDNA

To generate cDNA from isolated RNA the high capacity RNA to cDNA kit from Invitrogen is used according to the manufacturer's protocol. cDNA is frozen at -20°C.

6.2.14 Quantitative PCR (qPCR)

For quantification of RNA by qPCR the iQ SYBR green supermix from Biorad was used.

The 25µl reaction was set up as follows:

SYBR green mix	12.5
primer fwd	1µl
primer rev	1µl
cDNA	12ng
H2O	to 25µl

Program:

95°C	3min
95°C	15sec
60°C	30sec
72°C	30sec

Read after each cycle for 40 cycles

Melting curve after the program has finished from 54-90°C read every 0.2°C.

The data was analyzed with the ΔΔCt method:

Fold change KO/contr = $2^{-((Ct_{KO}-Ct_{contr}\ Gapdh)-(Ct_{KO}-Ct_{contr}\ Gapdh)}$

6.2.15 In vitro transcription (IVT) and generation of in situ probes

Before cDNA is transcribed the vector has to be linearized by cutting with a restriction enzyme at the future 3' end.

The IVT is set up as follows:

DEPC H2O	6µl
10x Transcription buffer	1 µl
10x Dig mix	1 µl
RNase inhibitor	0.5 µl
Sp6/T7 or T3 polymerase	0.5 µl
DNA linearized	500ng

The reaction is incubated for 3h at 37°C, afterwards 1µl DnaseI is added to digest the DNA vector. The mixture is incubated at 30 °C for 15 min to precipitate the RNA, 100 µl DEPC-H_2O, 10 µl 4 M LiCl and 300 µl 100 % ethanol are added and the reaction is incubated on dry ice for 15 min. Afterwards the mixture is centrifuged at 14000 rpm at 4 °C for 10 min. The pellet is washed once with 70 % ethanol, centrifuged and dried at RT for 5 min. The pellet is resuspended in 55 µl DEPC-H_2O. 5 µl are used to check the quality of the RNA probe on a 1 % RNA gel.

6.2.16 Agarose gel electrophoresis

Agarose gel is prepared at 1-2% depending on expected fragment size in TAE buffer. Agarose is melted in a microwave oven and ethidiumbromide (EtBr) is added to a final concentration of 1mg/ml. DNA samples are mixed with OrangeG dye (5x) and the gel is run at ca130V for 30min. DNA bands are visualized under UV light.

6.2.17 Extraction of proteins from cells

RIPA buffer supplemented with proteinase inhibitor cocktail (1:200) is added to the cells and vortexed extensively. The suspension is incubated for 10min on ice, centrifuged 10min at 1400rpm at 4°C and the supernatant frozen at -20°C.

6.2.18 Measuring protein concentration by Bradford assay

With the colorimetric Bradford assay protein concentration is measured by the absorbance shift of the Coomassie brilliant blue dye to 595nm. 1µl of protein sample ist diluted 1:10 with 9µl H2O and 990µl Bradford reagent is added. After 10min incubation at RT OD600 is measured compared to a standard curve.

6.2.19 Western blot

Denaturing SDS polyacrylamide gel electrophoresis

Solutions for 2 small 10% separating gels:

5 ml acrylamide/bisacylamide-mixture (ready-to-use)

3.75 ml 4x Tris.HCl/SDS buffer pH 8.8

6.25 ml H2O

20 µl TEMED

150 µl 10 % APS

The mixture is quickly filled between 2 sealed glass plates and covered with isopropanol. When the gel has polymerized the isopropanol is poured out and rests are removed with a paper towel.

For 2 small stacking gels:

650 µl acrylamide/bisacylamide-mixture (ready-to-use)

1.25 ml 4xTris/SDS pH 6.8

3.10 ml H2O

10 µl TEMED

50 µl 10 % APS

The stacking gel is filled on top of the separation gel and the comb is inserted without enclosing air bubbles.

Dithiothreitol (DTT) is added to 4 x SDS loading buffer before use and mixed with the protein sample in a ratio of 1:3. The protein sample is then denatures for 5min at95°C and put on ice afterwards.

The comb is removed from the gel, the pockets washed and cleaned and 30-60µg sample and size standard loaded into the pockets using a Hamilton syringe.

The gel is run for ca. 90-120min at 100V.

b) Semi-dry blot

After the gel electrophoresis the glass plates are separated and the gel is equilibrated for 10min in KP buffer. The PVDF membrane is activated for 15sec in MeOH, washed in H20 for 2min and incubated in APII buffer for 5min.

Setup of blot:

Cathode (top)

3 x blotting paper soaked with KP buffer

Acrylamide gel

PVDF membrane

1 x blotting paper soaked with APII buffer

2 x blotting paper oaked with API buffer

Anode (bottom)

The semi dry blot is run at 0.22A per gel for 30min. After blotting the membrane is incubated in Ponceau S solution to confirm successful blotting. The membrane is then washed with H2O until the red staining disappears.

c) Immunostaining

The membrane is blocked in 5% milk powder in TBST for 1h at RT. The membrane is then incubated in the desired antibody diluted in 5% milk over night at 4°C. The next day the membrane is washed 3x15min in TBST. The 2° antibody is incubated for 1h at RT in a dilution of 1:10000. After this the membrane is washed 3x15min in TBST and incubated with 1ml ECL solution for 1min. The excess liquid is dried an the membrane exposed for 1s to 5min to a BIOMAX film in a dark room. After exposure the film was developed.

6.2.20 Immunohistochemistry

Fluorescent staining of whole mount embryos

Embryos are fixed in 2% PFA for 20min after dissection, washed 3x10min with PBST and permeabilized for 10min (E7.0-7.5)-20min (E8.5) at RT. After washing 2 times in PBST embryos are blocked in blocking solution for 2-3h. 1° antibodies are added at the accurate dilution in blocking solution and incubated over night at 4°C.

The next day the embryos are stained another 2h at RT washed 3x10min with PBST and the 2° antibodies are added in blocking solution for at least 3h at RT. After staining embryos are washed 1x10min with PBST with DAPI and 3x10min with PBST. Before embedding embryos are dehydrated in an increasing glycerol series from 15-45% at 5min each and mounted on coverslips between 100µm spacer in mounting medium. Slides are stored at 4°C.

Staining of cryosections

Frozen sections are dries for 1h at RT, then they are washed 3x15min in PBS and permeabilzed for 10min with 0.1M glycine and 0.1% Triton X 100 in PBS. Afterwards they are washed 3x10min in PBST and blocked for at least 1h. Primary antibodies are diluted in blocking solution and incubated over night at 4°C. The next day sections are washed 3x10min in PBST and the secondary antibody added in blocking solution for at least 2h at RT. DAPI is used 1:500 in PBS and the sections stained for 30min at RT. Thereafter they are washed 3x10min in PBS and mounted in antifade embedding medium. Images are taken with a Leica SP5 confocal microscope.

Staining of cells

Medium is removed from plates by inverting the plate. The wells are washed twice with PBS, fixed with 4 % PFA for 5 min at room temperature, rinsed twice with PBS and permeablized with 1 % Triton X - 100, 1 % glycine in H_20 for 5 min. Cells are washed 10min in PBST and blocked in blocking solution for more than 30 min. Primary antibodies are diluted in blocking

solution and incubated overnight at 4 °C. The next day, the plates are rinsed twice with PBST and washed 3 x 10 min with PBST. The secondary antibodies were diluted in blocking solution and cells are incubated 1-2 h at room temperature. Afterwards, the cells are stained in PBST containing DAPI in a ratio 1:500 for 20 min at RT. The cells are washed 4 x 10 min with PBST. After washing, the wells are covered with 50 to 100 µl PBS and stored at 4 °C in the dark.

6.2.21 Mouse husbandry and matings

The mice are kept in a day-night cycle (6.30 am-6.30 pm). For determination of the embryonic stages, bred female mice where checked in the morning for the presence of a vaginal plug. At noon of the plug day the time point was considered as embryonic day 0.5 (E0.5). Detailed staging was done according to (Downs K and Davies T 1993)

6.2.22 Genotyping of mice by PCR

Mouse tail clips (TC) are digested in TC lysis buffer with proteinase K over night at 55°C. Tails are vortexed ant centrifuged at 14000rpm for 10min. The supernatant is transferred to a fresh tube and 500ul isopropanol added and mixed well. The tube is again centrifuged for 10 min and the pellet washed with 70% EtOH, dried for 10min at RT. The DNA pellet is resolved in 400µl MilliQ water on a shaker at 37°C.

Embryos are digested in yolk sac lysis buffer containing proteinase K (40µg/ml) at 55°C over night. Proteinase K is inactivated by incubation at 95°C for 30min.

<u>Set up of a 3primer PCR reaction</u>:

2 µl 10x Taq buffer with $(NH_4)_2SO_4$

2 µl 25 mM $MgCl_2$

1 µl 10 mM dNTPs

1 µl 10 µM primer a

1 µl 10 µM primer b

1 µl 10 µM primer c

0.2 µl Taq polymerase

10.8 µl nuclease-free water

1 µl genomic DNA

PCR program

95°C	5min	
95°C	30sec	35 cycles
X°C	40sec	
72°C	45sec	
72°C	10min	
16°C	pause	

a) Oct4 flox genotyping:

To distinguish the Oct4 flox allele from wt primers EP408 and EP409 are used at 58°C annealing temperature. The Oct4 flox band has a size of 450bp and the wt band of 415bp.

b) Oct4 flox deleted (FD) genotyping:

To distinguish the Oct4 FD allele from wt primers EP410 and EP411 are used at 58°C annealing temperature. The Oct4 FD band has a size of 245bp and for the wt allele no product is amplified.

c) Foxa2-2A-iCre genotyping:

To distinguish the Foxa2-2A-iCre allele from wt primers EP397, Ep398 and EP564 are used at 60°C annealing temperature. The Foxa2-2A-iCre band has a size of 457bp and the wt band of 207bp.

d) Rosa25 reporter (R26R) genotyping:

To distinguish the R26R allele from wt primers EP308, Ep309 and EP310 are used at 60°C annealing temperature. The R26R band has a size of 340bp and the wt band of 650bp.

e) Foxa2-Venus fusion (FVF) genotyping:

To distinguish the FVF allele from wt primers EP038, Ep397 and EP398 are used at 60°C annealing temperature. The FVF band has a size of 506bp and the wt band of 207bp.

6.2.23 Isolation of embryos and organs

Embryos and organs are dissected according to Nagy and Behringer („Manipulating the mouse embryo: a laboratory manual“). The stages of embryos from E6.5 to e8.5 are determined according to Downs and Davis (Downs and Davies, 1993)

6.2.24 LacZ staining with X-gal

Mouse Embryos or organs are fixed in fixation solution for 20-60min (E12.5 or earlier) or 60-90min (E13.5 and later). The tissue is washed 3x in PBS NP40 and stained in X-gal (5-bromo-4-chloro-3-indolyl β-D-galactopyranoside) staining solution at RT until the blue signal has the desired intensity. Stained tissues are washed 3x10min in PBS NP40 and fixed in 4% PFA over night at 4°C.

6.2.25 Whole mount in situ hybridization (WISH)

Embryos are dissected in DEPC PBS, transferred to a clean glass vial and fixed with 4% PFA for 1h at 4°C. Embryos are afterwards washed with PBT, dehydrated in a 25%-50%-100% MeOH series and stored at -20°C until use.

Day 1:

Embryos are rehydrated in a decreasing MeOH series for 5 min each and 2x5in in PBST. Then they are bleached in 3% H2O2 in PBT for 20min in the dark and washed 3x5min with PBT. After bleaching embryos are postfixed in in 4% PFA, 0.2% glutaraldehyde in PBT for 20min and washed again 3x5min. 1ml of prewarmed prehybridization buffer is added and the embryos swirled for 5min. Fresh prehybridization buffer is then added for 2h at 70°C. 1µg RNA probe is denatured for 5min at 80°C and exchanged with the prehybridization buffer. Embryos are incubated at 70°C overnight. Solution I and II are put at 70°C overnight.

Day 2:

The hybridization mix is removed and the probe saved for reuse. Embryos are washed 3x30min with prewarmed solution I and then 3x5min with TNT at RT. The tissue is then treated with 100µg/ml RNase in TNT for 60min at 37°C and washed with TNT/Solution II (1:1) for 5min, with solution II 3x30min at 65°C and 3x5min in MAB at RT. Embryos are then blocked in 10% sheep serum in MAB/2% blocking reagent for 2-3h. The blocking solutions is changed for the antibody solution an incubated overnight at4°C.

Day3:

Embryos are washed 3x10min in MAB at RT and once every hour throughout the day. Overnight the washing step is continued at 4°C.

Day 4:

Embryos are washed 3x10min in NTMT at TR and incubated in BM purple at TR until a clear signal is visible (if necessary over night at 4°C). The reaction is stopped by washing 3 times in PBT and fixed afterwards in 4% PFA for 1h at RT. Embryos are then imaged on a Zeiss Lumar V12 stereo microscope.

6.2.26 Histology

Dehydration and embedding in paraffin

Formaldehyde fixed samples are washed in PBS over night at 4°C. The next day dehydration is done in an increasing EtOH series:

E7.5-E8.5: 70%EtOH 15min-2h, 96%EtOH 5min, 100% EtOH 5min Xylene 5min

E9.5: 70%EtOH 15min-2h, 96%EtOH 10min, 100% EtOH 10min Xylene 5-10min

Organs: 70%-80%-96%-100% EtOH and Xylene for 30min each.

After the last step the Embryos or organs are transferred to molten paraffin at 65°C and incubated overnight. The tissue is embedded in plastic molds and after solidification mounted onto embedding cassettes.

Paraffin sections

Paraffin sections are cut at a thickness of 7-9µm, transferred to a 37°C waterbath and mounted onto charged glass slides. Sections are dried over night at 37°C before further processing.

Cryo sections

Embryos are fixed for 2h in 4% formaldehyde at 4°C and washed for 3x10min in PBS. Afterwards the tissue is incubated in 15% sucrose for 1h and 30% sucrose overnight. The next day the solution is changed to 30%sucrose/OCT (1:1) for 2h at RT. The organs are transferred to OCT in an embedding mold, oriented and frozen on dry ice. The blocks are stored at -20°C until sectioning.

For sectioning the block is mounted onto the holder of a cryostat and cut at a thickness of 10µm. Sections are picked up by non-cooled glass slides, dried for 30min at RT and stores at -20°C.

Counter staining with nuclear fast red (NFR)

Sections are dewaxed for 20min in 100% Xylene, thereafter rehydrated in a series of 100%-96%-80%-70% EtOH for 3min each and H2O for 3min. The slides are stained for 45sec in NFR

and afterwards washed in H2O. For dehydration slides the same EtOH concentrations as before are used from 70% to 100% each for 2min and fro 5min in 100% Xylene at the end. The sections are mounted in Histokit mounting medium and let dried at RT overnight. Images are taken with a Zeiss Lumar V12 stereo microscope.

6.2.27 Transcriptome analysis

Performed by Martin Irmler, IDG

RNA isolation

Total RNA was isolated employing the RNeasy Micro Plus kit (Qiagen) including removal of remaining genomic DNA. The Agilent 2100 Bioanalyzer was used to assess RNA quality and only high quality RNA (RIN>7) was used for microarray analysis.

Expression profiling

Total RNA (120 ng) was amplified using the one-cycle MessageAmp Premier labeling kit (Ambion). Amplified aRNA were hybridized on Affymetrix Mouse Genome 430 2.0 arrays containing about 45,000 probe sets. Staining and scanning was done according to the Affymetrix expression protocol.

Statistical transcriptome analysis

Expression console (v.1.3.0.187, Affymetrix) was used for quality control and to obtain annotated normalized RMA gene-level data (standard settings including median polish and sketch-quantile normalisation). Statistical analysis was performed by utilizing the statistical programming environment R (R Development Core Team Ref1) implemented in CARMAweb (Ref2). Genewise testing for differential expression was done employing the limma *t*-test and Benjamini-Hochberg multiple testing correction. Heatmaps were generated with CARMAweb and cluster dendrograms with R scripts based on agnes, diana or hclust.

[1] Team, R. D. C., R: A language and environment for statistical computing. 2005.

[2] **Rainer, J., Sanchez-Cabo, F., Stocker, G., Sturn, A. and Trajanoski, Z.** (2006). CARMAweb: comprehensive R- and bioconductor-based web service for microarray data analysis. *Nucleic Acids Res* **34**, W498-503.

6.2.28 Cell profiler analysis

Quantitative analysis of immuno fluorescence staining was done by Cell Profiler software (Jones TR, Kang IH, Wheeler DB, Lindquist RA, Papallo A, Sabatini DM, Golland P 2008). Fluorescent staining of nuclear antigens is identified as primary objects with the global Otsu threshold and the mean normalized intensity of the fluorescent signals recorded. Values for 2 antigens are plotted against each other by MS Excel as dotplot.

6.2.29 Gene Ontology term (GO) analysis

GO analysis was performed using Genomatix software (www.genomatix.de). Gene names were uploaded to the Gene Ranker module and analyzed for enrichment of GO terms

7 References

Aamar, E. & Dawid, I.B., 2010. Sox17 and chordin are required for formation of Kupffer's vesicle and left-right asymmetry determination in zebrafish. *Developmental Dynamics*, 239(11), pp.2980–2988.

Abu-Remaileh, M. et al., 2010. Oct-3/4 regulates stem cell identity and cell fate decisions by modulating Wnt/beta-catenin signalling. *The EMBO journal*, 29(19), pp.3236–3248.

Ackerman, K.G. et al., 2007. Gata4 is necessary for normal pulmonary lobar development. *American journal of respiratory cell and molecular biology*, 36(4), pp.391–7.

Ai, D. et al., 2006. Pitx2 regulates cardiac left-right asymmetry by patterning second cardiac lineage-derived myocardium. *Developmental biology*, 296(2), pp.437–49.

Van den Akker, E. et al., 2002. Cdx1 and Cdx2 have overlapping functions in anteroposterior patterning and posterior axis elongation. *Development (Cambridge, England)*, 129(9), pp.2181–93.

Aksoy, I. et al., 2013. Oct4 switches partnering from Sox2 to Sox17 to reinterpret the enhancer code and specify endoderm. *The EMBO Journal*, (November 2012), pp.1–16.

Ambrosetti, D.C. et al., 1997. Synergistic activation of the fibroblast growth factor 4 enhancer by Sox2 and Oct-3 depends on protein-protein interactions facilitated by a specific spatial arrangement of factor binding sites . Synergistic Activation of the Fibroblast Growth Factor 4 En. *Molecular and cellular biology*, 17(11).

Ang, S. & Rossant, J., 1994a. HNF3b Is Essential for Node and Notochord in Mouse Development. *Cell*, 78, pp.561–574.

Ang, S.L. et al., 1993. The formation and maintenance of the definitive endoderm lineage in the mouse: involvement of HNF3/forkhead proteins. *Development (Cambridge, England)*, 119(4), pp.1301–15.

Arnold, S.J. et al., 2000. Brachyury is a target gene of the Wnt/beta-catenin signaling pathway. *Mechanisms of development*, 91(1-2), pp.249–58.

Arnold, S.J. & Robertson, E.J., 2009. Making a commitment: cell lineage allocation and axis patterning in the early mouse embryo. *Nature reviews. Molecular cell biology*, 10(2), pp.91–103.

Athanasiadou, R. et al., 2010. Targeting of de novo DNA methylation throughout the Oct-4 gene regulatory region in differentiating embryonic stem cells. *PloS one*, 5(4), p.e9937.

Atkinson, S. & Armstrong, L., 2008. Epigenetics in embryonic stem cells: regulation of pluripotency and differentiation. *Cell and tissue research*, 331(1), pp.23–9.

Aulehla, A. et al., 2003. Wnt3a Plays a Major Role in the Segmentation Clock Controlling Somitogenesis. *Developmental Cell*, 4(3), pp.395–406.

Avilion, A. a et al., 2003. Multipotent cell lineages in early mouse development depend on SOX2 function. *Genes & development*, 17(1), pp.126–40.

Bafico, A. et al., 2001. Novel mechanism of Wnt signalling inhibition mediated by Dickkopf-1 interaction with LRP6/Arrow. *Nat Cell Biol*, 3(7), pp.683–686.

Bamforth, S. et al., 2004. Cited2 controls left-right patterning and heart development through a Nodal-Pitx2c pathway. *Nature Genetics*, 36(11), pp.1189–1196.

Barker, N., van de Wetering, M. & Clevers, H., 2008. The intestinal stem cell. *Genes & development*, 22(14), pp.1856–64.

Barnes, J.D. et al., 1994. Embryonic expression of Lim-1, the mouse homolog of Xenopus Xlim-1, suggests a role in lateral mesoderm differentiation and neurogenesis. *Developmental biology*, 161(1), pp.168–78.

Barrow, J.R., Stadler, H.S. & Capecchi, M.R., 2000. Roles of Hoxa1 and Hoxa2 in patterning the early hindbrain of the mouse. *Development (Cambridge, England)*, 127(5), pp.933–44.

Beddington, R.S. & Robertson, E.J., 1999. Axis development and early asymmetry in mammals. *Cell*, 96(2), pp.195–209.

Benahmed, F. et al., 2008. Multiple regulatory regions control the complex expression pattern of the mouse Cdx2 homeobox gene. *Gastroenterology*, 135(4), pp.1238–1247, 1247.e1–3.

Van den Berg, D.L.C. et al., 2010. An Oct4-centered protein interaction network in embryonic stem cells. *Cell stem cell*, 6(4), pp.369–81.

Berge, D. Ten et al., 2011. Embryonic stem cells require Wnt proteins to prevent differentiation to epiblast stem cells. *Nature Cell Biology*, 13(9), pp.1070–1075.

Bernstein, B.E. et al., 2006. A bivalent chromatin structure marks key developmental genes in embryonic stem cells. *Cell*, 125(2), pp.315–26.

Bessho, Y. et al., 2003. Periodic repression by the bHLH factor Hes7 is an essential mechanism for the somite segmentation clock. *Genes & development*, 17(12), pp.1451–6.

Boulet, A. & Capecchi, M., 2012. Signaling by FGF4 and FGF8 is required for axial elongation of the mouse embryo. *Dev. Biol.*, 371(2), pp.235–245.

Bradley, A. et al., 1984. Formation of germ-line chimaeras from embryo-derived teratocarcinoma cell lines. *Nature*, 309, pp.255–256.

Bradley, E.W. & Drissi, M.H., 2011. Wnt5b regulates mesenchymal cell aggregation and chondrocyte differentiation through the planar cell polarity pathway. *Journal of Cellular Physiology*, 226(6), pp.1683–1693.

Brennan, J. et al., 2001a. Nodal signalling in the epiblast patterns the early mouse embryo. *Nature*, 411(6840), pp.965–9.

Brennan, J., Norris, D.P. & Robertson, E.J., 2002a. Nodal activity in the node governs left-right asymmetry. *Genes & development*, 16(18), pp.2339–44.

Van den Brink, S.C. et al., 2014. Symmetry breaking, germ layer specification and axial organisation in aggregates of mouse embryonic stem cells. *Development*, 141(22), pp.4231–4242.

Briscoe, J. & Novitch, B.G., 2008. Regulatory pathways linking progenitor patterning, cell fates and neurogenesis in the ventral neural tube. *Philosophical transactions of the Royal Society of London. Series B, Biological sciences*, 363(1489), pp.57–70.

Brons, I.G.M. et al., 2007. Derivation of pluripotent epiblast stem cells from mammalian embryos. *Nature*, 448(7150), pp.191–5.

Buckingham, M., Meilhac, S. & Zaffran, S., 2005. Building the mammalian heart from two sources of myocardial cells. *Nature reviews. Genetics*, 6(11), pp.826–35.

Buecker, C. et al., 2014. Reorganization of Enhancer Patterns in Transition from Naive to Primed Pluripotency. *Cell Stem Cell*, 14(6), pp.838–853.

Burgess, S. et al., 2002. The zebrafish spiel-ohne-grenzen (spg) gene encodes the POU domain protein Pou2 related to mammalian Oct4 and is essential for formation of the midbrain and hindbrain, and for pre-gastrula morphogenesis. *Development (Cambridge, England)*, 129(4), pp.905–16.

Burtscher, I. et al., 2012. The Sox17-mCherry fusion mouse line allows visualization of endoderm and vascular endothelial development. *Genesis (New York, N.Y. : 2000)*, 50(6), pp.496–505.

Burtscher, I., Barkey, W. & Lickert, H., 2013. Foxa2-venus fusion reporter mouse line allows live-cell analysis of endoderm-derived organ formation. *Genesis (New York, N.Y. : 2000)*, 51(8), pp.596–604.

Burtscher, I. & Lickert, H., 2009. Foxa2 regulates polarity and epithelialization in the endoderm germ layer of the mouse embryo. *Development (Cambridge, England)*, 136(6), pp.1029–38.

Campbell, P. a & Rudnicki, M. a, 2013. Oct4 interaction with Hmgb2 regulates Akt signaling and pluripotency. *Stem cells (Dayton, Ohio)*, 31(6), pp.1107–20.

Campione, M. et al., 1999. The homeobox gene Pitx2: mediator of asymmetric left-right signaling in vertebrate heart and gut looping. *Development* , 126 (6), pp.1225–1234.

Carapuço M, Nóvoa A, Bobola N, M.M., 2005. Hox genes specify vertebral types in the presomitic mesoderm. *Genes Dev.*, 19(18), pp.2116–21.

Cedar, H., 1988. DNA methylation and gene activity. *Cell*, 53(1), pp.3–4.

Cervantes, S., Yamaguchi, T.P. & Hebrok, M., 2010. Wnt5a is essential for intestinal elongation in mice. *Dev Biol*, 326(2), pp.285–294.

Chambers, I. et al., 2003. Functional expression cloning of Nanog, a pluripotency sustaining factor in embryonic stem cells. *Cell*, 113(5), pp.643–55.

Chambers, I., 2004. The Molecular Basis of Pluripotency in Mouse Embryonic Stem Cells. *Cloning and stem cells*, 6(4), pp.386–391.

Chambers, I. & Tomlinson, S.R., 2009. The transcriptional foundation of pluripotency. *Development (Cambridge, England)*, 136(14), pp.2311–22.

Chazaud, C. et al., 2006. Early lineage segregation between epiblast and primitive endoderm in mouse blastocysts through the Grb2-MAPK pathway. *Developmental cell*, 10(5), pp.615–24.

Chen, C. & Shen, M.M., 2004. Two Modes by which Lefty Proteins Inhibit Nodal Signaling. *Current Biology*, 14(7), pp.618–624.

Chen, T. & Dent, S.Y.R., 2013. Chromatin modifiers and remodellers : regulators of cellular differentiation. *Nature*, 15(2), pp.93–106.

Chen, T.-W. et al., 2014. ChIPseek, a web-based analysis tool for ChIP data. *BMC Genomics*, 15(1), p.539.

Chen, X. et al., 2008. Integration of external signaling pathways with the core transcriptional network in embryonic stem cells. *Cell*, 133(6), pp.1106–17.

Chen, Z.-S. et al., 2014. Octamer-binding protein 4 affects the cell biology and phenotypic transition of lung cancer cells involving β-catenin/E-cadherin complex degradation. *Molecular Medicine Reports*.

Cheng, S.K. et al., 2004. Lefty Blocks a Subset of TGFβ Signals by Antagonizing EGF-CFC Coreceptors. *PLoS Biol*, 2(2), p.e30.

Cheng, X., Ying, L., Lu, L., Galvão, A.M., Mills, J., et al., 2012. Self-Renewing Endodermal Progenitor Lines Generated from Human Pluripotent Stem Cells Supplemental Information. *Cell Stem Cell*, 11.

Chiou, S.-H. et al., 2010. Coexpression of Oct4 and Nanog Enhances Malignancy in Lung Adenocarcinoma by Inducing Cancer Stem Cell–Like Properties and Epithelial–Mesenchymal Transdifferentiation. *Cancer Research* , 70 (24), pp.10433–10444.

Chiu, W.T. et al., 2014. Genome-wide view of TGF /Foxh1 regulation of the early mesendoderm program. *Development*, 141, pp.4537–4547.

Chuang, P.-T., Kawcak, T. & McMahon, A.P., 2003. Feedback control of mammalian Hedgehog signaling by the Hedgehog-binding protein, Hip1, modulates Fgf signaling during branching morphogenesis of the lung. *Genes & Development* , 17 (3), pp.342–347.

Chung, C. et al., 2013. Hippo-Foxa2 signaling pathway plays a role in peripheral lung maturation and surfactant homeostasis. *Proceedings of the National Academy of Sciences* , 110 (19), pp.7732–7737.

Cimmino, L. et al., 2011. TET Family Proteins and Their Role in Stem Cell Differentiation and Transformation. *Cell stem cell*, 9(3), pp.193–204.

Cirillo, L.A. et al., 2002. Opening of Compacted Chromatin by Early Developmental Transcription Factors HNF3 (FoxA) and GATA-4. *Molecular Cell*, 9(2), pp.279–289.

Cleaver, O. & Krieg, P., 2001. Notochord patterning of the endoderm. *Developmental biology*, 234(1), pp.1–12.

Clevers, H., 2013. The Intestinal Crypt, A Prototype Stem Cell Compartment. *Cell*, 154(2), pp.274–284.

Clevers, H., 2006. Wnt/beta-catenin signaling in development and disease. *Cell*, 127(3), pp.469–80.

Cole, M.F. et al., 2008. Tcf3 is an integral component of the core regulatory circuitry of embryonic stem cells. *Genes & development*, 22(6), pp.746–55.

Collignon, J., Varlet, I. & Roberston, E., 1996. Relations between assymetric nodal expression and direction of embryonic turning. *Nature*, 381, pp.155–158.

Conlon, F.L. et al., 1994. A primary requirement for nodal in the formation and maintenance of the primitive streak in the mouse. *Development (Cambridge, England)*, 120(7), pp.1919–28.

Creyghton, M.P. et al., 2010a. Histone H3K27ac separates active from poised enhancers and predicts developmental state. *Proceedings of the National Academy of Sciences of the United States of America*, 107(50), pp.21931–6.

Creyghton, M.P. et al., 2010b. Histone H3K27ac separates active from poised enhancers and predicts developmental state. *Proceedings of the National Academy of Sciences of the United States of America*, 107(50), pp.21931–6.

D'Amour, K. a et al., 2005. Efficient differentiation of human embryonic stem cells to definitive endoderm. *Nature biotechnology*, 23(12), pp.1534–41.

Davidson, K.C. et al., 2012. Wnt/β-catenin signaling promotes differentiation, not self-renewal, of human embryonic stem cells and is repressed by Oct4. *Proceedings of the National Academy of Sciences of the United States of America*, 109(12), pp.4485–90.

Deveale, B. et al., 2013. Oct4 is required ∼e7.5 for proliferation in the primitive streak. *PLoS genetics*, 9(11), p.e1003957.

Ding, J. et al., 1998. Cripto is required for correct orientation of the anterior-posterior axis in the mouse embryo. *Nature*, 395(6703), pp.702–707.

Ding, J. et al., 2012. Oct4 links multiple epigenetic pathways to the pluripotency network. *Cell research*, 22(1), pp.155–67.

Dixon, J.R. et al., 2015. Chromatin architecture reorganization during stem cell differentiation. *Nature*, 518(7539), pp.331–336.

Downs, K.M., 2008. Systematic localization of Oct-3/4 to the gastrulating mouse conceptus suggests manifold roles in mammalian development. *Developmental dynamics : an official publication of the American Association of Anatomists*, 237(2), pp.464–475.

Dunty, W.C. et al., 2008. Wnt3a/beta-catenin signaling controls posterior body development by coordinating mesoderm formation and segmentation. *Development (Cambridge, England)*, 135(1), pp.85–94.

Efroni, S. et al., 2008. Global transcription in pluripotent embryonic stem cells. *Cell stem cell*, 2(5), pp.437–47.

Engert, S. et al., 2009. Sox17-2A-iCre: a knock-in mouse line expressing Cre recombinase in endoderm and vascular endothelial cells. *Genesis (New York, N.Y. : 2000)*, 47(9), pp.603–10.

Engert, S. et al., 2013a. Wnt/β-catenin signalling regulates Sox17 expression and is essential for organizer and endoderm formation in the mouse. *Development* , 140 (15), pp.3128–3138.

Eon, J.P. et al., 2008. System for tamoxifen-inducible expression of Cre-recombinase from the Foxa2 locus in mice. *Developmental Dynamics*, 237(December 2007), pp.447–453.

Ericson, J. et al., 1995. Sonic hedgehog induces the differentiation of ventral forebrain neurons: A common signal for ventral patterning within the neural tube. *Cell*, 81(5), pp.747–756.

Evans JM; Kaufman MH, 1981. Establishment in culture of pluripotential cells from mouse embryos. *Nature*, 292.

Ezeh, U.I. et al., 2005. Human embryonic stem cell genes OCT4, NANOG, STELLAR, and GDF3 are expressed in both seminoma and breast carcinoma. *Cancer*, 104(10), pp.2255–2265.

Faunes, F. et al., 2013. A membrane-associated β-catenin/Oct4 complex correlates with ground-state pluripotency in mouse embryonic stem cells. *Development (Cambridge, England)*, 140(6), pp.1171–83.

Fausett, S.R., Brunet, L.J. & Klingensmith, J., 2014. BMP antagonism by Noggin is required in presumptive notochord cells for mammalian foregut morphogenesis. *Developmental Biology*, 391(1), pp.111–124.

Feldman, N. et al., 2006. G9a-mediated irreversible epigenetic inactivation of Oct-3/4 during early embryogenesis. *Nature cell biology*, 8(2), pp.188–94.

Ficz, G. et al., 2011. Dynamic regulation of 5-hydroxymethylcytosine in mouse ES cells and during differentiation. *Nature*, 3.

Filosa, S. et al., 1997. Goosecoid and HNF-3beta genetically interact to regulate neural tube patterning during mouse embryogenesis. *Development* , 124 (14), pp.2843–2854.

Forlani, S.K.A.L. and J.D., 2003. Acquisition of Hox codes during gastrulation and axial elongation in the mouse embryo. *Development*, 130(16), pp.3807–3819.

Francois, M., Koopman, P. & Beltrame, M., 2010. SoxF genes: Key players in the development of the cardio-vascular system. *The International Journal of Biochemistry & Cell Biology*, 42(3), pp.445–448.

Francou, A. et al., 2012. Second heart field cardiac progenitor cells in the early mouse embryo. *Biochimica et Biophysica Acta (BBA) - Molecular Cell Research*, 1833(4), pp.795–798.

Gadue, P. et al., 2005. Germ layer induction from embryonic stem cells. *Experimental hematology*, 33(9), pp.955–64.

Gadue, P. et al., 2006a. Wnt and TGF-beta signaling are required for the induction of an in vitro model of primitive streak formation using embryonic stem cells. *Proceedings of the National Academy of Sciences of the United States of America*, 103(45), pp.16806–11.

Galceran, J. et al., 1999. Wnt3a−/−-like phenotype and limb deficiency in Lef1−/−Tcf1−/− mice. *Genes & Development*, 13, pp.709–717.

Gao, N. et al., 2008. Dynamic regulation of Pdx1 enhancers by Foxa1 and Foxa2 is essential for pancreas development. *Genes & Development* , 22 (24), pp.3435–3448.

Gavalas, A. et al., 2003. Neuronal defects in the hindbrain of Hoxa1, Hoxb1 and Hoxb2 mutants reflect regulatory interactions among these Hox genes. *Development (Cambridge, England)*, 130(23), pp.5663–79.

Gesbert, F. et al., 2000. BCR/ABL regulates expression of the cyclin-dependent kinase inhibitor p27Kip1 through the phosphatidylinositol 3-Kinase/AKT pathway. *The Journal of biological chemistry*, 275(50), pp.39223–30.

Gifford, C. a et al., 2013. Transcriptional and Epigenetic Dynamics during Specification of Human Embryonic Stem Cells. *Cell*, pp.1–15.

Glinka, A. et al., 1998. Dickkopf-1 is a member of a new family of secreted proteins and functions in head induction. *Nature*, 391(6665), pp.357–362.

Göke, J. et al., 2011. Combinatorial Binding in Human and Mouse Embryonic Stem Cells Identifies Conserved Enhancers Active in Early Embryonic Development. *PLoS Comput Biol*, 7(12), p.e1002304.

Goldin, S.N. & Papaioannou, V.E., 2003. Paracrine action of FGF4 during periimplantation development maintains trophectoderm and primitive endoderm. *genesis*, 36(1), pp.40–47.

Goll, M.G. & Bestor, T.H., 2002. Histone modification and replacement in chromatin activation. *Genes & development*, 16(14), pp.1739–42.

Gregorieff, A., Grosschedl, R. & Clevers, H., 2004. Hindgut defects and transformation of the gastro-intestinal tract in Tcf4(-/-)/Tcf1(-/-) embryos. *The EMBO journal*, 23(8), pp.1825–33.

Guo, G. et al., 2009. Klf4 reverts developmentally programmed restriction of ground state pluripotency. *Development*, 1069, pp.1063–1069.

Hashimoto, M. et al., 2010. Planar polarization of node cells determines the rotational axis of node cilia. *Nature cell biology*, 12(2), pp.170–176.

Hata, K. et al., 2002. Dnmt3L cooperates with the Dnmt3 family of de novo DNA methyltransferases to establish maternal imprints in mice. *Development* , 129 (8), pp.1983–1993.

Heard, E., 2004. Recent advances in X-chromosome inactivation. *Current Opinion in Cell Biology*, 16(3), pp.247–255.

Heng, J.-C.D. et al., 2010. The Nuclear Receptor Nr5a2 Can Replace Oct4 in the Reprogramming of Murine Somatic Cells to Pluripotent Cells. *Cell Stem Cell*, 6(2), pp.167–174.

Hermesz, E., Mackem, S. & Mahon, K.A., 1996. Rpx : a novel anterior-restricted homeobox gene progressively activated in the prechordal plate , anterior neural plate and Rathke ' s pouch of the mouse embryo. , 52, pp.41–52.

Hirokawa, N. et al., 2006. Nodal Flow and the Generation of Left-Right Asymmetry. *Cell*, 125(1), pp.33–45.

Hochedlinger, K. et al., 2005. Ectopic expression of Oct-4 blocks progenitor-cell differentiation and causes dysplasia in epithelial tissues. *Cell*, 121(3), pp.465–77.

Horn, S. et al., 2012. Mind bomb 1 is required for pancreatic β -cell formation. *PNAS*, 109(19), pp.7356–7361.

Hu, J. et al., 2011. Downregulation of transcription factor Oct4 induces an epithelial-to-mesenchymal transition via enhancement of Ca(2+) influx in breast cancer cells. *Biochemical and biophysical research communications*, (July), pp.2–7.

Hu, J. et al., 2012. MiR-145 Regulates Epithelial to Mesenchymal Transition of Breast Cancer Cells by Targeting Oct4. *PloS one*, 7(9), p.e45965.

Hudson, C. et al., 1997. Xsox17alpha and -beta mediate endoderm formation in Xenopus. *Cell*, 91(3), pp.397–405.

Ikeya M, T.S., 2001. Wnt-3a is required for somite specification along the anteroposterior axis of the mouse embryo and for regulation of cdx-1 expression. *Mech Dev*, 103, pp.27–33.

Ito, S., D/'Alessio, A.C., et al., 2010. Role of Tet proteins in 5mC to 5hmC conversion, ES-cell self-renewal and inner cell mass specification. *Nature*, 466(7310), pp.1129–1133.

Jones TR, Kang IH, Wheeler DB, Lindquist RA, Papallo A, Sabatini DM, Golland P, C.A., 2008. CellProfiler Analyst: data exploration and analysis software for complex image-based screens. *BMC Bioinformatics*, 9(1).

JP, M.B. et al., 2000. The homeobox gene Hex is required in definitive endodermal tissues for normal forebrain, liver and thyroid formation. *Development*, 127(11), pp.2433–45.

Jukkola, T. et al., 2005. Meox1Cre: a mouse line expressing Cre recombinase in somitic mesoderm. *Genesis (New York, N.Y. : 2000)*, 43(3), pp.148–53.

Kadowaki, T. et al., 1996. The segment polarity gene porcupine encodes a putative multitransmembrane protein involved in Wingless processing. *Genes & Development* , 10 (24), pp.3116–3128.

Kanai, Y. et al., 1996. Identification of two Sox17 messenger RNA isoforms, with and without the high mobility group box region, and their differential expression in mouse spermatogenesis. *The Journal of cell biology*, 133(3), pp.667–81.

Kanai-Azuma, M. et al., 2002. Depletion of definitive gut endoderm in Sox17-null mutant mice. *Development (Cambridge, England)*, 129(10), pp.2367–79.

Karwacki-Neisius, V.A. et al., 2013. Reduced Oct4 Expression Directs a Robust Pluripotent State with Distinct Signaling Activity and Increased Enhancer Occupancy by Oct4 and Nanog. *Cell Stem Cell*, 12, pp.1–19.

Kathiriya, I.S. & Srivastava, D., 2000. Left-right asymmetry and cardiac looping: Implications for cardiac development and congenital heart disease. *American Journal of Medical Genetics*, 97(4), pp.271–279.

Katsanis, N., 2006. Ciliary proteins and exencephaly. *Nat Genet*, 38(2), pp.135–136.

Kehler, J. et al., 2004. Oct4 is required for primordial germ cell survival. *EMBO reports*, 5(11), pp.1078–83.

Keller, G., 2005. Embryonic stem cell differentiation: emergence of a new era in biology and medicine. *Genes & development*, 19(10), pp.1129–55.

Kemler, R. et al., 2004. Stabilization of beta-catenin in the mouse zygote leads to premature epithelial-mesenchymal transition in the epiblast. *Development (Cambridge, England)*, 131(23), pp.5817–5824.

Kiecker, C. & Niehrs, C., 2001. A morphogen gradient of Wnt/β-catenin signalling regulates anteroposterior neural patterning in Xenopus. *Development* , 128 (21), pp.4189–4201.

Kilian, B. et al., 2003. The role of Ppt/Wnt5 in regulating cell shape and movement during zebrafish gastrulation. *Mechanisms of development*, 120(4), pp.467–476.

Kim, J. et al., 2008. An extended transcriptional network for pluripotency of embryonic stem cells. *Cell*, 132(6), pp.1049–61.

Kim, S.K., Hebrok, M. & Melton, D.A., 1997. Notochord to endoderm signaling is required for pancreas development. *Development*, 4252, pp.4243–4252.

Kimura-Yoshida, C. et al., 2005. Canonical Wnt signaling and its antagonist regulate anterior-posterior axis polarization by guiding cell migration in mouse visceral endoderm. *Developmental cell*, 9(5), pp.639–50.

Kimura-Yoshida, C. et al., 2007. Crucial roles of Foxa2 in mouse anterior–posterior axis polarization via regulation of anterior visceral endoderm-specific genes. *Proceedings of the National Academy of Sciences* , 104 (14), pp.5919–5924.

Kinder, S.J. et al., 2001. The organizer of the mouse gastrula is composed of a dynamic population of progenitor cells for the axial mesoderm. *Development (Cambridge, England)*, 128(18), pp.3623–34.

Kitajima, K. et al., 2013. Wnt signaling regulates left-right axis formation in the node of mouse embryos. *Developmental biology*, 380(2), pp.222–32.

Koh, K.P. et al., 2011. Tet1 and Tet2 regulate 5-hydroxymethylcytosine production and cell lineage specification in mouse embryonic stem cells. *Cell stem cell*, 8(2), pp.200–13.

Kotkamp, K. et al., 2014. Pou5f1/Oct4 Promotes Cell Survival via Direct Activation of mych Expression during Zebrafish Gastrulation. *PloS one*, 9(3), p.e92356.

Kouzarides, T., 2007. Chromatin modifications and their function. *Cell*, 128(4), pp.693–705.

Kwon, G.S., Viotti, M. & Hadjantonakis, A.-K., 2008. The endoderm of the mouse embryo arises by dynamic widespread intercalation of embryonic and extraembryonic lineages. *Developmental cell*, 15(4), pp.509–20.

Labbé, E. et al., 1998. Smad2 and Smad3 Positively and Negatively Regulate TGFβ-Dependent Transcription through the Forkhead DNA-Binding Protein FAST2. *Molecular Cell*, 2(1), pp.109–120.

Lai, E. et al., 1990. HNF-3A, a hepatocyte-enriched transcription factor of novel structure is regulated transcriptionally. *Genes & Development* , 4 (8), pp.1427–1436.

Lee, C.S. et al., 2002. Foxa2 Controls Pdx1 Gene Expression in Pancreatic β-Cells In Vivo . *Diabetes* , 51 (8), pp.2546–2551.

Lee, C.S. et al., 2005. Foxa2 is required for the differentiation of pancreatic α-cells. *Developmental Biology*, 278(2), pp.484–495.

Lengerke, C. et al., 2008. BMP and Wnt Specify Hematopoietic Fate by Activation of the Cdx-Hox Pathway. *Cell Stem Cell*, 2(1), pp.72–82.

Lengner, C.J. et al., 2007. Oct4 expression is not required for mouse somatic stem cell self-renewal. *Cell stem cell*, 1(4), pp.403–15.

Lengner, C.J., Welstead, G.G. & Jaenisch, R., 2008. The pluripotency regulator Oct4. *Cell Cycle*, (March), pp.725–728.

Lewis, E.B., 1978. A gene complex controlling segmentation in Drosophila. *Nature*, 276(5688), pp.565–570.

Leyns, L. et al., 1997. Frzb-1 Is a Secreted Antagonist of Wnt Signaling Expressed in the Spemann Organizer. *Cell*, 88(6), pp.747–756.

Li, Y. et al., 2013a. Brief report: Oct4 and canonical Wnt signaling regulate the cardiac lineage factor Mesp1 through a Tcf/Lef-Oct4 composite element. *Stem cells (Dayton, Ohio)*, 31(6), pp.1213–7.

Li, Y. et al., 2013b. Oct4 and Canonical Wnt Signaling Regulate the Cardiac Lineage Factor Mesp1 through a Tcf/Lef-Oct4 Composite Element. *Stem cells (Dayton, Ohio)*.

Li, Z. et al., 2012. Foxa2 and H2A.Z Mediate Nucleosome Depletion during Embryonic Stem Cell Differentiation. *Cell*, 151(7), pp.1608–1616.

Liang, J. et al., 2008. Nanog and Oct4 associate with unique transcriptional repression complexes in embryonic stem cells. *Nature cell biology*, 10(6), pp.731–9.

Lickert, H. et al., 2005. Dissecting Wnt/beta-catenin signaling during gastrulation using RNA interference in mouse embryos. *Development (Cambridge, England)*, 132(11), pp.2599–609.

Lickert, H. et al., 2002. Formation of multiple hearts in mice following deletion of beta-catenin in the embryonic endoderm. *Developmental cell*, 3(2), pp.171–81.

Lickert, H. et al., 2000. Wnt/(beta)-catenin signaling regulates the expression of the homeobox gene Cdx1 in embryonic intestine. *Development (Cambridge, England)*, 127(17), pp.3805–13.

Lickert, H. & Kemler, R., 2002. Functional analysis of cis-regulatory elements controlling initiation and maintenance of early Cdx1 gene expression in the mouse. *Developmental dynamics : an official publication of the American Association of Anatomists*, 225(2), pp.216–20.

Lin, C.R. et al., 1999. Pitx2 regulates lung asymmetry, cardiac positioning and pituitary and tooth morphogenesis. *Nature*, 401(6750), pp.279–282.

Lin, H. et al., 2014. Knockdown of OCT4 suppresses the growth and invasion of pancreatic cancer cells through inhibition of the AKT pathway. *Molecular Medicine Reports*, 10(3), pp.1335–134.

Lindsley, R.C. et al., 2006. Canonical Wnt signaling is required for development of embryonic stem cell-derived mesoderm. *Development (Cambridge, England)*, 133(19), pp.3787–96.

Linker, C. et al., 2005. beta-Catenin-dependent Wnt signalling controls the epithelial organisation of somites through the activation of paraxis. *Development (Cambridge, England)*, 132(17), pp.3895–905.

Liu, P. et al., 1999. Requirement for Wnt3 in vertebrate axis formation. *Nature genetics*, 22(4), pp.361–5.

Liu, X. et al., 2008. Yamanaka factors critically regulate the developmental signaling network in mouse embryonic stem cells. *Cell research*, 18(12), pp.1177–89.

Liu, Y. et al., 2007. Sox17 is essential for the specification of cardiac mesoderm in embryonic stem cells. *Proceedings of the National Academy of Sciences* , 104 (10), pp.3859–3864.

Livigni, A. et al., 2013. A conserved Oct4/POUV-dependent network links adhesion and migration to progenitor maintenance. *Current biology*, 23(22), pp.2233–44.

Loh, K.M. et al., 2014. Efficient Endoderm Induction from Human Pluripotent Stem Cells by Logically Directing Signals Controlling Lineage Bifurcations. *Cell Stem Cell*, 14, pp.1–16.

Loh, Y.-H. et al., 2006. The Oct4 and Nanog transcription network regulates pluripotency in mouse embryonic stem cells. *Nature genetics*, 38(4), pp.431–40.

Lu, X. et al., 2014. The retrovirus HERVH is a long noncoding RNA required for human embryonic stem cell identity. *Nat Struct Mol Biol*, 21(4), pp.423–425.

Lunde, K., Belting, H.-G. & Driever, W., 2004. Zebrafish pou5f1/pou2, Homolog of Mammalian Oct4, Functions in the Endoderm Specification Cascade. *Current Biology*, 14(1), pp.48–55.

Luo, W. et al., 2013. Embryonic Stem Cells Markers SOX2, OCT4 and Nanog Expression and Their Correlations with Epithelial-Mesenchymal Transition in Nasopharyngeal Carcinoma. *PLoS ONE*, 8(2), p.e56324.

Lyashenko, N. et al., 2011. Differential requirement for the dual functions of β-catenin in embryonic stem cell self-renewal and germ layer formation. *Nature cell biology*, 13(7), pp.753–61.

Mahaffey, J.P. et al., 2013. Cofilin and Vangl2 cooperate in the initiation of planar cell polarity in the mouse embryo. *Development (Cambridge, England)*, 140(6), pp.1262–71.

Mallo, M., Wellik, D. & Deschamps, J., 2011. Hox Genes and Regional Patterning of the Vertebrate Body Plan. *Dev. Biol.*, 344(1), pp.7–15.

Maloof, J.N. et al., 1999. A Wnt signaling pathway controls hox gene expression and neuroblast migration in C. elegans. *Development* , 126 (1), pp.37–49.

Marikawa, Y. et al., 2011. Dual roles of Oct4 in the maintenance of mouse P19 embryonal carcinoma cells: as negative regulator of Wnt/β-catenin signaling and competence provider for Brachyury induction. *Stem cells and development*, 20(4), pp.621–33.

Marson, A. et al., 2008a. Connecting microRNA genes to the core transcriptional regulatory circuitry of embryonic stem cells. *Cell*, 134(3), pp.521–33.

Martelli, A.M. et al., 2012. The emerging multiple roles of nuclear Akt. *Biochimica et Biophysica Acta (BBA) - Molecular Cell Research*, 1823(12), pp.2168–2178.

Martin, B.L. & Kimelman, D., 2008. Regulation of canonical Wnt signaling by Brachyury is essential for posterior mesoderm formation. *Developmental cell*, 15(1), pp.121–33.

Martinez-Ceballos, E. & Gudas, L.J., 2008. Hoxa1 is required for the retinoic acid-induced differentiation of embryonic stem cells into neurons. *Journal of neuroscience research*, 86(13), pp.2809–19.

Masui, S. et al., 2007. Pluripotency governed by Sox2 via regulation of Oct3/4 expression in mouse embryonic stem cells. *Nature cell biology*, 9(6), pp.625–35.

Mathur, D. et al., 2008. Analysis of the mouse embryonic stem cell regulatory networks obtained by ChIP-chip and ChIP-PET. *Genome biology*, 9(8), p.R126.

McKnight, K.D., Hou, J. & Hoodless, P.A., 2010. Foxh1 and Foxa2 are not required for formation of the midgut and hindgut definitive endoderm. *Developmental Biology*, 337(2), pp.471–481.

McPherson, C.E. et al., 1993. An active tissue-specific enhancer and bound transcription factors existing in a precisely positioned nucleosomal array. *Cell*, 75(2), pp.387–398.

Meissner, A. et al., 2008. Genome-scale DNA methylation maps of pluripotent and differentiated cells. *Nature*, 454(7205), pp.766–70.

Meno, C. et al., 2001. Diffusion of nodal signaling activity in the absence of the feedback inhibitor Lefty2. *Developmental cell*, 1(1), pp.127–38.

Meno, C. et al., 1998. Lefty-1 Is Required for Left-Right Determination As a Regulator of Lefty-2 and Nodal. *Cell*, 94(3), pp.287–97.

Meno, C. et al., 1999. Mouse Lefty2 and zebrafish antivin are feedback inhibitors of nodal signaling during vertebrate gastrulation. *Molecular cell*, 4(3), pp.287–98.

Mitsui, K. et al., 2003. The homeoprotein Nanog is required for maintenance of pluripotency in mouse epiblast and ES cells. *Cell*, 113(5), pp.631–42.

Morris, S. a et al., 2010. Origin and formation of the first two distinct cell types of the inner cell mass in the mouse embryo. *Proceedings of the National Academy of Sciences of the United States of America*, 107(14), pp.6364–9.

Morrison, G.M. & Brickman, J.M., 2006. Conserved roles for Oct4 homologues in maintaining multipotency during early vertebrate development. *Development (Cambridge, England)*, 133(10), pp.2011–22.

Mukhopadhyay, M. et al., 2001. Dickkopf1 is required for embryonic head induction and limb morphogenesis in the mouse. *Developmental cell*, 1(3), pp.423–34.

Mullen, A.C. et al., 2011. Master transcription factors determine cell-type-specific responses to TGF-β signaling. *Cell*, 147(3), pp.565–76.

Nakaya, M. et al., 2005. Wnt3a links left-right determination with segmentation and anteroposterior axis elongation. *Development (Cambridge, England)*, 132(24), pp.5425–36.

Nichols, J. et al., 1998. Formation of pluripotent stem cells in the mammalian embryo depends on the POU transcription factor Oct4. *Cell*, 95(3), pp.379–91.

Nichols, J. & Smith, A., 2009. Naive and primed pluripotent states. *Cell stem cell*, 4(6), pp.487–92.

Nishita, M. et al., 2010. Ror2/Frizzled Complex Mediates Wnt5a-Induced AP-1 Activation by Regulating Dishevelled Polymerization. *Molecular and Cellular Biology* , 30 (14), pp.3610–3619.

Niwa, H. et al., 2005a. Interaction between Oct3/4 and Cdx2 determines trophectoderm differentiation. *Cell*, 123(5), pp.917–29.

Niwa, H., Miyazaki, J. & Smith, a G., 2000. Quantitative expression of Oct-3/4 defines differentiation, dedifferentiation or self-renewal of ES cells. *Nature genetics*, 24(4), pp.372–6.

Nonaka, S. et al., 1998. Randomization of left-right asymmetry due to loss of nodal cilia generating leftward flow of extraembryonic fluid in mice lacking KIF3B motor protein. *Cell*, 95(6), pp.829–37.

Nordström, U. et al., 2006. An Early Role for Wnt Signaling in Specifying Neural Patterns of Cdx and Hox Gene Expression and Motor Neuron Subtype Identity . *PLoS Biol*, 4(8), p.e252.

Norris, D.P. et al., 2002. The Foxh1-dependent autoregulatory enhancer controls the level of Nodal signals in the mouse embryo. *Development (Cambridge, England)*, 129(14), pp.3455–68.

Okita, K., Ichisaka, T. & Yamanaka, S., 2007. Generation of germline-competent induced pluripotent stem cells. *Nature*, 448(7151), pp.313–317.

Palmieri, S.L. et al., 1994. Oct-4 transcription factor is differentially expressed in the mouse embryo during establishment of the first two extraembryonic cell lineages involved in implantation. *Developmental biology*, 166(1), pp.259–67.

Pardo, M. et al., 2010. An expanded Oct4 interaction network: implications for stem cell biology, development, and disease. *Cell stem cell*, 6(4), pp.382–95.

Park, K.-S. et al., 2006. Sox17 influences the differentiation of respiratory epithelial cells. *Developmental biology*, 294(1), pp.192–202.

Perea-Gomez, a, Rhinn, M. & Ang, S.L., 2001. Role of the anterior visceral endoderm in restricting posterior signals in the mouse embryo. *The International journal of developmental biology*, 45(1), pp.311–20.

Perea-Gomez, A. et al., 2002. Nodal antagonists in the anterior visceral endoderm prevent the formation of multiple primitive streaks. *Developmental cell*, 3(5), pp.745–56.

Piccolo, S. et al., 1999. The head inducer Cerberus is a multifunctional antagonist of Nodal, BMP and Wnt signals. *Nature*, 397(6721), pp.707–710.

Pilon, N. et al., 2006. Cdx4 is a direct target of the canonical Wnt pathway. *Developmental Biology*, 289(1), pp.55–63.

Pinson, K.I. et al., 2000. An LDL-receptor-related protein mediates Wnt signalling in mice. *Nature*, 407(6803), pp.535–538.

Qi, X. et al., 2004. BMP4 supports self-renewal of embryonic stem cells by inhibiting mitogen-activated protein kinase pathways. *Proceedings of the National Academy of Sciences of the United States of America* , 101 (16), pp.6027–6032.

Qian, D. et al., 2007. Wnt5a functions in planar cell polarity regulation in mice. *Developmental Biology*, 306(1), pp.121–133.

Radzisheuskaya, A. et al., 2013. A defined Oct4 level governs cell state transitions of pluripotency entry and differentiation into all embryonic lineages. *Nature Cell Biology*, 15(5), pp.1–14.

Ralston, A. & Rossant, J., 2008. Cdx2 acts downstream of cell polarization to cell-autonomously promote trophectoderm fate in the early mouse embryo. *Developmental biology*, 313(2), pp.614–29.

Rattner, A. et al., 1997. A family of secreted proteins contains homology to the cysteine-rich ligand-binding domain of frizzled receptors. *Proceedings of the National Academy of Sciences* , 94 (7), pp.2859–2863.

Reim, G. et al., 2004. The POU domain protein spg (pou2/Oct4) is essential for endoderm formation in cooperation with the HMG domain protein casanova. *Developmental cell*, 6(1), pp.91–101.

Reya, T. & Clevers, H., 2005. Wnt signalling in stem cells and cancer. *Nature*, 434(7035), pp.843–50.

Roberts, D.J. et al., 1995. Sonic hedgehog is an endodermal signal inducing Bmp-4 and Hox genes during induction and regionalization of the chick hindgut. *Development (Cambridge, England)*, 121(10), pp.3163–74.

Rochais, F., Mesbah, K. & Kelly, R.G., 2009. Signaling pathways controlling second heart field development. *Circulation Research*, 104(8), pp.933–942.

Rodríguez-Seguel, E. et al., 2013. Mutually exclusive signaling signatures define the hepatic and pancreatic progenitor cell lineage divergence. *Genes & development*, 27(17), pp.1932–46.

Rosner, M. et al., 1990. A POU domain transcription factor in early stem cells and germ cells of the mammalian embryo. *Nature*, 345.

Sakamoto, Y. et al., 2007. Redundant roles of Sox17 and Sox18 in early cardiovascular development of mouse embryos. *Biochemical and biophysical research communications*, 360(3), pp.539–44.

Sánchez-tilló, E. et al., 2011. β-catenin/TCF4 complex induces the epithelial- to-mesenchymal transition (EMT)-activator ZEB1 to regulate tumor invasiveness. *PNAS*, 108(48), pp.19204–19209.

Sasai, Y. et al., 1994. Xenopus chordin: A novel dorsalizing factor activated by organizer-specific homeobox genes. *Cell*, 79(5), pp.779–790.

Sasaki, H. & Hogan, B.L., 1993. Differential expression of multiple fork head related genes during gastrulation and axial pattern formation in the mouse embryo. *Development* , 118 (1), pp.47–59.

Sasaki, H. & Hogan, B.L.M., 1994. HNF-3β as a regulator of floor plate development. *Cell*, 76(1), pp.103–115.

Savory, J.G. a et al., 2009. Cdx2 regulation of posterior development through non-Hox targets. *Development (Cambridge, England)*, 136(24), pp.4099–110.

Schneider, S. et al., 1996. Beta-catenin translocation into nuclei demarcates the dorsalizing centers in frog and fish embryos. *Mechanisms of development*, 57(2), pp.191–8.

Schöler, H.R. et al., 1990. New type of pou domain in germ line-specific Oct-4. *Nature*, 344.

Shawlot, W. & Behringer, R.R., 1995. Requirement for Liml in head-organizer function. *Nature*, 374.

Shen, M.M., 2007. Nodal signaling: developmental roles and regulation. *Development (Cambridge, England)*, 134(6), pp.1023–34.

Sherwood, R.I. et al., 2011. Wnt signaling specifies and patterns intestinal endoderm. *Mechanisms of development*, 128(7-10), pp.387–400.

Silva, J. & Smith, A., 2008. Capturing pluripotency. *Cell*, 132(4), pp.532–6.

Simeone, A. et al., 1993. homeodomain of the bicoid class and demarcates anterior neuroectoderm in the gastrulating mouse embryo. *EMBO*, 12(7), pp.2735–2747.

Simeone, A. et al., 1992. Nested expression domains of four homeobox genes in developing rostral brain. *Nature*, 358(6388), pp.687–690.

Singh, A.M. et al., 2014. Signaling Network Crosstalk in Human Pluripotent Cells: A Smad2/3-Regulated Switch that Controls the Balance between Self-Renewal and Differentiation. *Cell Stem Cell*, 10(3), pp.312–326.

Sinner, D. et al., 2004. Sox17 and beta-catenin cooperate to regulate the transcription of endodermal genes. *Development (Cambridge, England)*, 131(13), pp.3069–80.

Smith, Z.D. & Meissner, A., 2013. DNA methylation: roles in mammalian development. *Nature Reviews Genetics*, 14(3), pp.204–220.

Song, H. et al., 2010. Planar cell polarity breaks bilateral symmetry by controlling ciliary positioning. *Nature*, 466(7304), pp.378–382.

Soriano, P., 1999. Generalized lacZ expression with the ROSA26 Cre reporter strain. *Nature genetics*, 21(1), pp.70–1.

Soriano, P. et al., 1986. Tissue-Specific and Ectopic Expression of Genes Introduced into Transgenic Mice by Retroviruses. *Science*, 234, pp.1409–1413.

Spence, J.R. et al., 2010a. Directed differentiation of human pluripotent stem cells into intestinal tissue in vitro. *Nature*, pp.1–6.

Spence, J.R. et al., 2010. Sox17 regulates organ lineage segregation of ventral foregut progenitor cells. *Developmental Cell*, 17(1), pp.62–74.

Srinivas, S. et al., 2004. Active cell migration drives the unilateral movements of the anterior visceral endoderm. *Development (Cambridge, England)*, 131(5), pp.1157–64.

Stefanovic, S. et al., 2009. Interplay of Oct4 with Sox2 and Sox17: a molecular switch from stem cell pluripotency to specifying a cardiac fate. *The Journal of cell biology*, 186(5), pp.665–73.

Van Straaten, H.W.M. & Copp, A.J., 2001. Curly tail: a 50 year history of the mouse spina bifida model. *Anatomy and embryology*, 203(4), pp.225–237.

Suzuki, M.M. & Bird, A., 2008. DNA methylation landscapes: provocative insights from epigenomics. *Nature reviews. Genetics*, 9(6), pp.465–76.

Tabin, C.J. & Vogan, K.J., 2003. A two-cilia model for vertebrate left-right axis specification. *Genes and Development*, 17, pp.1–6.

Tada, M. & Kai, M., 2009. Noncanonical Wnt/PCP signaling during vertebrate gastrulation. *Zebrafish*, 6(1), pp.29–40.

Takada, S. et al., 1994. Wnt-3a regulates somite and tailbud formation in the mouse embryo. *Genes & Development*, 8(2), pp.174–189.

Tam, P.P., 1981. The control of somitogenesis in mouse embryos. *Journal of embryology and experimental morphology*, 65 Suppl, pp.103–28.

Tamplin, O.J. et al., 2008. Microarray analysis of Foxa2 mutant mouse embryos reveals novel gene expression and inductive roles for the gastrula organizer and its derivatives. *BMC genomics*, 9, p.511.

Tan, Y. et al., 2013. Acetylated histone H3K56 interacts with Oct4 to promote mouse embryonic stem cell pluripotency. *Proceedings of the National Academy of Sciences*, 110(28).

Tanaka, Y., Okada, Y. & Hirokawa, N., 2005. FGF-induced vesicular release of Sonic hedgehog and retinoic acid in leftward nodal flow is critical for left-right determination. *Nature*, 435(7039), pp.172–177.

Teo, A.K.K., Arnold, S., et al., 2011. Pluripotency factors regulate definitive endoderm specification through eomesodermin. *Genes & development*, pp.1–5.

Teo, A.K.K., Arnold, S.J., et al., 2011. Pluripotency factors regulate definitive endoderm specification through eomesodermin. *Genes & development*.

Tesar, P.J. et al., 2007. New cell lines from mouse epiblast share defining features with human embryonic stem cells. *Nature*, 448(7150), pp.196–9.

Thomas, P. & Beddington, R., 1996. Anterior primitive endoderm may be responsible for patterning the anterior neural plate in the mouse embryo. *Current biology : CB*, 6(11), pp.1487–96.

Thomson, J.A. et al., 1998. Embryonic Stem Cell Lines Derived from Human Blastocysts. *Science* , 282 (5391), pp.1145–1147.

Thomson, M. et al., 2011. Pluripotency factors in embryonic stem cells regulate differentiation into germ layers. *Cell*, 145(6), pp.875–89.

Toshiko, T. et al., 2004. Dual roles of Sema6D in cardiac morphogenesis through region-specific association of its receptor, Plexin-A1, with off-track and vascular endothelial growth factor receptor type 2. *Genes & development*, 18(4), pp.435–47.

Toyofuku, T. et al., 2004. Guidance of myocardial patterning in cardiac development by Sema6D reverse signalling. *Nat Cell Biol*, 6(12), pp.1204–1211.

Tsai, L.-L. et al., 2014. Oct4 Mediates Tumor Initiating Properties in Oral Squamous Cell Carcinomas through the Regulation of Epithelial-Mesenchymal Transition. *PLoS ONE*, 9(1), p.e87207.

Wan, H. et al., 2004. Foxa2 is required for transition to air breathing at birth. *Proceedings of the National Academy of Sciences of the United States of America* , 101 (40), pp.14449–14454.

Wang, J. et al., 2006. A protein interaction network for pluripotency of embryonic stem cells. *Nature*, 444(7117), pp.364–8.

Warmflash, A. et al., 2014. A method to recapitulate early embryonic spatial patterning in human embryonic stem cells. *Nature methods*, 11(8), pp.847–854.

Watanabe, S. et al., 2006. Activation of Akt signaling is sufficient to maintain pluripotency in mouse and primate embryonic stem cells. *Oncogene*, 25(19), pp.2697–2707.

Weigel, D. & Jäckle, H., 1990. The fork head domain: A novel DNA binding motif of eukaryotic transcription factors? *Cell*, 63(3), pp.455–456.

Weinstein, D.C. et al., 1994. The winged-helix transcription factor HNF-3β is required for notochord development in the mouse embryo. *Cell*, 78(4), pp.575–588.

Wells, J.M. & Melton, D. a, 2000. Early mouse endoderm is patterned by soluble factors from adjacent germ layers. *Development (Cambridge, England)*, 127(8), pp.1563–72.

Wen, J. et al., 2010. Oct4 and Nanog Expression Is Associated With Early Stages of Pancreatic Carcinogenesis. *Pancreas*, 39(5).

Weninger, W.J. et al., 2005. Cited2 is required both for heart morphogenesis and establishment of the left-right axis in mouse development. *Development (Cambridge, England)*, 132(6), pp.1337–48.

Williams, R.L. et al., 1988. Myeloid leukaemia inhibitory factor maintains the developmental potential of embryonic stem cells. *Nature*, 336(6200), pp.684–687.

Wolfrum, C. et al., 2004. Foxa2 regulates lipid metabolism and ketogenesis in the liver during fasting and in diabetes. *Nature*, 432(7020), pp.1027–1032.

Wray, J. et al., 2011. Inhibition of glycogen synthase kinase-3 alleviates Tcf3 repression of the pluripotency network and increases embryonic stem cell resistance to differentiation. *Nature cell biology*, 13(7), pp.838–845.

Xie, W. et al., 2013. Epigenomic Analysis of Multilineage Differentiation of Human Embryonic Stem Cells. *Cell*, pp.1–15.

Yamada, T. et al., 2013. Involvement of Crosstalk between Oct4 and Meis1a in Neural Cell Fate Decision. *PloS one*, 8(2), p.e56997.

Yamaguchi, T.P. et al., 1999. T (Brachyury) is a direct target of Wnt3a during paraxial mesoderm specification. *Genes and Development*, 13(24), pp.3185–3190.

Yamamoto, M. et al., 2004a. Nodal antagonists regulate formation of the anteroposterior axis of the mouse embryo. *Nature*, 428(6981), pp.387–92.

Yamamoto, M. et al., 2004b. Nodal antagonists regulate formation of the anteroposterior axis of the mouse embryo. *Nature*, 428(6981), pp.387–92.

Yang, S.-H., Kalkan, T., Morissroe, C., Marks, H., Stunnenberg, H., Smith, A. & Sharrocks, A.D., 2014. Otx2 and Oct4 Drive Early Enhancer Activation during Embryonic Stem Cell Transition from Naive Pluripotency. *Cell Reports*, pp.1–14.

Yang, S.-H., Kalkan, T., Morissroe, C., Marks, H., Stunnenberg, H., Smith, A. & Sharrocks, A.D., 2014. Otx2 and Oct4 Drive Early Enhancer Activation during Embryonic Stem Cell Transition from Naive Pluripotency. *Cell reports*, 7(6), pp.1968–81.

Yeom, Y.I. et al., 1996. Germline regulatory element of Oct-4 specific for the totipotent cycle of embryonal cells. *Development (Cambridge, England)*, 122(3), pp.881–94.

Ying, Q.-L. et al., 2008a. The ground state of embryonic stem cell self-renewal Suppl. *Nature*, 453(7194), pp.519–23.

Yoshiba, S. et al., 2012. Cilia at the Node of Mouse Embryos Sense Fluid Flow for Left-Right Determination via Pkd2. *Science*, 226.

Yoshiba, S. & Hamada, H., 2014. Roles of cilia, fluid flow, and Ca(2+) signaling in breaking of left-right symmetry. *Trends in genetics : TIG*, 30(1), pp.10–7.

Yoshioka, H. et al., 1998. Pitx2, a Bicoid-Type Homeobox Gene, Is Involved in a Lefty-Signaling Pathway in Determination of Left-Right Asymmetry. *Cell*, 94(3), pp.299–305.

Young, R. a, 2011. Control of the embryonic stem cell state. *Cell*, 144(6), pp.940–54.

Young, T. & Deschamps, J., 2009. Hox, Cdx, and anteroposterior patterning in the mouse embryo. *Current topics in developmental biology*, 88, pp.235–55.

Yuan, H. et al., 1995. Developmental-specific activity of the FGF-4 enhancer requires the synergistic action of Sox2 and Oct-3. *Genes & Development*, 9(21), pp.2635–2645.

Yuan, P. et al., 2009a. Eset partners with Oct4 to restrict extraembryonic trophoblast lineage potential in embryonic stem cells. *Genes & development*, 23(21), pp.2507–20.

Zeineddine, D. et al., 2006. Oct-3/4 dose dependently regulates specification of embryonic stem cells toward a cardiac lineage and early heart development. *Developmental cell*, 11(4), pp.535–46.

Zhang, K. et al., 2010. Distinct functions of BMP4 during different stages of mouse ES cell neural commitment. *Development (Cambridge, England)*, 137(13), pp.2095–105.

Zhang, L. et al., 2007. Successful co-immunoprecipitation of Oct4 and Nanog using cross-linking. *Biochemical and Biophysical Research Communications*, 361(3), pp.611–614.

Zhang, X. et al., 2010. Prognostic Significance of OCT4 Expression in Adenocarcinoma of the Lung. *Japanese Journal of Clinical Oncology* , 40 (10), pp.961–966.

Zhao, T. et al., 2014. β-catenin regulates Pax3 and Cdx2 for caudal neural tube closure and elongation. *Development* , 141 (1), pp.148–157.

Zhu, J. et al., 2013. Genome-wide chromatin state transitions associated with developmental and environmental cues. *Cell*, 152(3), pp.642–54.

Zorn, A.M. & Wells, J.M., 2009. Vertebrate endoderm development and organ formation. *Annual review of cell and developmental biology*, 25, pp.221–51.

8 List of abbreviations

aa	amino acid
ADE	anterior definitive endoderm
AJ	adherens junctions
AME	anterior mesendoderm
AP	anterior-posterior
AVE	anterior visceral endoderm
β-gal	β-galactosidase
BMP	bone morphogenetic protein
bp	base pair
BSA	bovine serum albumin
°C	Celsius
Cdx	caudal-related homeobox
Cer	Cerberus
ChIP	chromatin immuno precipitation
CKO	conditional knock out
D1,2,3	day1,2,3…
DE	definitive endoderm
Dkk	Dickkopf
DNA	deoxyribonucleic acid
DTT	Dithiothreitol
DV	dorsoventral

DVE	distal visceral endoderm
E	embryonic day
EB	embryoid body
ECL	enhanced chemiluminescence
eGFP	enhanced green fluorescent protein
EMT	epithelial-mesenchymal transition
ESC	embryonic stem cell
EtOH	ethanol
ExE	extraembryonic ectoderm
FACS	fluorescent activated cell sorting
FBS	fetal bovine serum
Fg	foregut
FGF	fibroblast growth factor
Foxa2	forkhead box transcription factor a 2
fp	floorplate
Fwd	forward
Fz	Frizzled
GI	gastrointestinal
GO	gene onthology
Gsk3β	glycogen synthase 3 beta
Hex	haematopoetically expressed homeobox gene
Hg	hindgut

HH	hedgehog
HNF	hepatocyte nuclear factor
HRP	horseradish peroxidase
HT	heart
ICM	inner cell mass
iCre	improved Cre recombinase
IP	immunoprecipitation
IRES	internal ribosomal entry site
kb	kilo base
kDa	kilo Dalton
Lefty	left right determination factor
LIF	leukemia inhibitory factor
Lef	lymphoid enhancer factor
LR	left-right
LSM	laser scanning microscopy
MEF	murine embryonic fibroblast
MEK	mitogen-activated protein kinase
Mg	midgut
Mes	Mesoderm
MeOH	Methanol
Min	minute(s)
MMC	mitomycin C

lN_2	liquid nitrogen
NC	notochord
NFR	nuclear fast red
NLS	nuclear localization signal
NT	neural tube
OCT	optimal cutting temperature
ON	over night
ORF	open reading frame
P1,2,3	postnatal day 1,2,3…
PBS	phosphate buffered saline
PCR	polymerase chain reaction
PrE	primitive endoderm
PFA	paraformaldehyde
PS	primitive streak
qPCR	quantitative polymerase chain reaction
R26R	ROSA26 reporter
RA	retinoic acid
Rev	reverse
RT	room temperature
Rpm	rounds per minute
Sec	second(s)
Shh	sonic hedgehog

T2A	a 2A-like
TAE	Tris-acetate, EDTA
TE	trophectoderm
TE	Tris, EDTA
TSS	transcriptional start site
UTR	untranslated region
VE	visceral endoderm
WISH	whole mount *in situ* hybridization
WT	wild type

9 Apendix

9.1 List of publications

Ingo Burtscher, Silvia Engert, Stefan Hasenöder, Daniela Padula, Heiko Lickert
Steuerungsmechanismen der Entodermentwicklung in der Maus (Biospektrum; 5/2011; non-peer reviewed)

Gegg M, Böttcher A, Burtscher I, Hasenöder S, Van Campenhout C, Aichler M, Walch A, Grant SG, Lickert
Flattop regulates basal body docking and positioning in mono- and multiciliated cells
eLife 2014;3:e03842

Hasenöder S, Engert S, Burtscher I, Gegg M, Irmler M, Liao P, Beckers P, Lickert H
Oct4 regulates Left-right asymmetry through Wnt and Tgf-β/Nodal pathway activation
(Manuscript in preparation)

9.2 Conference contributions

- **Joint Meeting of the German and Japanese Societies of Developmental Biologists**, Dresden, 2011
- **Stem cells in development and disease**, Berlin 2011
- **4th International Congress on stem cells and tissue regeneration**, Dresden 2012